Titre: Title:	Development of Graphene-Based Polymer Nanocomposites for Electrical Conductors and Supercapacitors
Auteur: Author:	Ali Moayeri
Date:	2015
Type:	Mémoire ou thèse / Dissertation or Thesis
Référence: Citation:	Moayeri, A. (2015). Development of Graphene-Based Polymer Nanocomposites for Electrical Conductors and Supercapacitors [Thèse de doctorat, École Polytechnique de Montréal]. PolyPublie. https://publications.polymtl.ca/2007/

URL de PolyPublie: PolyPublie URL:	https://publications.polymtl.ca/2007/
Directeurs de recherche: Advisors:	Abdellah Ajji
Programme: Program:	Génie chimique

UNIVERSITÉ DE MONTRÉAL

DEVELOPMENT OF GRAPHENE-BASED POLYMER NANOCOMPOSITES FOR ELECTRICAL CONDUCTORS AND SUPERCAPACITORS

ALI MOAYERI

DÉPARTEMENT DE GÉNIE CHIMIQUE

ÉCOLE POLYTECHNIQUE DE MONTRÉAL

THÈSE PRÉSENTÉE EN VUE DE L'OBTENTION

DU DIPLÔME DE PHILOSOPHIÆ DOCTOR

(GÉNIE CHIMIQUE)

DÉCEMBRE 2015

UNIVERSITÉ DE MONTRÉAL

ÉCOLE POLYTECHNIQUE DE MONTRÉAL

Cette thèse intitulée:

DEVELOPMENT OF GRAPHENE-BASED POLYMER NANOCOMPOSITES FOR ELECTRICAL CONDUCTORS AND SUPERCAPACITORS

présentée par : MOAYERI Ali

en vue de l'obtention du diplôme de : Philosophiæ Doctor

a été dûment acceptée par le jury d'examen constitué de :

M. PERRIER Michel, Ph. D., président

M. AJJI Abdellah, Ph. D., membre et directeur de recherche

M. THERRIAULT Daniel, Ph. D., membre

Mme DEMARQUETTE Nicole Raymonde., Ph. D., membre

DEDICATION

“To my lovely wife and daughter, and beloved father, mother and sister”

ACKNOWLEDGEMENTS

I would like to express my everlasting gratitude to my father, Masoud, mother, Haleh, and sister, Valeh, who have always been there for me. Words are powerless to express what I feel in my heart towards them. I send my deepest gratitude to my wife, Kiana, and my newborn daughter, Liana, for being there for me in all the moments. Words are incapable to express what I feel in my heart towards them.

I would like to express the deepest appreciation to my supervisor, Prof. Abdellah Ajji, who is inspiring for me in many aspects, which are not limited to research. His kind consideration, support and affability besides of his guidance in repute to research provided a medium full of spirit of adventure in regard to research and innovation which are much more than what is written in this thesis.

I take this opportunity to place my sincere thanks to all the members of Prof. Ajji's research group, particularly to Claire Cerclé and Richard Silverwood for their help and support. I would like to express my special thanks to Mounia Arkoun for her help in translating the abstract of this thesis to French.

I would also like to thank the supervisory committee members for their insight and helpful comments, namely Prof. Michel Perrier, Prof. Daniel Therriault and Prof. Nicole R. Demarquette.

In addition, I am grateful to all my friends who were there for me during my Ph.D. studies at Polytechnique Montreal. I cannot list them all as it would be a very long list so to anyone who thinks I am his/her friend; I express my deepest gratitude.

I would like to thank Nicole MacDonald and Jean-Philippe Masse from CM^2 for their help and assistance with microscopy imaging. I would also like to thank Dr. Josianne Lefebvre for her

guidance and help with the XPS analysis and Dr. Gwenaël Chamoulaud at NanoQAM - Université du Québec à Montréal for his assistance with carbonization process and electrochemical tests.

The administrative staff of our department had a significant role in helping us and providing us with a calm atmosphere in order to advance our projects, namely Evelyne Rousseau, Lyne Henley and Carmen Elena Membreno Aguilar.

The financial support from the Natural Science and Engineering Research Council (NSERC) and the Fonds de recherche du Québec – Nature et technologies (FRQNT) is highly appreciated.

RÉSUMÉ

L’électrofilage est une méthode pratique et avantageuse pour obtenir des nanofibres de polymères avec des diamètres contrôlés de l'ordre de quelques dizaines de nanomètres à quelques micromètres. Les mats de fibres non-tissées résultants ont des surfaces spécifiques élevées de l'ordre de 1 à 100 m^2/g. La combinaison de ces propriétés avec la conductivité électrique intrinsèquement élevée de certains polymères conducteurs donne lieu à des mats de fibres conducteurs qui sont très prometteurs pour diverses applications dans divers domaines dont : l’électronique, le magnétique, le biomédical, mais encore des applications en optique et dans le domaine des capteurs.

Une nouvelle classe de polymère connue sous le nom de polymères intrinsèquement conducteurs (PIC) a été découverte en 1960. Les PIC sont de nature intrinsèquement conducteurs en raison de la présence d'un système d'électrons π conjugué dans leur structure. Les PIC possèdent des bonnes propriétés électroniques, des faibles potentiels d'ionisation et une électroaffinité élevée. La polyaniline (PANi) est l'un des PIC les plus étudiés. Elle est unique en raison de la facilité de sa synthèse, de sa stabilité environnementale et de la simplicité de sa chimie de dopage/dédopage. En revanche, elle est relativement difficile à mettre en forme par rapport à la plupart des autres polymères conventionnels, ce qui est typique des PIC. En effet, la polyaniline a un squelette assez rigide en raison de son aromaticité élevée. Ainsi, l'élasticité des solutions de PANi est généralement insuffisante pour qu'elles puissent être électrofilées pour en faire des nanofibres. En outre, la PANi a une mauvaise solubilité dans la plupart des solvants communs, ce qui rend son électrofilabilité encore plus difficile. Cependant, si les limitations de solubilité et de rigidité suscitées pouvaient être résolues, la PANi pourrait être électrofilée en mats de fibres conductrices pouvant être utilisés

dans une large gamme d'applications telles que les capteurs chimio-résistants, les surfaces hydrophobes réversibles et les substrats pour la fonctionnalisation.

Le but ultime de la première partie de cette thèse est de préparer des nanofibres de PANi électrofilées avec du graphène intégré pour une utilisation potentielle comme capteurs pour la détection de gaz et de pathogènes. À cette fin, deux stratégies ont été utilisées pour obtenir les nanofibres électrofilées de PANi:

Mélanger de la PANi dopée avec des polymères isolants et facilement électrofilables comme le poly(oxyde d'éthylène) ou PEO. Cependant, la présence du polymère isolant réduit la conductivité des fibres en raison de la diminution des composés conducteurs dans le mélange. Une bonne stratégie pour compenser l'addition du polymère isolant et améliorer les propriétés électriques globales des fibres électrofilées, est d'y incorporer des nanocharges conductrices à base de carbone. À cet effet, le graphène a été sélectionné. Depuis sa découverte en 2004, le graphène a suscité un intérêt considérable en recherche. Il est constitué d'un simple feuillet d'une seule épaisseur en deux dimensions, lui-même composé d'atomes de carbone organisés en une structure cristalline en nid d'abeilles. Il possède une surface, une résistance ainsi qu'une conductivité thermique et électrique exceptionnellement élevées.

Par conséquent, compte tenu des excellentes propriétés du graphène et de la PANi, des nanofibres de PANi contenant des nanocharges de graphène comme agent de remplissage peuvent être obtenues. Ainsi, des nanofibres conductrices de PANi dopée avec de l'acide camphre-10-sulfonique (ACS), mélangée à du PEO et remplie avec du graphène fonctionnalisé ester succinimidyle de l'acide 1-pyrènebutanoïque ou (G-PBASE) ont été préparées par électrofilage. La microscopie électronique à balayage (MEB), la microscopie électronique à transmission (MET), la spectroscopie de photoélectrons par rayons X (XPS), la spectroscopie infrarouge à transformée de

Fourier (FTIR) et l'analyse thermogravimétrique (TGA) ont été utilisées pour caractériser la morphologie des fibres de PANi/PEO/G-PBASE ainsi que leurs propriétés. Les observations montrent que les fibres électrofilées sont fortement interconnectées et possèdent une surface relativement lisse. Le diamètre moyen des fibres est d'environ 220 nm. La conductivité électrique des fibres de PANi/PEO et PANi/PEO/G-PBASE à température ambiante a également été étudiée. Les fibres composites nanostructurées PANi/PEO/G-PBASE avec une faible charge de G-PBASE (5 % en poids par rapport à la PANi) a montré une augmentation de la conductivité électrique de deux ordres de grandeur et une amélioration d'un ordre de grandeur de la stabilité thermique en comparaison avec les nanofibres de PANi/PEO.

Utiliser la technique d'électrofilage coaxial pour préparer des nanofibres structurées en cœur-enveloppe avec la PANi au centre de la fibre et un polymère facilement électrofilable tel que le poly(méthacrylate de méthyle) (PMMA). Par la suite, l'enveloppe externe a été retirée par extraction-solvant pour obtenir des nanofibres de PANi pures. La méthode d'électrofilage coaxial constitue une alternative et un moyen efficace pour l'obtention de fibres de polymères non-électrofilables. Dans cette technique, deux solutions différentes sont électrofilées simultanément à travers une filière composée de deux capillaires coaxiaux pour produire des nanofibres structurées en cœur-enveloppe avec le polymère non-électrofilable au centre de la fibre. Par conséquent, des nanofibres cœur-enveloppe de PANi/PMMA contenant du G-PBASE sont préparées par électrofilage coaxial, avec la PANi et le G-PBASE étant au cœur des fibres et le PMMA l'enveloppe externe, respectivement. Les nanofibres de PANi/G-PBASE/PMMA obtenues possèdent des diamètres de ~420 nm. En outre, des nanofibres de pure PANi et de PANi/G-PBASE ont été obtenues par extraction-solvant de l'enveloppe de PMMA, ce qui a réduit le diamètre des fibres à

230 nm. La morphologie des nanofibres a été analysée par MEB et MET. La structure cœur-enveloppe et l'existence de feuillets de graphène dans la couche centrale des fibres ont été confirmées par les images en MET, obtenues avant et après extraction-solvant du PMMA. La conductivité électrique des fibres obtenues à température ambiante a été étudiée par la méthode de la sonde à quatre points. Les nanofibres de PANi/G-PBASE ont montré une conductivité électrique de 30,25 S/cm, laquelle est trois fois plus élevée que celle des nanofibres de PANi pure.

Dans la deuxième partie de cette thèse, nous investiguons l'ajout de graphène à du polyacrylonitrile (PAN) renforcé par des nanofibres de carbone (NFC). L'objectif étant d'améliorer la surface spécifique et la capacitance des fibres obtenues, en vue d'applications où une densité de haute énergie est requise, tel que dans les supercondensateurs. Récemment, beaucoup de recherches ont été menées sur des matériaux à base de PAN et NFC pour des applications de stockage d'énergie. Cependant, la faible conductivité et densité de puissance des NFC représentent un obstacle à leur utilisation potentielle dans les supercondensateurs. Par conséquent, dans cette étude, des NFC électrofilées en structure cœur-enveloppe et additionnées de différentes quantités de graphène fonctionnalisé de façon non covalente ont été préparées. La technique employée à cet effet est l'électrofilage à une seule buse en utilisant une solution biphasée de polyacrylonitrile et de polyvinylpyrrolidone (PAN/PVP), avec comme solvant du N,N-diméthylformamide (DMF). La concentration en graphène varie de 0% à 15% en poids (par rapport au PAN). Les nanofibres électrofilées structurées en cœur-enveloppe ont d'abord été stabilisées à 250 °C dans l'air puis, par la suite carbonisées à 850 °C dans une atmosphère sous azote pour produire les NFC. Les fibres ultra-minces résultantes ont des diamètres moyens de l'ordre de 60 à 80 nm. La morphologie et la microstructure des nanofibres ont été caractérisées par SEM, TEM, spectroscopie Raman, XPS et

BET pour l'adsorption d'azote à 77 K. Après incorporation des nanofeuillets de graphène, les résultats ont montré une augmentation de la surface spécifique et du volume des pores des mats de fibres allant jusqu'à 627 $m^2 g^{-1}$ et 0,35 $cm^3 g^{-1}$, respectivement. La performance électrochimique des nanocomposites NFC/graphène a été étudiée dans une solution de KOH (6M). Les analyses électrochimiques de ces mêmes nanofibres révèlent une capacitance spécifique maximale de 265 $F g^{-1}$, après ajout de 10% en poids de nanofeuillets de graphène.

ABSTRACT

Electrospinning is a convenient method to produce polymer nanofibers with controlled diameters on the order of tens of nanometers to micrometers. The resulting non-woven fiber mats have high specific surface areas of around 1−100 m^2/g. Combining these properties with the high electrical conductivity of intrinsically conductive polymers yields conductive electrospun fiber mats that are very promising for a variety of applications such as electronic, magnetic, biomedical, sensor and optical fields.

A new class of polymer known as intrinsically conducting polymers (ICPs) were discovered in 1960. ICPs are intrinsically conducting in nature due to the presence of a conjugated π electron system in their structure. ICPs possess electronic properties, low ionization potentials and a high electroaffinity. Polyaniline (PANi) is one of the most studied ICPs and it is unique due to its ease of synthesis, environmental stability, and simple doping/dedoping chemistry, yet it is relatively hard to process compared to most other polymers. As is common among ICPs, it has a fairly rigid backbone due to its high aromaticity. Thus, the elasticity of its solutions is generally insufficient for it to be electrospun directly into fibers. Moreover, PANi has poor solubility in common solvents, which further complicates it electrospinnability. However, if aforementioned processing limitations of PANi can addressed and it can be electrospun into conductive fiber mats, it can be used for a variety of applications such as chemoresistive sensors, reversible hydrophobic surfaces and substrates for functionalization.

The ultimate purpose of first part of this thesis is to fabricate electrospun PANi nanofibers embedded with graphene for potential sensor applications such as gas and pathogen detection. To this end, two strategies were utilized to electrospin PANi nanofibers:

1) Blending doped-PANi with insulating polymers which are easily electrospinnable such as polyethylene oxide (PEO). However, the presence of the insulator polymer will decrease the fibers conductivity due to a reduction of the conducting component in the blend and a good strategy to compensate for the addition of insulating polymer and to improve the overall electrical properties of the electrospun fibers blend is to incorporate carbon-based conductive nanofillers into the fibers and in this work graphene was selected. Since the discovery of graphene in 2004, it has attracted tremendous research interest. Graphene is a single-atom-thick, two-dimensional sheet of sp^2-hybrized carbon atoms arranged in a honeycomb crystal structure with exceptionally high strength, surface area, thermal conductivity, and electronic conductivity. Therefore, considering the excellent properties of graphene and PANi, highly conductive PANi nanofibers with graphene as nanofiller can be obtained. To this end, conducting nanofibers of PANi doped with camphor-10-sulfonic acid (HCSA), blended with PEO, and filled with 1-pyrenebutanoic acid, succinimidyl ester functionalized graphene (G-PBASE) have been fabricated using electrospinning. Scanning electron microscopy (SEM), transmission electron microscopy (TEM), X-ray photoelectron spectroscopy (XPS), Fourier transforms infrared (FTIR) and thermal gravimetric analyzer (TGA) were utilized to characterize the PANi/PEO/G-PBASE fibers morphology and properties. The observations show that electrospun fibers are highly interconnected and possess a relatively smooth surface. The average diameter of fibers was ~ 220 nm. The electrical conductivity of PANi/PEO and PANi/PEO/G-PBASE at room temperature was also studied. The unique nanostructured composite of PANi/PEO/G-PBASE with small loading of G-PBASE (5 wt.% relative to PANi) showed two order of magnitude enhancement in the electrical conductivity and one order of magnitude enhancement in thermal stability in comparison to PANi/PEO nanofibers.

2) Utilizing coaxial electrospinning technique to produce core−shell structured nanofiber with PANi at the core layer and an easily electrospinnable polymer such as poly(methyl methacrylate) (PMMA) at shell segment. Subsequently, the shell segment was removed by solvent etching to produce pure PANi nanofibers. The coaxial electrospinning method provides an alternative and effective way for fabrication of unspinnable polymer with unique core−shell structured fibers. In this technique, two dissimilar solutions are spun simultaneously through a spinneret composed of two coaxial capillaries to produce core−shell structured nanofibers with unspinable polymer at the core section. Therefore, Core−shell structured PANi/PMMA nanofibers embedded with G-PBASE are produced by a coaxial electrospinning setup. PANi/G-PBASE and PMMA solutions were used as core and shell layer respectively. The as-prepared PANi/G-PBASE/PMMA nanofibers possessed diameters in the range of ~420 nm. Moreover, neat PANi/G-PBASE and PANi nanofibers were obtained by solvent etching of PMMA shell which reduced the fiber diameter to 230 nm. The morphology of the nanofibers was investigated by SEM and TEM. The core−shell structure and the existence of graphene sheets in the core layer were confirmed by TEM images obtained before and after solvent etching of PMMA. The electrical conductivity of the fibers at room temperature was investigated by four-point probe method. The PANi/G-PBASE nanofibers exhibited electrical conductivity as high as of 30.25 S/cm which was 3 times higher than that of neat PANi nanofibers.

The second part of this thesis investigates the addition of graphene to polyacrylonitrile (PAN)-based carbon nanofibers (CNFs) in order to improve their surface area and capacitance for applications where high-energy density is required such as in supercapacitors. Recently, a lot of research has been conducted on PAN-based CNFs for energy storage applications. However, CNFs low conductivity and power density is an obstacle for their potential application in supercapacitors.

Therefore, in this study core–shell structured CNFs embedded with various amounts of non-covalently functionalized graphene were fabricated by single-nozzle electrospinning technique using phase-separated solution of polyacrylonitrile and polyvinylpyrrolidone (PAN/PVP) in N,N-dimethylformamide (DMF). The concentration of graphene varied from 0 wt% to 15 wt% (relative to PAN). These core-shell structured electrospun nanofibers were first stabilized at 250 °C in air and consecutively carbonized at 850 °C in nitrogen atmosphere to produce CNFs. The resulting ultra-fine fibers have average fiber diameters in the range of 60-80 nm. The morphology and microstructure of the nanofibers were characterized by SEM, TEM, Raman spectroscopy, XPS and BET nitrogen adsorption at 77 K. The result showed that the specific surface area and pore volume of nanofiber mats increased to 627 $m^2 g^{-1}$ and 0.35 $cm^3 g^{-1}$ respectively by embedding graphene nanosheets. The electrochemical performance of as-synthesized CNF/G nanocomposites was investigated in 6M KOH electrolyte by cyclic voltammetry and galvanostatic charge/discharge. Electrochemical measurements of CNF/G nanofibers exhibited a maximum specific capacitance of 265 F g^{-1} after addition of 10 wt% graphene nanosheets.

TABLE OF CONTENTS

LIST OF TABLES

LIST OF FIGURES

LIST OF SYMBOLS AND ABBREVIATIONS

AFD	Average fiber diameter
APW	Average pore width
ATR	Attenuated total reflectance
BET	Brunauer–emmett–teller
CNF	Carbon nanofiber
CNT	Carbon nanotube
CRGO	Chemically reduced graphene
CVD	Chemical vapor deposition
DFT	Density functional theory
DI water	Deionized water
DMF	N,n-dimethylformamide
EDX	Energy-dispersive X-ray spectroscopy
FTIR	Fourier transform infrared spectroscopy

G-PBASE	1-pyrenebutanoic acid, succinimidyl ester functionalized graphene
GNPC	Graphene-based polymer nanocomposites
GO	Graphene oxide
HCSA	Camphor-10-sulfonic acid
HDPE	High-density polyethylene
HOPG	Highly oriented pyrolytic graphite
ICP	Intrinsically conducting polymers
IPA	Isopropanol / Isopropyl alcohol
LEI	Lower secondary electron image
MIBK	Methyl isobutyl ketone
PAN	Polyacrylonitrile
PANi	Polyaniline
PBASE	1-Pyrenebutanoic acid, succinimidyl ester
PC	Polycarbonate
PDT	Polydodecylthiophene

PE	Polyethylene
PEO	Polyethylene oxide
PET	Polyethylene terephthalate
PI	Polyimide
PLA	Polylactic acid
PMMA	Polymethyl methacrylate
PP	Polypropylene
PS	Polystyrene
PTFE	Polytetrafluoroethylene
PVP	Polyvinylpyrrolidone
RGO	Reduced graphene oxide
SEM	Scanning electron microscope
TEM	Transmission electron microscopy
TGA	Thermogravimetric analysis
THF	Tetrahydrofuran
TRGO	Thermally reduced graphene

XPS	X-ray photoelectron spectroscopy

CHAPTER 1 INTRODUCTION

Nanocomposites have made advancement in many industries after it was shown that most mechanical, thermal and electrical properties can be significantly enhanced by dispersing only small quantities of nanoparticles in polymer matrices. In particular, electrically conducting polymer nanocomposites have received significant attention since they exhibited sufficient conductivity for replacement of metals and inorganic materials for applications in sensors, actuators, and energy storage devices.

Electrospinning is an efficient, relatively simple and low-cost procedure to produce polymer and composite fibers with diameters ranging from several nanometers to a few micrometers. Nanofibers fabricated via electrospinning have large aspect ratios and specific surface approximately one to two orders of the magnitude larger than flat films. In this process, a charged polymeric solution ejects out of a syringe and accelerates toward a collector, mounted at a fixed distance from the needle and during this flight the polymer solution elongates and whips until it is deposited on the collector, resulting in formation of non-woven random nanofibers. The prepared non-woven electrospun mats exhibit remarkable characteristics such as high specific surface area, high porosity and interconnected porous structure. These properties make the electrospun mats a good candidate for gas or pathogen detection and energy storage applications.

A new class of polymer known as intrinsically conducting polymers (ICPs) were discovered in 1960. ICPs are intrinsically conducting in nature due to the presence of a conjugated π electron system in their structure. ICPs posse electronic properties, low ionization potentials and a high electroaffinity. This extended π-conjugated system of conducting polymer is linked to the single and double bonds in their structure. The conductivity level of ICPs can reached near to that of a

metal depending on their oxidation states and doping level. These properties have attracted many studies for application of ICPs in electronics, electrochemical, electromagnetic and sensor applications. Polyaniline (PANi) is one of the most studied ICPs and it is unique due to its ease of synthesis, environmental stability, and simple doping/dedoping chemistry, yet it is relatively hard to process compared to most other polymers. As is common among ICPs, it has a fairly rigid backbone due to its high aromaticity. Thus, the elasticity of its solutions is generally insufficient for it to be electrospun directly into fibers. Moreover, PANi has poor solubility in common organic solvents, which further complicates it electrospinability. However, if aforementioned processing limitations of PANi can be addressed to obtain conductive fiber mats, it can be used for a variety of applications such as chemoresistive sensors. In this thesis, two strategies were followed to electrospun PANi for the mentioned application:

1) By blending doped-PANi with insulating polymers, which are easily electrospinnable. However, the presence of an insulator polymer will decrease the fibers conductivity due to reduction of the conducting component in the blend. A good strategy to compensate for the addition of insulating polymer and to improve the overall electrical properties of the electrospun fibers blend is to incorporate carbon-based conductive nanofillers into the fibers and in this work graphene was selected.

2) By utilizing coaxial electrospinning technique to produce core-shell structured nanofiber with PANi at the core segment and an easily electrospinnable polymer at shell segment. Subsequently, the shell segment is removed by solvent etching to produce pure PANi nanofibers.

Since the discovery of graphene in 2004, it has attracted tremendous research interest. Graphene is a single-atom-thick, two-dimensional sheet of sp^2-hybrized carbon atoms arranged in a honeycomb crystal structure with outstanding properties such as extraordinary physical properties (high values

of its Young's modulus (~1,100 GPa), fracture strength (125 GPa), high thermal conductivity ~5,000 W $m^{-1}K^{-1}$), excellent mobility of charge carriers (200,000 cm^2 V^{-1} s^{-1}), and high specific surface area (calculated value, 2,630 m^2 g^{-1}). Therefore, considering the excellent properties of graphene, a highly conductive PANi composite with graphene as nanofillers can be obtained.

In the second part of this thesis, fabrication of polyacrylonitrile (PAN) based carbon nanofibers (CNFs) embedded with graphene nanosheets for supercapacitor applications is investigated. In recent years, there has been an extensive research on the fabrication of PAN based carbon CNFs as a great candidate for electrode material of energy storage devices mainly due to CNFs high surface area and chemical resistance. However, the low conductivity of CNFs has limited their power densities and hindered their potential usage in application where high power densities are sought after, such as in supercapacitors. Graphene nanosheets have demonstrated attractive properties as a new family of carbon nanomaterials for use in electrochemical energy generation and storage application. Thus, given the high surface area and electrical conductivity of graphene, an essential characteristics of an electrode material for energy production and storage, it is an attractive material for applications in energy storage systems and provides the possibility of improving the power density of CNFs by embedding graphene nanosheets into the precursor polymer matrix.

This dissertation is based on three articles that have been published or submitted to scientific journals and is comprised of the following sections:

Chapter 2 provides a literature review on the related topics investigated in this dissertation and followed by **Chapter 3**, which discusses the originality and main objectives of this dissertation.

The summary and organization of the articles are described in **Chapter 4**. **Chapter 5** and **Chapter 6** present result for the first part of this thesis where fabrication PANi nanofibers embedded with graphene by blending and coaxial electrospinning method is studied. **Chapter 7** presents results of second part of this thesis where graphene filled CNFs for supercapacitor applications is studied. **Chapter 8** provides a general discussion on the results obtained in this thesis followed by **Chapter 9** where conclusions and recommendations for this work is presented.

CHAPTER 2 LITERATURE REVIEW

This chapter provides a comprehensive literature review covering many aspects of graphene-based polymer nanofiber fabrication which forms the backbone of this research. In Section 2.1, an overview of single nozzle electrospinning and coaxial electrospinning is provided. Section 2.2 focuses on intrinsically conductive polymers and particularly polyaniline. Section 2.3 focuses on carbon nanofibers, their preparation via electrospinning and applications in supercapacitors. Section 2.4 deals with overview of graphene, its fabrication followed by highlight of its properties.

2.1 Electrospinning

2.1.1 Single-nozzle electrospinning

Electrospinning is an efficient, relatively simple and low-cost procedure to produce polymer and composite fibers with diameters ranging from several nanometers to a few micrometers (Doshi and Reneker 1995, Reneker and Chun 1996). The main advantages of the electrospinning process are its technical simplicity and its easy adaptability. Nanofibers fabricated via electrospinning have large aspect rations and specific surface approximately one to two orders of the magnitude larger than flat films, making them excellent candidates for potential applications in sensors (Prasad, Das et al. 2009). There are basically three components to fulfill the process: a high voltage supplier, a micro-syringe with a needle of small diameter, and a collecting screen. The schematic of this process is illustrated in Figure 2-1. The collector can be made of any shape according to product requirements such as flat plate, rotating drum, or patterned collector. In most cases, the collector is simply grounded, as shown in Figure 2-1.

The electric field is applied to the end of the micro-syringe that contains the solution fluid held by its surface tension. This induces a charge on the surface of the liquid. Mutual charge repulsion and the contraction of the surface charges to the counter electrode cause a force directly opposite to the surface tension (Fang and Reneker 1997). As the intensity of the electric field is increased, the hemispherical surface of the fluid at the tip of the micro-syringe needle elongates to form a conical shape known as the Taylor cone. By further increasing the electric field, a critical value is attained with which the repulsive electrostatic force overcomes the surface tension and charged jet of the fluid is ejected from the tip of the micro-syringe.

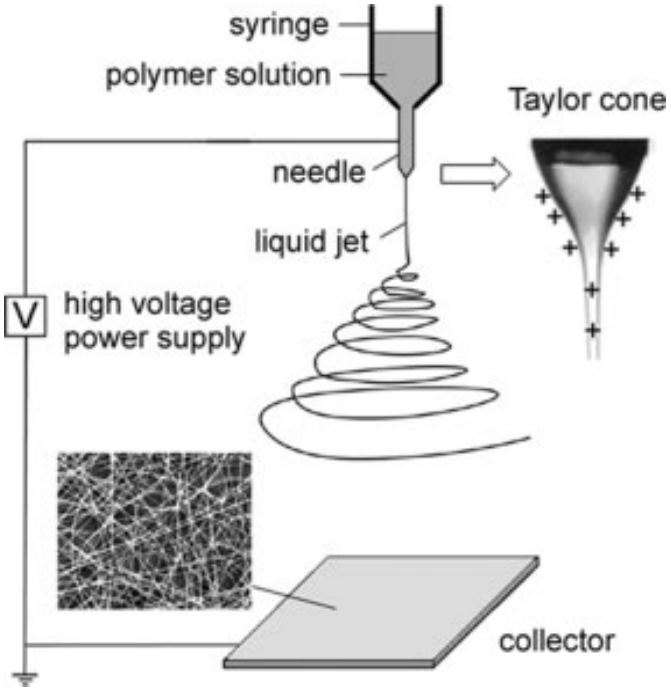

Figure 2-1: Schematic illustration of the fabrication of polymer nanofiber composite by electrospinning. The insets show a hemispherical surface of the fluid at the tip of the micro-syringe needle known as the Taylor cone (image is reproduced from reference (Li and Xia 2004)).

The discharged polymer solution undergoes an instability and elongation process, which allows the jet to become very long and thin. Meanwhile, the solvent evaporates, leaving behind a charged

polymer fiber. In the case of the melt, the discharged jet solidifies when it travels in the air (Huang, Zhang et al. 2003).

2.1.1.1 Control of Fiber Morphology and Diameter

As studies on the electrospinning process have been conducted, there have been some efforts to characterize the structure and morphology of nanofibers as a function of polymer solution and process parameters. Many parameters can influence the electrospinning of nanofibers. These parameters include: i) the intrinsic properties of the solution such as viscosity, elasticity, conductivity, and surface tension. ii) the operational conditions such as electric potential at the needle, the feeding rate for the polymer solution, and the distance between the syringe and the collector screen (Reneker and Chun 1996). iii) ambient parameters such as temperature, humidity and air velocity (Doshi and Reneker 1995). Two of the important factors that affect the viscosity of the solution are the molecular weight of the polymer and the solution concentration. Generally, when a polymer of higher molecular weight is dissolved in a solvent, its viscosity will be higher than solution of the same polymer but of a low molecular weight. One of the conditions necessary for electrospinning to occur where fibers are formed is that the solution consists of polymer of sufficient molecular weight and the solution must be of sufficient viscosity. As the jet leaves the needle tip during electrospinning, the polymer solution is stretched as it travels towards the collection plate. During the stretching of the polymer solution, it is the entanglement of the molecule chains that prevents the electrically driven jet from breaking up thus maintaining a continuous solution jet. The molecular weight of the polymer represents the length of the polymer chain, which in turn have an effect on the viscosity of the solution since the polymer length will determine the amount of entanglement of the polymer chains in solvent. Another way to increase

the viscosity of the solution is to increase the polymer concentration. Similar to increasing the molecular weight, an increased in the concentration will result in greater polymer chain entanglements within the solution which is necessary to maintain the continuity of the jet during electrospinning. Fibers measuring less than 1 μm in diameter were first spun by electrostatic means from N,N-dimethylformamide (DMF) solutions of acrylic resin (Baumgarten 1971) and this study highlighted the effects of solution viscosity on the fiber diameter and jet length. The experiment showed that the fiber diameter increased with the solution viscosity. The relationship between the fiber diameter and solution viscosity was established by Baumgart and can be expressed by the Equation 2-1, where d is fiber diameter and η is solution viscosity in poise.

$$d = \eta^{0.5} \qquad 2\text{-}1$$

One challenge in electrospinning is the occurrence of defects such as beads in polymer nanofibers. As shown in Figure 2-2 (A) (Jaeger, Schönherr et al. 1996), The formation of beads can be attributed to three forces: i) surface tension tends to convert the liquid jet into one or many spherical droplets (Rayleigh instability) ii) the electrostatic repulsion between charges on the jet surface tends to increase the surface area and favors the formation of a thin jet rather than beads. iii) Viscoelastic force also resists rapid changes in shape and supports the formation of fibers with smooth surfaces (Li and Xia 2004). Fong et al. have shown that polymer concentration also affects the formation of the beads in nanofibers and in general the higher the polymer concentration, the lower number of beads will form (Fong and Reneker 1999). The authors showed that as the viscosity increased for PEO/water solutions, the fiber diameter increased and the shape of beads changed from spherical to spindle-shaped and gradually disappeared, as shown in Figure 2-2.

Reneker et al. have reported that the nanofibers beads can be minimized by reducing the surface-tension of the polymer solution (Doshi and Reneker 1995).

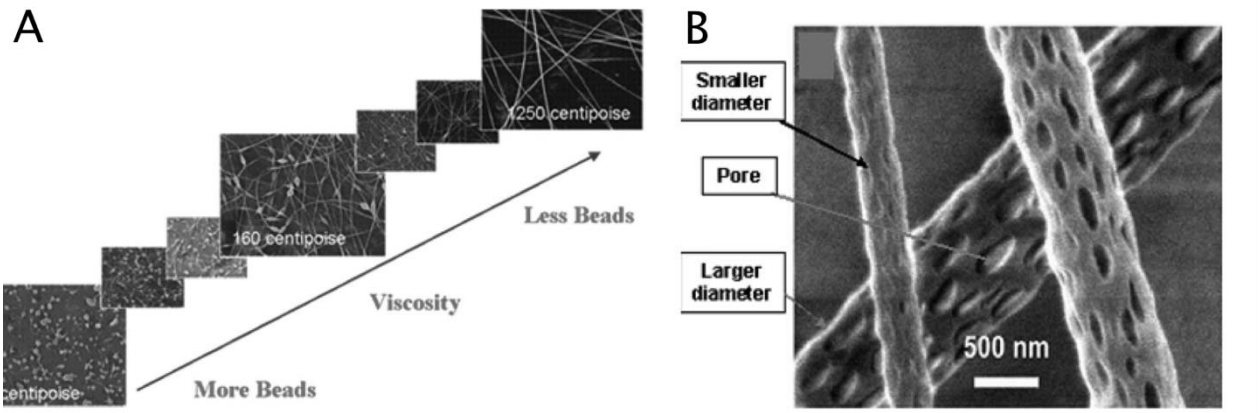

Figure 2-2: A) SEM photographs of electrospun nanofibers from different polymer concentration solutions (image is reproduced from reference (Fong and Reneker 1999)). B) nanofibers with different diameters and pores (image is reproduced from reference (Bognitzki, Czado et al. 2001).

Researchers showed the influence of solution properties on electrospun fiber diameter and morphology. Studies with poly(styrene), poly(urethane), poly(lactide), poly(vinyl chloride), and poly(vinylpyrrolidone) have yielded similar trends in fiber morphology with polymer concentration or solution viscosity. In general, as the polymer concentration increases, and subsequently the entanglement density in solution increases, the fiber morphology gradually changes from droplets to beaded fibers to uniform fibers. Thus, for electrospinning to occur a minimum solution concentration must be attained, and below this concentration, the Rayleigh instability domains and electrospraying occurs. To quantify the effect of entanglements on electrospun fiber formation process, the Berry number (*Be*), a dimensionless parameter, is used. In this equation, η is the intrinsic viscosity and C is the polymer concentration (Chen, Berry et al.).

$$Be = [\eta]C \qquad 2\text{-}2$$

In very diluted solutions, when the *Be* is less than unity, the molecules of the polymer are sparsely distributed in the solution. There is a low probability of individual molecules being entangled to each other. At a *Be* of greater than unity and as the concentration of the polymers increases, the level of molecular entanglement increases, resulting in more favorable conditions for the formation of fibers. Frank et al. electrospun poly(lactide)/chloroform solutions and have evaluated systematically the effects of polymer concentration and *Be*, on the average fiber diameter (AFD) and fiber morphology, shown in Figure 2-3 (Tao and Institute 2005).

Region I, where *Be <1*, is characterized by a very diluted polymer solution with molecular chains that barely touch each other. This makes it almost impossible to form fibers by electrospinning of such a solution, since the chains are not entangled enough to form a continuous fiber and the effect of surface tension will make the extended conformation of a single molecule unstable. As a result, only polymer droplets are formed. In region II, where *1<Be <3*, AFD increases slowly with *Be* from ~ 100 nm to ~ 500 nm. In this region, the degree of molecular entanglement is just sufficient for fibers to form. The coiled macromolecules of dissolved polymer are transformed by the elongational flow of the polymer jet into oriented molecular assemblies with some level of inter and intra-molecular entanglement. These entangled networks persist as fiber solidifies. In this region, some bead formations are observed as a result of the relaxation of the polymers and the effect of surface tension. In region III, where *3< Be <4*, AFD increases rapidly with *Be*, from ~ 1700 nm to ~ 2800 nm. In this region the entanglement of the molecular chain becomes more intensive, contributing to an increase in the viscosity of the polymer. Because of the intense level of molecular entanglement, a stronger electric field is needed for fibers to form by electrospinning.

In region IV, where *Be >4*, the AFD is less dependent on *Be*. With a high degree of inter and intra-molecular chain entanglement, other processing parameters such as the strength of the electric field and spinning distance become dominant factors that affect the diameter of the fiber.

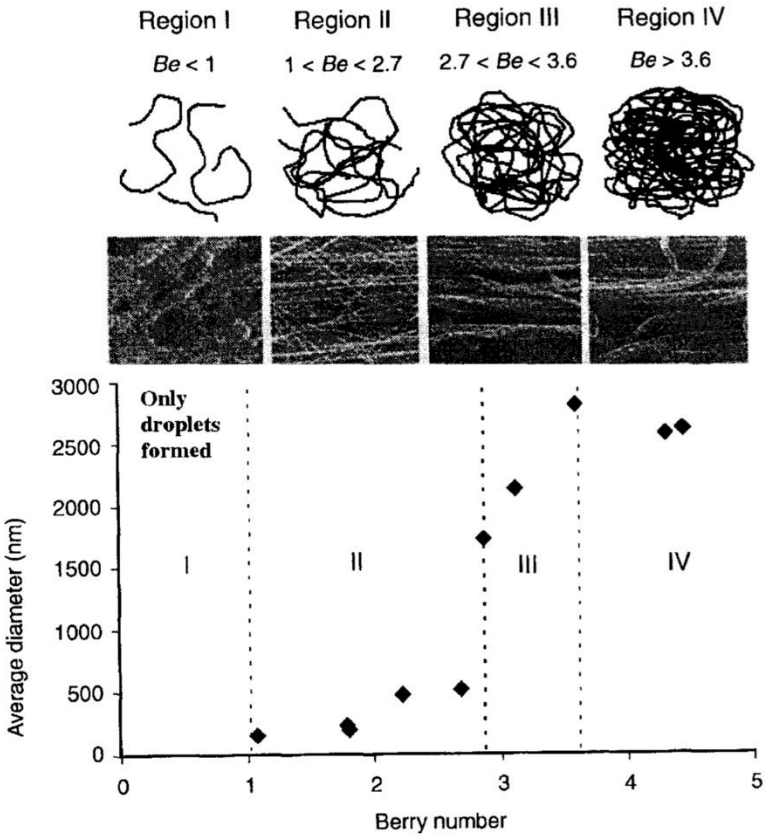

Figure 2-3: Fiber diameter and morphology as a function of Berry number (*Be*) (image is reproduced from reference (Ko 2006)).

Another significant factor in nanofiber's diameter, is the applied electrical voltage and as the voltage gets higher more fluid ejects from the needle resulting in a larger fiber diameter (Demczyk, Wang et al. 2002). Moreover, a higher feeding rate for the solution always leads to the formation of thicker fibers (Li and Xia 2004).

Generally, the electrospun fibers are deposited on a fixed collector as randomly oriented, three-dimensional non-woven membrane structure with a wide range of fiber diameter distribution. However, for many applications it is necessary to control the spatial orientation of the nanostructures. It was shown that be using a cylinder with high rotating speed collector, it is possible to fabricate aligned electrospun nanofibers and the collected fibers were oriented parallel to each other (Theron, Zussman et al. 2001).

2.1.2 Coaxial Electrospinning

Coaxial electrospinning is a branch of electrospinning which was developed in order to address the need for electrospinning of materials that was not previously electrospinnable using the single nozzle electrospinning technique and to develop nanofibers that posses a core-shell structure (Qu, Wei et al. 2013). Sun et al. first demonstrated the use of coaxial electrospinning setup in 2003 by using the same polymer, poly(ethyleneoxide) (PEO) for both core and shell segment of the nanofibers. They also electrospun unspinnable polymer, such as poly(dodecylthiophene) (PDT) and palladium(II) acetate ($Pd(OAc)_2$), in the core segment of fibers by using easily electrospinnable polymers, such as PEO and poly(L-lactide) (PLA) as a guide for the shell segment.

The general set up adopted by most researchers is quite similar to that used for single nozzle electrospinning (Elahi, Lu et al. 2013). In coaxial electrospinning, a smaller (inner) capillary is fitted concentrically inside the bigger (outer) capillary to make the coaxial spinneret and two syringes will feed the core and shell solutions to the spinneret. As the two solutions meet at the tip of the needle they form a compound Taylor cone with a core-shell structure when under the electric

field. The stress generated in the shell solution causes shearing of the core solution by viscous dragging and contact friction which deforms the core solution into the conical shape with the shell solution and forms the compound Taylor cone at the tip of the needle (Li and Xia 2004). The schematic of this process is shown in Figure 2-4. As the electrostatic force is applied on the compound Taylor cone, the shell solution elongates and stretches and once the charge accumulation reaches the threshold value, due to the increased applied potential, the jet is ejected towards the collector. The core-shell structure is kept intact as the jet is drawn by electrostatic force and flies towards the collector resulting in formation of nanofibers with core-shell structure at the collector.

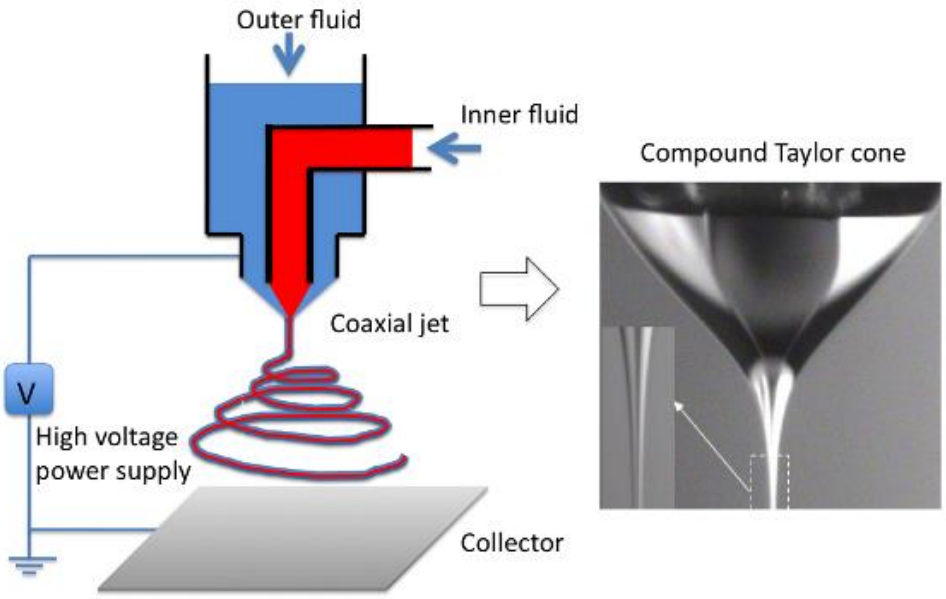

Figure 2-4: The configuration of coaxial electrospinning setup showing the formation of compound Taylor cone at the tip of the needle [(Li, Zhao et al. 2010)].

Coaxial electrospinning processing parameters are similar to those discussed earlier for single nozzle electrospinning. However, the introduction of second phase complicates to electrospinning process as miscibility and stress due to viscosity differences of the two solutions and difference between conductivity of two phases can play an important role in formation of fibers (Qu, Wei et al. 2013). Some of the important parameters in the coaxial electrospinning is discussed in the next sections.

2.1.2.1 Solution concentration

The polymer concentration is vital to electrospinability of a solution and the concentration should be high enough for entanglements to occur. For coaxial electrospinning the increase in solution concentration causes an increase in fiber diameter, the same relationship which is valid for single nozzle electrospinning. Zhang et al. increased the core-solution concentration while keeping the shell-solution concentration constant (Zhang, Huang et al. 2004). They observed an increase in core diameter as the concentration of core solution was increased. Also as expected, as the core diameter increased the shell diameter decreased and overall fiber diameter increased.

2.1.2.2 Solution viscosities

The key driver for formation of core-shell structured fibers in coaxial electrospinning is the shell solution. The shell solution viscosity should be high enough that can exert sufficient viscous stress on the core solution and overcome the interfacial tension between the two solutions and result in formation of compound Taylor cone (Díaz, Barrero et al. 2006).

2.1.2.3 Immiscibility of core-shell solutions

The selection of solvents and polymers in shell and core solutions are key in formation of compound Taylor cone and successful coaxial electrospinning. In a coaxial system, it is important

that the solvent in each of solutions do not precipitate the polymer in other phase as they meet at the tip of the needle (Yu, Fridrikh et al. 2004) and the interfacial tension between the two phases be as low as possible to yield an stable compound Taylor cone (Díaz, Barrero et al. 2006). It is also reported that when two miscible solutions are used, coaxial electrospinning can be also successful and the core-shell structured fibers can still be obtained (Sun, Zussman et al. 2003, Yu, Fridrikh et al. 2004). Although, certain degree of diffusion between core and shell layers can occur and it will be challenging to maintain the stable coaxial electrospinning process due to precipitation problem that can occur when two solutions at the tip of the needle (Li and Xia 2004).

2.1.2.4 Solvent vapor pressure:

The morphology of fibers can be strongly affected by the types of solvents used in the core and shell solutions. It is reported that usage of high vapour pressure solvents such as chloroform or acetone for core solution creates a thin layer at the interface of core and shell layers due to fast evaporation rate of the solvent which will cause the core segment to ultimately collapses. This phenomenon is due to creation of vacuum because the thin layer traps the solvent and when the solvent fully leaves the structure, the structure collapses and ribbon-like structures are created (Li, Babel et al. 2004). Therefore, high vapour pressure solvents should not be used as they can also disrupt the formation of compound Taylor cone (Larsen, Spretz et al. 2004).

2.1.2.5 Solution conductivity

Another important factor in the formation of fibers in coaxial electrospinning is the the conductivity of the solution. Solutions with high conductivity usually lead to fibers with smaller diameter since these solutions have higher surface charge density which cause an increase in the elongational force on the jet due to self-repulsion of the excess charges under a given electrical field (Hohman, Shin et al. 2001). In coaxial electrospinning the difference between conductivities of shell and core

solution can affect the fiber formation. Yu et al. shown that the more conductive core solutions are pulled at the higher rate by electrical field and therefore causes a discontinuity in the core-shell structure (Yu, Fridrikh et al. 2004). On the other hand, higher shell conductivity would result in higher shear stress on the core layer and will cause formation of a thinner core layer (Li and Xia 2004). Therefore, it is possible to embed solutions with low conductivity inside of a high conductivity shell layer (Elahi, Lu et al. 2013).

2.2 Intrinsically conductive polymers (ICPs)

Conducting polymers are a unique class of materials which structurally resemble organic insulating polymers but are actually semiconductors or conductors. Most conducting polymers such as polyacetylene, polypyrrole, polyaniline and polythiophene require a change in oxidation state to be converted into their conducting forms. Polyacetylene, possibly the most conducting of these polymers, has conductivities reported above 10^5 S/cm, however, it degrades upon exposure to air. Polythiophene and polypyrrole are difficult to process even with very polar organic solvents due to strong inter-chain attractions.

2.2.1 Polyaniline (PANi)

Polyaniline (PANi) has been of significant interest due to its low cost, stability, increased processability, relative to other conduction polymers (Stenger-Smith 1998). The fact that it can be synthesized to obtain thin or thick films, nanoparticles, composites and even can be drawn into nanofibers of diameters of a few nanometers gives it a distinct edge over a lot of other materials.

The monomer aniline was first synthesized in 1862 (Letheby 1862). The polymeric oxidation products of aniline were commonly refereed to as ``aniline black" and were widely used in the

textile industries for dyeing and also heat resistant in paints (Stenger-Smith 1998). The base structure of polyaniline, as shown in Figure 2-5, consists of a reduced unit or benzenoid attached to an amine (-NH-), and an oxidized unit or quinoid attached to an imine (-N=). The amines and imines are the nitrogenous centers of polyaniline which may react with dopant agents and/or analyte and the ratio of amines to imines dictates the oxidation state. Polyaniline exists in several oxidized forms. The most studied and widely accepted are the leucoemeraldine which is the fully reduced form, y = 1 in Figure 2-5, the emeraldine form which is half oxidized, half reduced, y = 0.5, and the pernigraniline form which is the fully oxidized form, y = 0 (Haynes 2008).

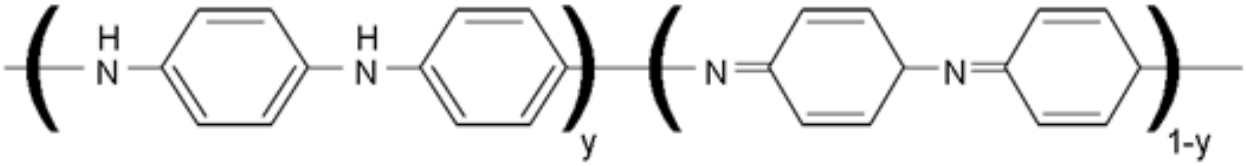

Figure 2-5: Base structure of polyaniline for y=1 the oxidation state is leucoemeraldine, for y=0 the polymer is in the pernigraniline oxidation state and for y=0.5 the polymer is in the emeraldine oxidation state (image is reproduced from reference (Haynes 2008).

Polyaniline has been known for 150 years, however it was after the discovery of its conducting properties that research area in this area has increased tremendously. Polyaniline is environmentally stable, easy to synthesize and can be reversibly transformed from conduction to insulation from using acid-base reactions (Syed and Dinesan 1991). It has advantages over other conducting polymers in that it can be transformed from one oxidation state to another by simply oxidation/reduction chemistry. Thus, polyaniline has found increasing applications in the area of sensors, field effect transistors, rechargeable batteries, capacitors, electronic devices, etc. (Skotheim, Elsenbaumer et al. 1998, Wessling 1998). All the three oxidation states of polyaniline mentioned above exist in two forms, salt form (doped state) and base from (undoped state) and of

these oxidation states only the emeraldine salt form is conductor and the rest are insulators (Kolla, Surwade et al. 2005).

2.3 Carbon nanofibers

2.3.1 Introduction

Energy is one of the top global issues facing the world for the next 50 years and nanotechnology is providing a platform to solve this challenge by fabricating nanofibers optimized for energy storage applications. Supercapacitors (Zhang and Zhao 2009) and lithium ion batteries (LIBs) (Bruce, Scrosati et al. 2008) are at the frontier of this efforts, and currently they are powering numerous portable consumer electronic devices from wearable smart-devices to laptops. In 1879, Thomas Edison prepared first carbon fiber (CF) by carbonization of cotton and bamboo which was subsequently used as the filament of a light bulb. CFs has developed tremendously scientific research and applications (Lu, Zu et al. 2012). Carbon nanofibers (CNFs) have been applied as promising materials in many fields but mainly as energy conversion and storage (Wangxi, Jie et al. 2003, Feng, Xie et al. 2014). There are some differences between CFs and CNFs. First, CFs have diameters in the range of several micrometers, whereas, CNFs have diameters of 50-200 nm. Second, as Figure 2-6 illustrates the structure of CF and CNF is different (Feng, Xie et al. 2014). The CNFs can be mainly fabricated by catalytic vapor deposition growth (Tibbetts, Lake et al. 2007) (Rodriguez 1993) and electrospinning. CNFs are normally produced from three polymeric precursors: polyacrylonitrile (PAN), cellulose, and pitch (Zhang, Aboagye et al. 2014).

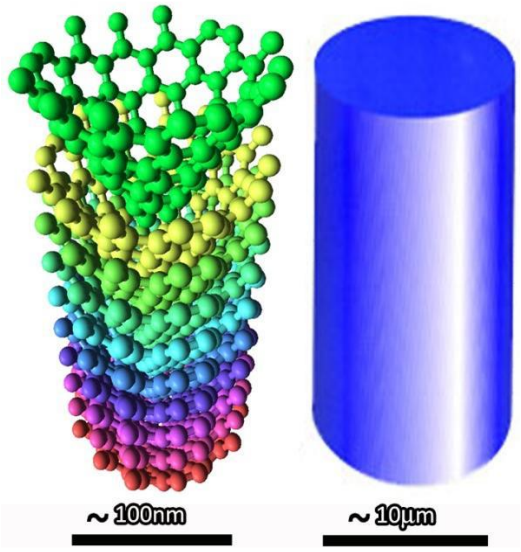

Figure 2-6: Schematic illustration of the difference between CF (~100nm) and CNF (~10 nm). Image is adapted from reference (Feng, Xie et al. 2014).

However, PAN is the one that received most attention due to its high carbon yield and superior mechanical properties of the resultant carbon fibers and currently 90 % of CNFs manufactured are PAN-based (Rahaman, Ismail et al. 2007). In the following section preparation of PAN-based CNFs by electrospinning is discussed.

2.3.2 Preparation of CNFs by electrospinning

Electrospinning is a widely used method to prepare CNFs (Zhang, Aboagye et al. 2014) and extensive researches have been conducted on electrospinning of PAN-based CNFs (Qin, Wan et al. 2004, Kalayci, Patra et al. 2005, Lifeng and You-Lo 2006). To fabricate the PAN-based CNFs by the electrospinning, PAN nanofibers should be prepared as the precursors of the CNFs. The properties of the final CNFs are governed by the polymer solution and the processing parameters. Once the PAN nanofibers are prepared, heat treatment will be performed on the nanofibers (Zhang,

Aboagye et al. 2014). The heat treatment consist of two-steps: stabilization and carbonization under an inert atmosphere to carbonize the CNFs (Feng, Xie et al. 2014). Various conditions for stabilization and carbonization process is reported in the literature. Stabilization is usually carried out in air at temperature between 200 °C to 300 °C and carbonization is conducted in an inert atmosphere from 800 °C to 2800 °C (Wang, Serrano et al. 2003, Hou, Ge et al. 2005, Zussman, Chen et al. 2005, Kim, Yang et al. 2006, Wu, Wang et al. 2012). The heat treatment parameters such as atmosphere and temperature plays an important role on the morphology, purity, diameters and porosity (Zhang, Aboagye et al. 2014). For energy storage applications, such as supercapacitors or Li-ion batteries, controlling the pore structure of the CNFs is the most important factor. This is because the transport performance of the ions in the electrolyte is largely dependent on the pore structure of CNFs electrode material (Feng, Xie et al. 2014).

2.3.3 PAN-based carbon nanofibers application in supercapacitors

Supercapacitors also known as, electric double layer capacitors (EDLCs), have recently received a lot of attention due to their a high energy density and providing better power density than batteries (Zhang, Aboagye et al. 2014). One of the common methods to make CNFs is by embedding other components in the PAN electrospinning solution followed by electrospinning, stabilization and carbonization. As reported in the literature, the presence of Si-containing compounds such as phenylsilane (PS) (Kim, Yang et al. 2011), tetraethyl orthosilicate (TEOS) (Kim, Yang et al. 2011), and polymethylhydrosiloxane (PMHS) (Kim, Yang et al. 2011) in the electrospun PAN nanofibers will create micropores on the surface of CNFs after the carbonization process and the final CNFs can possess surface areas up to 1200 m^2/g. Thus, due to increased surface area these CNFs exhibited much higher specific capacitance than the neat CNFs. In another study, vanadium pentoxide (V_2O_5) were added to the electrospinning solution of PAN (Kim, Kim et al. 2012). It was shown that CNFs

obtained from this system 150 F g^{-1} and energy density of 18.8 W h kg^{-1}. Also, the addition of boric acid (H_3BO_3) and urea were investigated in the PAN electrospinning solution (Kim, Seung Yang et al. 2013). The electrodes fabricated from these setups exhibited higher specific capacitance (180 F g^{-1}) due introduction of boron and nitrogen functional groups in CNFs and the increase in the surface area. Graphene-integrated CNFs were prepared by dispersing graphene in PAN/PMMA (Kim, Yang et al. 2012) or PAN/TEOS (Kim, Kim et al. 2012) electrospinning solutions. The CNFs made from these systems exhibited hierarchical pore structures with ultramicropores and mesopores were introduced and the CNFs exhibited specific capacitance up to 150 F g^{-1} while the neat CNFs values were only 60 F g^{-1}. Moreover, PAN crystallinity in has been reported to be unfavorable during the stabilization process of CNFs. To reduce PAN crystallinity of PAN, 9 % vinylimidazole was added to the PAN molecules through co-polymerization (Jung, Deng et al. 2012). The CNFs reached a high surface area of 1120 m^2/g and exhibited specific capacitances up to 122 F g^{-1} .

2.4 Graphene

In the past 20 years the field of nanoscience has blossomed. Polymer nanocomposite based on carbon black, carbon nanotubes and layered silicates have been extensively studied for the improvement of mechanical, thermal, electrical and gas barrier properties of polymers (Huang 2002, Moniruzzaman and Winey 2006). The discovery of graphene with its combination of extraordinary physical properties (high values of its Young's modulus ~ 1,100 GPa) (Lee, Wei et al. 2008), fracture strength (130 GPa) (Lee, Wei et al. 2008), thermal conductivity (~ 5,000 W m^{-1} K^{-1} (Balandin, Ghosh et al. 2008), mobility of charge carriers (200,000 cm^2 V^{-1} s^{-1}) (Bolotin, Sikes

et al. 2008) and specific surface area (calculated value, 2,630 $m^2 g^{-1}$) (Stoller, Park et al. 2008) and ability to be dispersed in various polymer matrices has created a new class of polymer nanocomposites (Kuilla, Bhadra et al. 2010). Therefore, graphene and graphene based nanocomposites play a key role in the future of nanoscience (Stankovich, Dikin et al. 2006). The promising mechanical, electrical, optical, thermal and magnetic properties of graphene have led to the creation of a new subfield of nanoscience that studies graphene based polymer nanocomposites.

2.4.1 Discovery of Graphene

In 1940, it was established by Wallace that graphene is the building block for graphite (Wallace 1947). In 2004, Geim et al. identified single layers of graphene and other 2-D crystals (Novoselov, Geim et al. 2004). Graphene is an atomically thick, two dimensional sheet composed of sp^2 carbon atoms arranged in a honeycomb crystal lattice (Kim, Abdala et al. 2010). It is the basic structural unit for carbon allotropes such as graphite, carbon nanotubes and fullerenes (Figure Figure 2-7). For instance, graphite (3-D carbon allotrope) is made of graphene sheets stacked on top of each other and separated by 3.37 Å. The fullerenes which are a dimensionless carbon allotrope is made by wrapping the graphene sheets. Moreover, it is possible to roll the graphene sheets to make the 1-D carbon nanotubes.

One-carbon-atom thick graphene can be a very promising reinforcement, providing combined benefits of both layered silicates and carbon nanotubes. Unlike layered silicates, it has exceptional electrical and thermal transport properties (Smith and Rasor 1956, Novoselov, Geim et al. 2004). Unlike carbon nanotubes (CNT), these 2-dimensional carbon layers can reduce gas permeability of host membranes (Kim and Macosko 2008), and can be derived from naturally occurring graphite at a fraction of cost. Moreover, its in-plane mechanical properties are similar to those of CNT

(Young's modulus ~1 TPa, ultimate strength ~130 GPa) (Kelly 1981). The potentially high aspect ratio of single graphene sheets indicates that graphene can greatly improve mechanical and gas barrier properties at small incorporation if it is well exfoliated in a polymer matrix.

2.4.2 Synthesis of Graphene

The first reported method for production of graphene nanosheets can be traced back to 1970 (Eizenberg and Blakely 1979). However, it was only until 2004 that the isolation of free-standing single-layer graphene was achieved by separation of graphene from graphite using micro-mechanical cleavage (Novoselov, Geim et al. 2004). Today, graphene can be prepared either by bottom-up processes or by top-down processes. In bottom-up processes, graphene is synthesized by methods such as chemical vapor deposition (CVD) (Di, Wei et al. 2008, Chae, Güneş et al. 2009, Li, Cai et al. 2009, Wang, You et al. 2009), arc discharge (Li, Wang et al. 2010), epitaxial growth on SiC (Rollings, Gweon et al. 2006, de Heer, Berger et al. 2007, Mattausch and Pankratov 2008, Sutter, Flege et al. 2008, Sprinkle, Soukiassian et al. 2009), chemical conversion (Carissan and Klopper 2006, Yang, Dou et al. 2008, Zhi and Mullen 2008), reduction of carbon monoxide (CO) (Kim, Min et al. 2009), unzipping carbon nanotubes (Hirsch 2009, Jiao, Zhang et al. 2009, Kosynkin, Higginbotham et al. 2009), and self-assembly of surfactants (Zhang, Cui et al. 2009). The CVD and epitaxial growth methods, produce a small amount of large-size, defect free graphene sheets (Kim, Kim et al. 2012). Therefore, these methods are more suited for fundamental studies and electronic application than fabrication of polymer nanocomposites since in fabrication of nanocomposites, a large amount of graphene sheets is required. In top-down processes, graphene or modified graphene sheets are produced by separation/exfoliation of graphene or graphite derivatives (such as graphite oxide (GO) and graphite fluoride (Worsley, Ramesh et al. 2007) with methods such as mechanical cleavage, direct sonication, superacid dissolution (Figure 2-8).

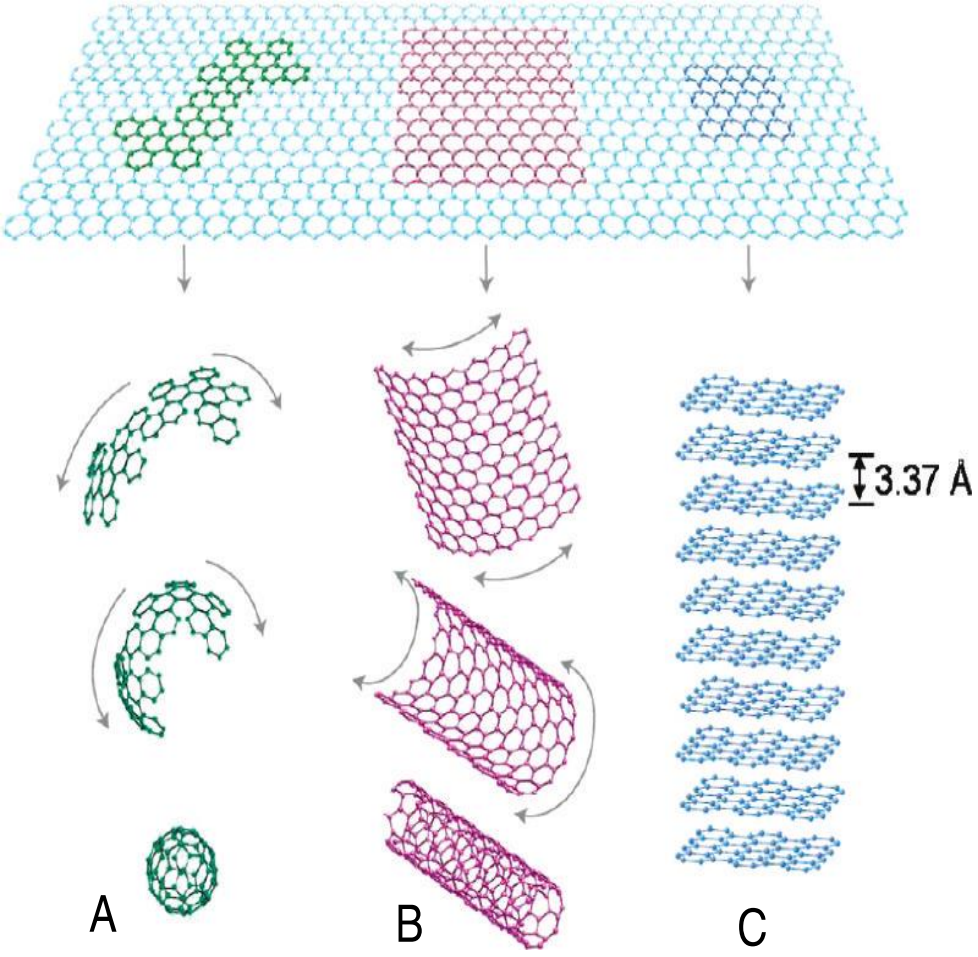

Figure 2-7: Graphene is the building block of all graphitic forms. It can be wrapped to form (A) the 0-D fullerene, rolled to form (B) the 1-D nanotubes, and stacked to form (C) the 3-D graphite. The figure is reproduced from the reference (Kim, Abdala et al. 2010).

These methods are more suited for large scale production than the bottom-up processes and therefore they can be used for polymer nanocomposites. The most common top-down methods will be discussed in the following section.

2.4.2.1 Micromechanical exfoliation

Micromechanical exfoliation was the start of the interest in graphene. This method led to the first isolation of graphene by Geim et al. in 2004 (Novoselov, Geim et al. 2004). In order to exfoliate a single sheet of graphene, van der Waals attraction between the first and second layers of graphite should be overcome without disturbing any subsequent sheets.

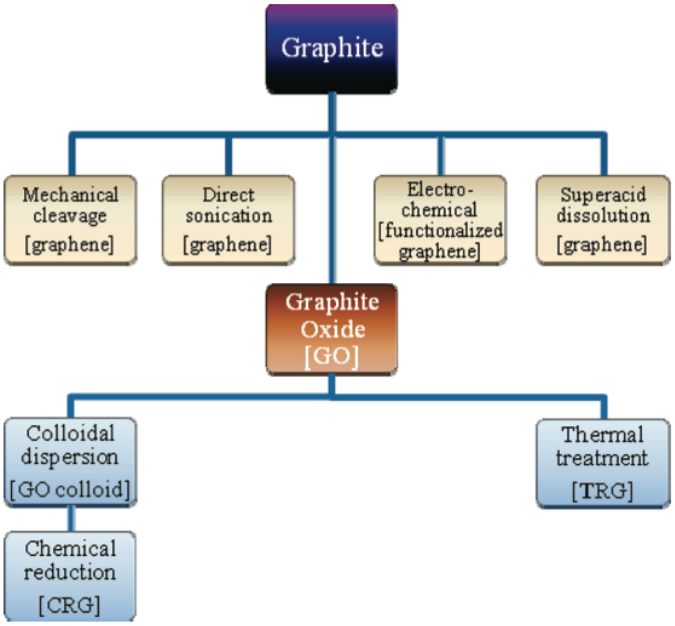

Figure 2-8: Top-down methods for production of graphene and modified graphene starting from graphite or via graphite oxide (GO) (image is reproduced from reference (Kim, Abdala et al. 2010)).

Utilizing this method, sheets with large size and high quality can be produced but in very limited quantities. This is due to the extremely low output of this process (several hours to produce a single sheet of graphene). Thus, it is more suitable for fundamental studies or electronic applications. The process to exfoliate graphite involves repeated peeling of a graphite block or highly oriented

pyrolytic graphite (HOPG) using an adhesive tape until a single layer of graphene is produced. This process is illustrated in Figure 2-9.

2.4.2.2 Chemical Exfoliation of Graphite

Deriving graphene from graphite was regarded nearly impossible for decades, however; recently developed strategies have paved a way for polymer nanocomposites reinforced with graphene. As discussed in the section 2.4.2, Geim et al. first demonstrated free-standing single layer carbons from repeated mechanical cleavages of graphite with Scotch tapes (Novoselov, Geim et al. 2004). However, this technique is less effective for large-scale manufacturing and chemical approach is more practical. The common approach for chemical exfoliation of graphite is to use strong acids and oxidizing agents to produce intermediary graphite oxide (GO).

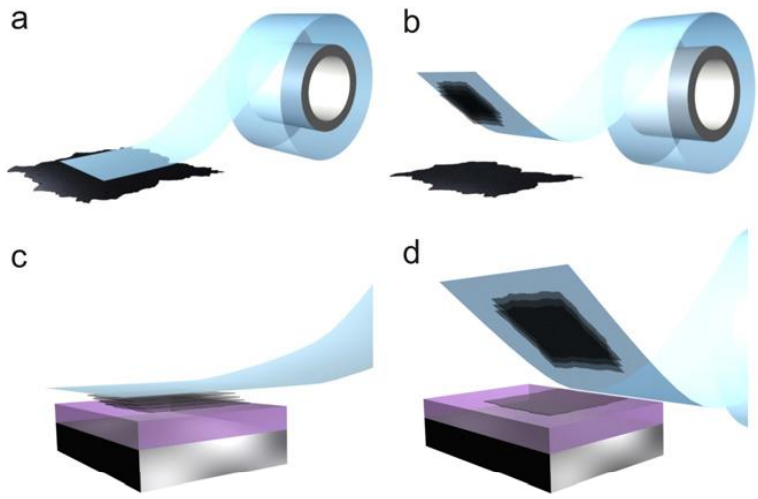

Figure 2-9: Micromechanical exfoliation of graphene. (a and b) Adhesive tape is pressed against graphite flakes so that the top few layers are attached to the tape (c) The tape with graphite sheets is pressed against a surface of choice. (d) by peeling off the tape, the bottom layer of graphene is left on the substrate (image is reproduced from reference (Novoselov and Neto 2012)).

The GO is layered stack of sheets with AB stacking which can be converted to reduced graphene oxide (RGO) upon sonication and subsequent reduction of the GO sheets. GO can be reduced into RGO by utilizing various reagents such as hydrazine hydrate (Novoselov, Geim et al. 2005), sodium hydrosulfite (Zhou, Chen et al. 2010), sodium borohydride (Shin, Kim et al. 2009), ascorbic aicd (Zhang, Yang et al. 2010) or thermal treatment (Zhu, Murali et al. 2010, Galal, Atta et al. 2012).

Schematic representation of chemical exfoliation of graphite is illustrated in Figure 2-10. Another chemical exfoliation technique for production of graphene is via sonication in the presence of polyvinylpyrrolidone or N-methylpyrrolidone which can produce single-layer or multiple-layer graphene (Hernandez, Nicolosi et al. 2008, Bourlinos, Georgakilas et al. 2009). If the challenge of separating exfoliated graphene sheets from the graphite is overcome, this method can be a viable option for production of large quantities of single and multiple layer graphene which can be utilized for nanocomposite fabrication (Kim, Abdala et al. 2010). Also, dissolution of graphite in a super acid can be used to exfoliate graphite and produce single and multiple layer graphene but the hazardous nature of super acids and the high cost of its removal can limit its potential (Behabtu, Lomeda et al. 2010).

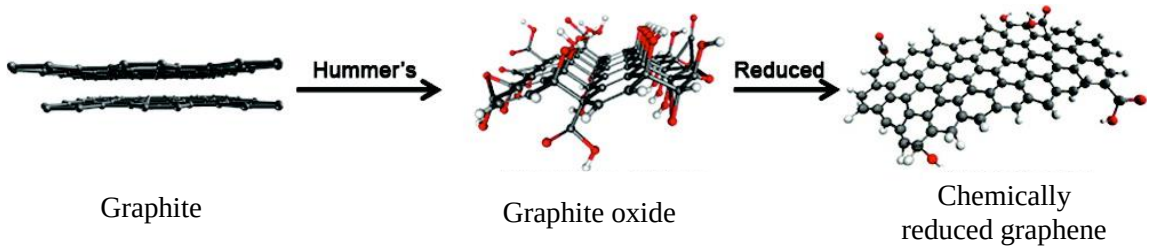

Figure 2-10: Schematic illustration of conversion of graphite to graphite oxide (GO) using Hummer's method and reduction of GO to graphene (image is reproduced from reference (Tung, Allen et al. 2009)).

2.4.2.2.1 Synthesis of Graphite Oxide

Graphite oxide (GO) was first synthesized in 1859 by British chemist Brodie by repeated treatment of ceylon graphite with an oxidation mixture consisting of potassium chlorate and fuming nitric acid (Brodie 1859). Later, Staudenmaier (Staudenmaier 1898) and Hummers (Hummers and Offeman 1958) had also developed different variation of this method to fabricate GO. In all of these three methods strong acids such as H_2SO_4, H_3PO_4 or HNO_3 and oxidants such as $KMnO_4$, $KClO_3$ and $NaNO_2$ is used to oxidize graphite (Park and Ruoff 2009). Recently Tour et al. have developed an improved method by utilizing 9:1 mixture of H_2SO_4:H_3PO_4 to improve the efficiency of the oxidation process and their method did not produce any toxic gas or a large exothereme (Marcano, Kosynkin et al. 2010). Also, by employing Tour et al. method a higher percentage of graphites are oxidized. The resultant graphite oxide (GO) made by any of the mentioned method is composed of graphene oxide sheets stacked on each other. Currently, the most promising method for production of large quantities of graphene are based on exfoliation of GO. This method is considered to be the perspective source for cheap graphene. Extensive studies have been done in order to understand the chemical structure of graphite oxide and several models are still being debated in the literature (Park and Ruoff 2009). However, the Lerf-Klinowski model is believed to be the most accurate description of GO structure (He, Klinowski et al. 1998, Lerf, He et al. 1998). This model is depicted in Figure 2-11. It describes GO as built of pristine aromatic ``island'' separated from each other by aliphatic regions containing epoxide and hydroxyl groups and double bonds (Kim, Abdala et al. 2010). Like graphite which is composed of stacks of graphene sheets with interlaying spacing of 3.37 Å, GO is composed of graphene oxide sheets stacked on top of each other with interlaying spacing of 6 to 10 Å, which depends on its water content (Kim, Abdala et al. 2010).

GO can be easily dispersed in water (Stankovich, Dikin et al. 2006) and in organic solvents after chemical modification. However, GO is electronically insulating due to presence of the oxygen functional groups in its structure and thermally unstable (undergoes pyrolysis at elevated temperatures). It has been demonstrated that by reduction of GO to graphene it is possible to restore its electrical conductivity and presumably its thermal stability (Stankovich, Dikin et al. 2007).

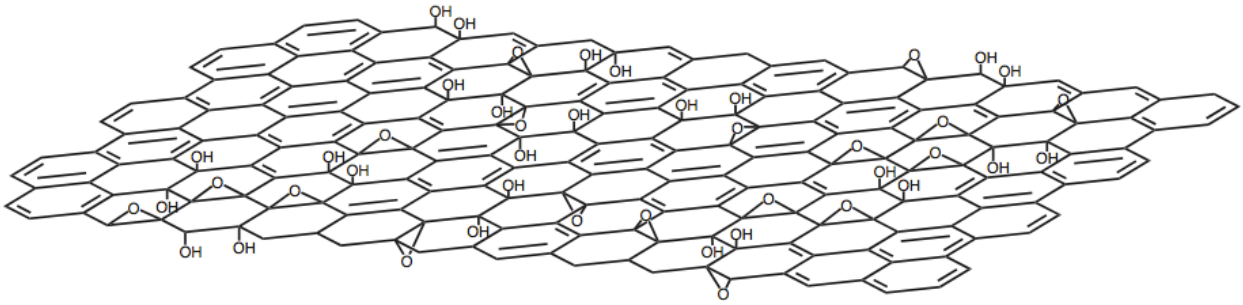

Figure 2-11: Chemical structure of graphite oxide consisting of aromatic islands seperated by aliphatic regions containing oxygen bonded carbons as described by Lerf-Kilnowski model. This figure is reproduced from the reference (He, Klinowski et al. 1998).

2.4.2.2.2 Chemical Reduction of Graphite Oxide to Graphene

In chemical reduction of GO, dispersed GO in water is sonicated to produced stable colloidal dispersion of graphene oxide. Thereafter, the colloidal of graphene oxide can be chemically reduced to graphene using reagents such as hydrazine hydrate (Novoselov, Geim et al. 2005), sodium borohydride (Shin, Kim et al. 2009) ascorbic acid (Zhang, Yang et al. 2010) and etc. The chemical reduction of graphite oxide provides an efficient route for production of graphene, however most of the regents used for this process are hazardous and expensive which limits its application. Recently, Fu et al. proposed a non-toxic, efficient method which was inspired by

reducing agent used in textile industry (sodium hydrosulfite) due to similarity of GO structure with the vat dye (both have aromatic benzene rings covalently attached with oxygen functional groups) (Zhou, Chen et al. 2010). The advantages of using this reagent compared to other reducing reagents are: i) it is a simple and efficient method. ii) the by-product Na_2SO_3) can be easily removed by water, with no accompanying side-effect on the resultant graphene and its composites. iii) the reducing process is a very fast (takes only few minutes) compared to other reducing methods.

2.4.3 Properties of Graphene

In the following sections, properties of graphene which are significant for this research are discussed.

2.4.3.1 Structure of Graphene

Dimensionality is one of the most defining material parameters. Carbon exists in various structural forms such as zero-dimensional Buckminster fullerene discovered by Kroto et al. in 1985 (Kroto, Heath et al. 1985), 1D carbon nanotubes discovered in 1991, 2D graphene isolated by Geim et al. in 2004 and 3D graphite. Graphene is an allotrope of carbon with sp^2 carbon atoms which are packed in honeycomb crystal structure. A carbon atom has six electrons in the atomic orbitals as $1s^2\ 2s^2\ 2p^2$ (Figure 2-12). The 1s electrons are considered inert and do not contribute to the chemical bond (Peres 2009). In the graphene structure, three atomic orbitals 2s, $2p_x$ and $2p_y$ hybridize to form three new planar orbitals known as sp^2 (Park 2009). The sp^2 hybridizations form σ bonds between the adjacent carbon atoms and show high-energy gap of 14.26 eV. These bonds have an angle of 120° between them which are responsible for the hexagonal lattice structure of graphene as illustrated in Figure 2-13.

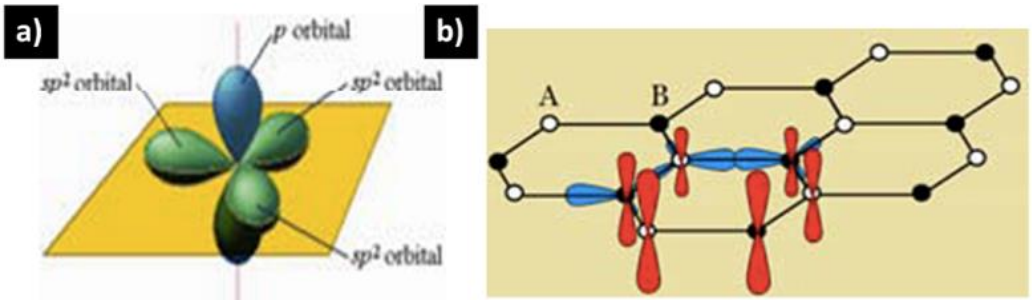

Figure 2-12: (a) Electron orbitals in graphite. (b) Electron orbital of graphene: sp^2 hybridized orbital responsible for the bonding on x-y plan; 2p orbital perpendicular to the x-y plan, image adapted from reference (Yang).

These sp^2 hybridization orbitals closely pack the carbons on the x-y plane, but do not contribute to the electronic transport. The remaining 2p orbital takes place in p_z states which form π bonds out of the plane of graphene.

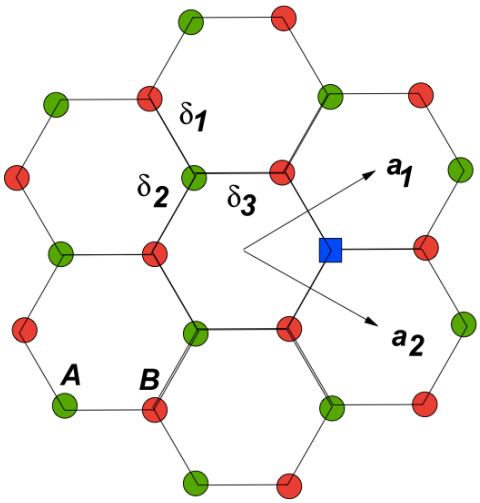

Figure 2-13: Schematic illustration of honeycomb lattice of graphene. a_1 and a_2 are the lattice unit vectors and δ_i =1, 2, 3 are the nearest-neighbor vectors (image adapted from reference (Peres 2009)).

Therefore, in a finite graphene sheet p_z electrons are contributing one conducting electron per carbon and responsible for the week van der Waals force between graphene layers in graphite (Johnston 1955).

2.4.3.2 Chemical Properties

Graphene exhibits unique chemical properties which are mostly due to its sp^2 bonded hybridization and its ultimate incarnation of the surface (two faces with no bulk left in between) (Geim 2009). The surface of graphene, like graphite, can adsorb and desorb various atoms and molecules such as NO_2, NH_3, K and OH. These attached adsorbates can act as donors or acceptors and lead to changes in the carrier concentration so that graphene remains highly conductive. These give an excellent basis for graphene sensing abilities. The operational principle of graphene for sensing is based on changes in their electrical conductivity σ due to gas molecules adsorbed on graphene's surface and acting as donors or acceptors (Schedin, Geim et al. 2007).

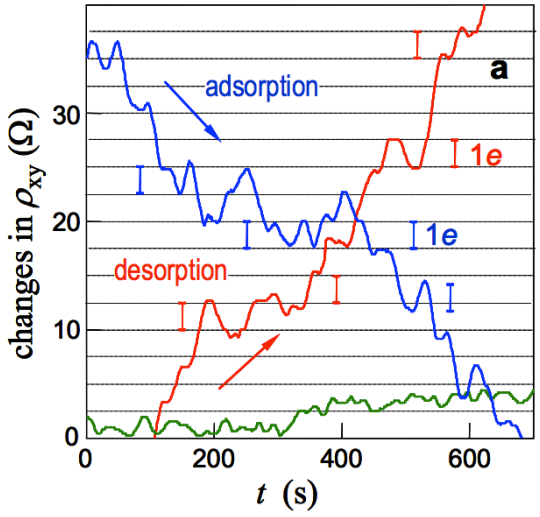

Figure 2-14: Blue curve illustrates the step-by-step decrease in the Hall resistivity upon adsorption of strongly diluted NO_2 and a red curve demonstrates the step-by-step increase upon its desorption. The green curve is the control, which is exposed to pure He. (image is reproduced from reference (Schedin, Geim et al. 2007)).

The characteristics of graphene that makes it ideal for sensing includes: i) it is a two-dimensional material and therefore its whole volume is exposed to surface adsorbates ii) it is highly conductive (exhibiting metallic conductivity) iii) it has a few crystal defects which leads to low intrinsic noise. Schedin et al. demonstrated the sensing abilities of graphene for detection of individual gas molecules such as adsorbed on graphene. As demonstrated in Figure 2-14 various gas molecules such as NO_2 and NH_3 on pristine graphene was successfully detected and lead to step-by-step modulation of local carrier concentration resulting in step-like changes in electrical resistance.

2.4.3.3 Mechanical Properties

Graphene exhibits unusual toughness among materials found in the universe. A lot of studies were conducted on mechanical properties of graphene, however most of these studies did not definitively measure the intrinsic strength of this material due to problems such as inevitable presence of defects, grain boundaries in macroscopic samples, uncertainty in the sample geometry and stress concentration at clamping points (Krishnan 1998) (Salvetat 1999). It was with recent experimental advancements which allowed Lee et al. to study mechanical properties of single sheet of graphene using atomic force microscopy (AFM) nano-indentation (Lee, Wei et al. 2008). The schematic representation of this process is illustrated in Figure 2-15. The authors reported that for a defect free sheet of monolayer graphene Young's modulus (E) is ~1 TPa and the intrinsic breaking strength is ~130 GPa (compared to 1.86 GPa for steel and 2.8 GPa for diamond), suggesting the strongest material ever measured (Lee, Wei et al. 2008). As a comparison, Figure 2-16 compiles the Young's modulus and densities of various materials. Graphene is a 2D material and therefore its behavior under tensile loading is properly described by a 2D stress σ^{2D} and elastic constant E^{2D} and D^{2D} with units of force/length.

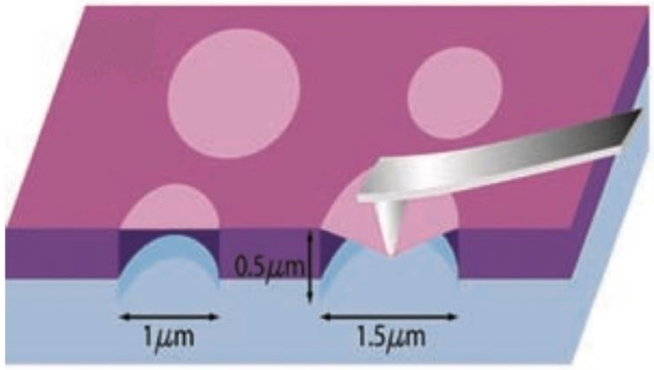

Figure 2-15: Schematic illustration showing nano-indentation of graphene suspended over a hole using AFM cantilever for determination of its mechanical properties (image is adapted from reference (Lee, Wei et al. 2008)).

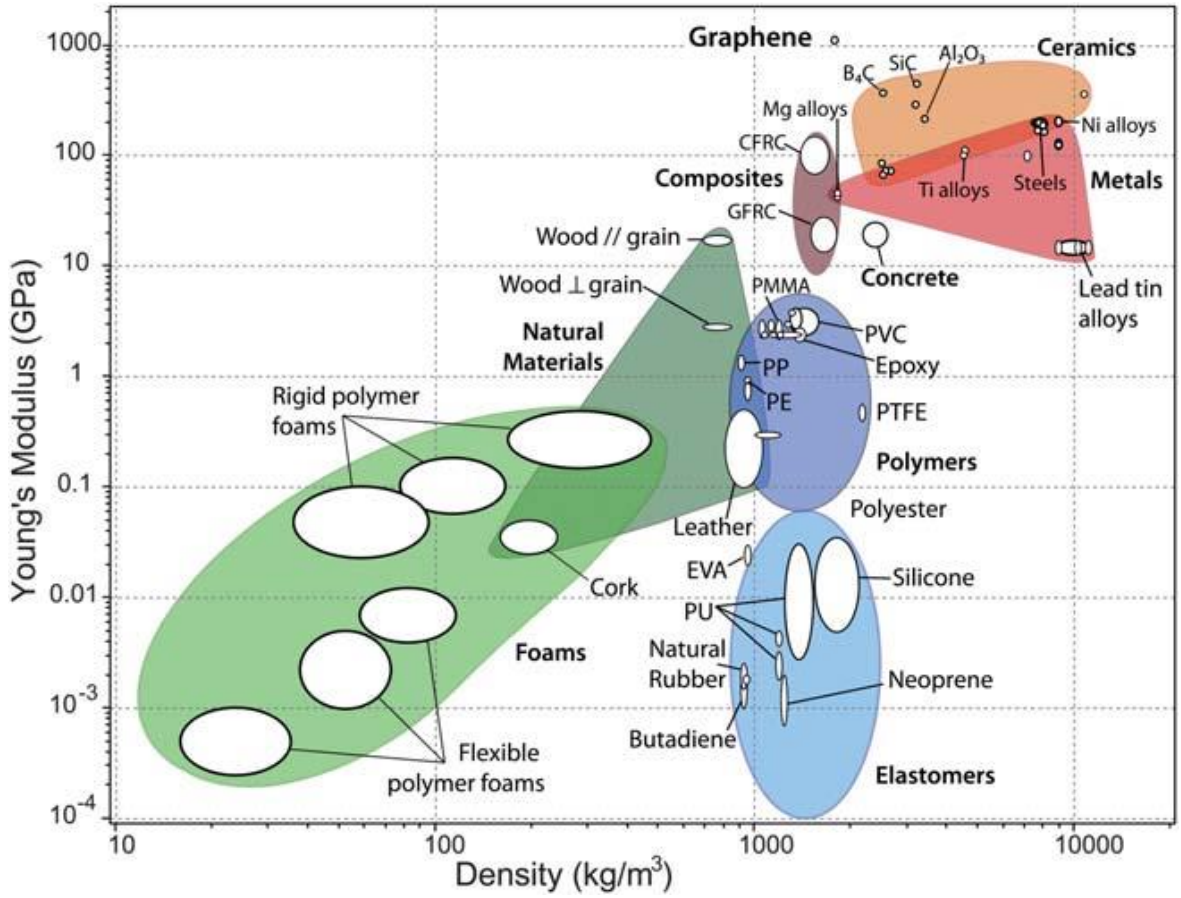

Figure 2-16: Chart of Young's modulus as a function of density comparing graphene properties to more traditional materials. Graphene density was taken as 2200 kg m^{-3} (image is adapted from reference (Verdejo, Bernal et al. 2011)).

The maximum stress at central point of graphene can be described by Equation 2-3 where σ^{2D} is the maximum stress at the central point of graphene, R is the indenter tip radi, E is the Young's modulus and F can be described by Equation 2-4 where a is radius of graphene membrane, δ is the deflection at center point of graphene, σ_0^{2D} is pre-tension in the film, q is given by Equation 2-5 with the Poisson's ratio γ being 0.165 for graphite in basal plane.

$$\sigma = \left(\frac{FE^{2D}}{4\pi R}\right)^{\frac{1}{2}} \quad 2\text{-}3$$

$$F = \sigma_0^{2D}(\pi a)\left(\frac{\delta}{a}\right) + E^{2D}(q^3 a)\left(\frac{\delta}{a}\right)^3 \quad 2\text{-}4$$

$$q = \frac{1}{1.049 - 0.15\gamma - 0.16\gamma^2} \quad 2\text{-}5$$

2.5 Graphene-based Polymer Nanocomposites

Graphene has opened new pathways for developing a wide range of novel functional materials (Park and Ruoff 2009). To take full advantage of its properties, integration of individual graphene sheets in polymer matrices to form advanced multi-functional composites is of the most promising routes. This is because polymer composites usually have exceptional specific modulus, specific strength, and wide application in many industries. Polymer composites can be easily processed and fabricated into intricately shaped components with excellent preservation of the structure and properties of graphene using conventional processing methods, which is very important to make full use of the outstanding properties of graphene. Although significant advances have been made in the use of carbon nanotubes as reinforcements of polymer matrices, there are still unresolved

issues such as the tendency of nanotubes to agglomerate during processing, the limited availability of high-quality nanotubes in large quantities and the high cost of their production (Stankovich, Dikin et al. 2006). Hence, graphene sheets provide an alternative option to produce functional nanocomposites. The following advantages of graphene over CNTs as a filler in polymer matrices have been reported: (i) graphene has a higher surface-to-volume ratio than CNTs because of the inaccessibility of the inner nanotube surface to polymer molecules (Stankovich, Dikin et al. 2006) which makes graphene potentially more favorable for altering matrix properties. (ii) The flat surface of graphene minimizes the geometric contribution to thermal interface resistance (Yu, Ramesh et al. 2007), and plane-to-plane contacts minimize the contact electrical resistance between graphene. (iii) The wrinkled nature together with the high surface area of graphene leads to stronger interfacial interactions with polymer matrices and thus has a substantially larger influence on the properties of the host polymers (Ramanathan, Abdala et al. 2008). (iv) The low cost of GO and chemically reduced graphene oxide that can be fabricated from a cheap precursor material, graphite (Du and Cheng 2012). These will make graphene potentially more favorable for improving the properties of polymer matrices and therefore, graphene-based polymer nanocomposites (GNPC) have attracted both academic and industrial interest. Polymers such as epoxy, polystyrene (PS), polypropylene (PP), polyethylene (PE), polycarbonate (PC), polyimide (PI), and poly(vinyl alcohol) (PVA) have been widly used as a matrix of GPNCs (Teng, Ma et al. 2011) (Wang, Hu et al. 2011) (Zhao, Zhang et al. 2011) (Shen, Zhai et al. 2011) (Yun, Bae et al. 2011) (Kuila, Bose et al. 2011) (Yoonessi and Gaier 2010). In these studies the mechanical, electrical, thermal properties of GNPCs have been extensively investigated and some results have been compared with CNT/polymer composites. The properties reported in literature are scattered and even lower than for CNT/polymer composites in some instances. This can be explained by delicate nature of the incorporation of graphene in polymer matrices and the fact that factors such as the type of graphene

used, its interfacial tension, morphological organization, fine interface control, uniform dispersion can affect the performance of the resulting composites (Schadler, Kumar et al. 2007). These challenges are discussed in more details in the next section. In spite of this, it is expected that with rapid development of the fabrication techniques for graphene and GPNCs and functionalization of graphene, these issues are being progressively overcome (Du and Cheng 2012) and GNPCs can have a universal application in many fields.

2.5.1 Fabrication of Graphene/Polymer Nanocomposites

The graphene that is mostly used for fabrication of GPNCs is the chemically reduced graphene (CRGO) or thermally reduced graphene (TRGO) and both are derived from graphene oxide (GO) due to its low cost and high-yield of production. These types of graphene can be dispersed in the polymeric matrix by using techniques such as solution mixing, melt blending, or in situ polymerization (Zhang, Zheng et al. 2010). The general fabrication routes of GNPCs using GO or its reduced from (RGO) as nanofillers are illustrated in Figure 2-17. Based on starting material, there are three main routes for fabrication of GNPCs. (i) taking GO as the starting material, it can be either melt blended in polymer matrix and after curing and/or polymerization GNPC is obtained or (ii) in situ chemical or thermal reduction can be performed during the melt blending to fabricate CRGO or TRGO/polymer composites. (iii) Another route is by starting from CRGO or TRGO and then melt blending it with polymer matrix fabricate CRGO or TRGO/polymer composites. These routes depend on polarity, molecular weight, hydrophobicity, reactive groups, etc. present in the polymer, graphene and solvent. The mechanisms required for dispersion of graphene and its derivatives in polymeric matrix are discussed below.

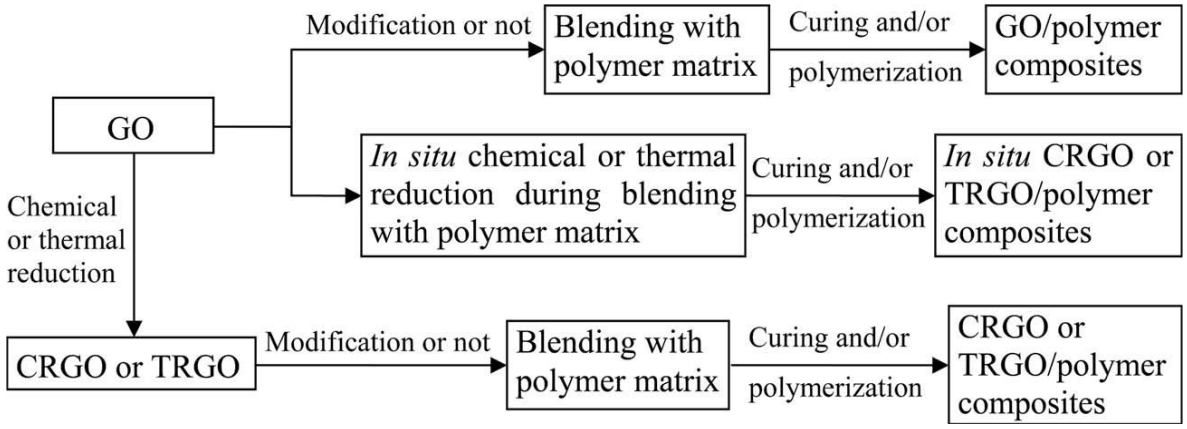

Figure 2-17: The general fabrication routes for graphene-based polymer composites (GNPCs) with GO or RGO as fillers (image is adapted from reference (Du and Cheng 2012)).

2.5.1.1 Solution mixing

Solution mixing is the most straightforward method for preparation of polymer composites. The solvent compatibility of the polymer and the filler is critical in achieving good dispersity (Huang, Qi et al. 2012. In this system, a polymer or a pre-polymer and graphene layers are solubilized in a solvent {Kuilla, 2010 #272). If a suitable solvent is chosen, the graphene layers can be easily dispersed since the layers are stacked together by a weak force. The typical solvents for this process are water, acetone, chloroform, tetrahydrofuran (THF), dimethyl formamide (DMF) or toluene. After that the graphene sheets are delaminated, the polymer chains will be absorbed to them and by evaporating the solvent the sheets will reassemble and the polymer will be sandwiched between them and as a result of this the nanocomposite will be formed (Lee and Im 2007). Polymer nanocomposites based on polyethylene-grafted maleic anhydride poly(E-g-MA)/graphite (Hussain, Hojjati et al. 2006), poly(styrene) (Stankovich, Dikin et al. 2006), poly(vinyl alchohol) (PVA)/graphene (Liang, Huang et al. 2009), etc., have been made using this method. In this method

re-stacking, aggregation and folding of the graphene based nanosheets are unavoidable, which significantly reduce the specific surface area of the 2D fillers. To overcome this problem, surface functionalization of graphene-based fillers will be carried out.

2.5.1.2 Melt Blending

This method is a popular method for preparing thermoplastic nanocomposites (Kuilla, Bhadra et al. 2010). In this method high shear and high temperature is utilized to blend the filler and the matrix. Also, in contrast with solution intercalation, no solvent is required and graphene layers are mixed with a thermoplastic polymer matrix in molten state. The method that are used for mixing the two components together are conventional methods such as extrusion or injection molding (Kim, Inoue et al. 2006). After mixing, the polymer chains are intercalated or exfoliated to form the nanocomposite. The advantage that this technique has is that the polymers that are unsuitable for other techniques can be processed by using this technique. However, the high shear forces employed in melt intercalation can sometimes result in the breakage of the graphene nanosheets (Dasari, Yu et al. 2009). Polymer nanocomposites such as HDPE/exfoliate graphite (Kim, Abdala et al. 2010), PS/exfoliate graphite (Chen, Wu et al. 2003), PP/exfoliate graphite (Kalaitzidou, Fukushima et al. 2007), and PET/reduced graphite oxide (Zhang, Zheng et al. 2010) were successfully prepared by using melt blending.

2.5.1.3 In Situ Polymerization

In situ polymerization is another method that is used to prepare graphene-filled polymer composites. In this method, the graphene is immersed in a liquid monomer which cause the graphene to get swollen (Kuilla, Bhadra et al. 2010). Thereafter, a suitable initiator will be added

to the mixture and then a stimuli such as heat or radiation will be used to initiate the polymerization (Zheng, Lu et al. 2004). Using this method polymer nanocomposites such as poly(styrene)/graphene (Zheng, Lu et al. 2004), poly(methyl methacrylate)/exfoliated graphite (Ye, Meng et al. 2009), polyaniline (PANi)/graphene (Zhou, Wu et al. 2010) were fabricated. The advantages of this method is first, it provides a strong interaction between the incorporated particles and the polymer matrix, facilitating stress transfer. Second, it enables an outstanding and homogeneous dispersion. However, it is usually accompanied by a viscosity increase that hinders manipulation and loading fraction (Verdejo, Bernal et al. 2011).

2.5.2 Challenges in Fabrication of Graphene/Polymer Nanocomposites

Although graphene is promising filler for improvement of properties of polymers and has wide potentials in many fields, there are some challenges that should be overcome before its universal application for advanced composites can be realized. One of these challenges is the technical barriers involving structure control, dispersion of graphene in the matrix, interfacial interaction between graphene and matrix, and contact between individual graphene. The other challenge is the consistency in mass fabrication of graphene. At present, large quantities of graphene are prepared by the exfoliation of graphite but the synthesized CRGO or TRGO are not consistent in their structure, morphology, aspect ratio, layer number, surface characteristics, electrical conductivity, and mechanical properties as they depend on how the GO is exfoliated and reduced. Therefore, how to fabricate a large amount of high quality graphene with controlled structure and at low cost is still a challenge in mass fabrication of GPNCs. Furthermore, a good dispersion of graphene in polymers for advanced applications is also a fundamental challenge. The properties of GPNCs depend strongly on the distribution of graphene in the polymer matrices. The GO and RGO that

are used in GNPCs are flat sheets (unlike entangled bundles of CNTs), GO has abundant oxygen-containing functional groups, and RGO obtained by reduction also has some residual groups on the surface, which will increase the interlayer spacing and decrease the van der Waals interaction between the graphene. These effects can facilitate uniform dispersion and further functionalization of graphene in polymer matrices. However, restacking of the flat graphene sheets can occurs, making uniform dispersion of graphene difficult and thus decreasing the reinforcing effectiveness of graphene in GNPCs. Furthermore, the uniaxial alignment of graphene sheets in a polymer matrix has not been thoroughly investigated, this can be attributed to fact that control of the spatial distribution of two-dimensional graphene is more difficult than one-dimensional materials. Another challenge in the design of GNPCs is the difference in the surface chemistry of graphene and polymer matrices which can create difficulty in obtaining a strong interfacial interaction between graphene and polymers matrix which can be addressed by functionalization of graphene.

2.6 Summary and problem identification

Fabrication of conductive polymer nanocomposites for energy related applications are of great interest. Moreover, dispersing carbonaceous nanomaterials in a polymeric matrix for the purpose of development of products with improved properties have received great attention in recent years. Particularly, graphene due to its exceptional electrical and mechanical properties. However, as the literature review in this section highlighted, good dispersion of graphene in polymer nanocomposites is daunting and there are many challenges in the fabrication of graphene-based polymer nanofibers. Dispersion of graphene in the initial solution before electrospinning is one of

the most important factors for producing nanofibers that have good graphene dispersion and directly effects the performance of the final product. In addition, PANi is not electrospinnable, mainly due to its rigid backbone, low-molecular weights and poor solubility in common organic solvents. In summary, the combined usage of graphene and conductive electrospun fibers for energy related applications are very scarce as still there are great deal of complications in dispersion of graphene in the nanofibers and electrospinning of conductive polymers. The first part of this work aims to electrospin PANi nanofibers and with highly dispersed graphene nanosheets in the nanofibers.

As discussed in the literature review section, carbon nanofibers are very promising materials for energy storage solutions and in particular supercapacitors. However, their performance is very much dependent on the surface area of the final fibers and they fall short for applications where high energy density is required. The second part of this thesis aims to produce carbon nanofibers embedded with graphene to overcome these issues and investigate the effect of graphene on the properties of final nanofibers.

2.7 References

Balandin, A. A., S. Ghosh, W. Bao, I. Calizo, D. Teweldebrhan, F. Miao and C. N. Lau (2008). "Superior thermal conductivity of single-layer graphene." Nano Letters **8**(3): 902-907.

Baumgarten, P. K. (1971). "Electrostatic spinning of acrylic microfibers." Journal of Colloid and Interface Science **36**(1): 71--79.

Behabtu, N., J. R. Lomeda, M. J. Green, A. L. Higginbotham, A. Sinitskii, D. V. Kosynkin, D. Tsentalovich, A. N. G. Parra-Vasquez, J. Schmidt, E. Kesselman, Y. Cohen, Y. Talmon, J. M. Tour and M. Pasquali (2010). "Spontaneous high-concentration dispersions and liquid crystals of graphene." Nature Nano **5**(6): 406--411.

Bognitzki, M., W. Czado, T. Frese, A. Schaper, M. Hellwig, M. Steinhart, A. Greiner and J. H. Wendorff (2001). "Nanostructured fibers via electrospinning." Advanced Materials **13**(1): 70--72.

Bolotin, K. I., K. J. Sikes, Z. Jiang, M. Klima, G. Fudenberg, J. Hone, P. Kim and H. L. Stormer (2008). "Ultrahigh electron mobility in suspended graphene." Solid State Communications **146**(9–10): 351-355.

Bourlinos, A. B., V. Georgakilas, R. Zboril, T. A. Steriotis and A. K. Stubos (2009). "Liquid-phase exfoliation of graphite towards solubilized graphenes." Small **5**(16): 1841--1845.

Brodie, B. C. (1859). "On the atomic weight of graphite." Philosophical Transactions of the Royal Society of London **149**: 249-259.

Bruce, P. G., B. Scrosati and J.-M. Tarascon (2008). "Nanomaterials for rechargeable lithium batteries." Angewandte Chemie International Edition **47**(16): 2930-2946.

Carissan, Y. and W. Klopper (2006). "Growing graphene sheets from reactions with methyl radicals: A quantum chemical study." ChemPhysChem **7**(8): 1770--1778.

Chae, S. J., F. Güneş, K. K. Kim, E. S. Kim, G. H. Han, S. M. Kim, H.-J. Shin, S.-M. Yoon, J.-Y. Choi, M. H. Park, C. W. Yang, D. Pribat and Y. H. Lee (2009). "Synthesis of large-area graphene layers on poly-nickel substrate by chemical vapor deposition: Wrinkle formation." Advanced Materials **21**(22): 2328--2333.

Chen, G., C. Wu, W. Weng, D. Wu and W. Yan (2003). "Preparation of polystyrene/graphite nanosheet composite." Polymer **44**(6): 1781--1784.

Chen, S. J., G. C. Berry and D. J. Plazek (1995). "Moderately concentrated-solutions of polystyrene .6. Gel formation in carbon-disulfide." Macromolecules **28**(19): 6539--6550.

Dasari, A., Z.-Z. Yu and Y.-W. Mai (2009). "Electrically conductive and super-tough polyamide-based nanocomposites." Polymer **50**(16): 4112--4121.

de Heer, W. A., C. Berger, X. Wu, P. N. First, E. H. Conrad, X. Li, T. Li, M. Sprinkle, J. Hass, M. L. Sadowski, M. Potemski and G. Martinez (2007). "Epitaxial graphene." Exploring graphene Recent research advances **143**(1-2): 92--100.

Demczyk, B. G., Y. M. Wang, J. Cumings, M. Hetman, W. Han, A. Zettl and R. O. Ritchie (2002). "Direct mechanical measurement of the tensile strength and elastic modulus of multiwalled carbon nanotubes." Materials Science and Engineering: A **334**(1--2): 173--178.

Di, C.-a., D. Wei, G. Yu, Y. Liu, Y. Guo and D. Zhu (2008). "Patterned graphene as source/drain electrodes for bottom-contact organic field-effect transistors." Advanced Materials **20**(17): 3289--3293.

Díaz, J. E., A. Barrero, M. Márquez and I. G. Loscertales (2006). "Controlled encapsulation of hydrophobic liquids in hydrophilic polymer nanofibers by co-electrospinning." Advanced Functional Materials **16**(16): 2110-2116.

Doshi, J. and D. H. Reneker (1995). "Electrospinning process and applications of electrospun fibers." Selected papers from the special technical session "Electrostatics in Polymer Processing and Charge Monitoring", 1993 IEEE Industry Applications Society Meeting **35**(2--3): 151--160.

Du, J. and H.-M. Cheng (2012). "The fabrication, properties, and uses of graphene/polymer composites." Macromolecular Chemistry and Physics **213**(10-11): 1060--1077.

Eizenberg, M. and J. M. Blakely (1979). "Carbon monolayer phase condensation on ni(111)." Surface Science **82**(1): 228-236.

Elahi, M. F., W. Lu, G. Guoping and F. Khan (2013). "Core-shell fibers for biomedical applications-a review." J Bioengineer & Biomedical Sci 3: 121. doi.

Fang, X. and D. H. Reneker (1997). "DNA fibers by electrospinning." Journal of Macromolecular Science, Part B **36**(2): 169-173.

Feng, L., N. Xie and J. Zhong (2014). "Carbon nanofibers and their composites: A review of synthesizing, properties and applications." Materials **7**(5): 3919-3945.

Fong, H. and D. H. Reneker (1999). "Elastomeric nanofibers of styrene--butadiene--styrene triblock copolymer." Journal of Polymer Science Part B: Polymer Physics **37**(24): 3488--3493.

Galal, A., N. F. Atta and H. K. Hassan (2012). "Graphene supported-pt-m (m = ru or pd) for electrocatalytic methanol oxidation." International Journal of Electrochemical Science **7**(1): 768--784.

Geim, A. K. (2009). "Graphene: Status and prospects." Science **324**(5934): 1530--1534.

Haynes, A. S. (2008). Electrospun conducting polymer composites for chemo-resistive environmental and health monitoring applications, State University of New York at Stony Brook.

He, H., J. Klinowski, M. Forster and A. Lerf (1998). "A new structural model for graphite oxide." Chemical Physics Letters **287**(1-2): 53-56.

Hernandez, Y., V. Nicolosi, M. Lotya, F. M. Blighe, Z. Sun, S. De, M. T, B. Holland, M. Byrne, Y. K. Gun'Ko, J. J. Boland, P. Niraj, G. Duesberg, S. Krishnamurthy, R. Goodhue, J. Hutchison, V. Scardaci, A. C. Ferrari and J. N. Coleman (2008). "High-yield production of graphene by liquid-phase exfoliation of graphite." Nature Nano **3**(9): 563--568.

Hirsch, A. (2009). "Unzipping carbon nanotubes: A peeling method for the formation of graphene nanoribbons." Angewandte Chemie International Edition **48**(36): 6594--6596.

Hohman, M. M., M. Shin, G. Rutledge and M. P. Brenner (2001). "Electrospinning and electrically forced jets. I. Stability theory." Physics of Fluids (1994-present) **13**(8): 2201-2220.

Hou, H., J. J. Ge, J. Zeng, Q. Li, D. H. Reneker, A. Greiner and S. Z. D. Cheng (2005). "Electrospun polyacrylonitrile nanofibers containing a high concentration of well-aligned multiwall carbon nanotubes." Chemistry of Materials **17**(5): 967-973.

Huang, J.-C. (2002). "Carbon black filled conducting polymers and polymer blends." Advances in Polymer Technology **21**(4): 299--313.

Huang, X., X. Qi, F. Boey and H. Zhang (2012). "Graphene-based composites." Chemical Society Reviews **41**(2): 666--686.

Huang, Z.-M., Y. Z. Zhang, M. Kotaki and S. Ramakrishna (2003). "A review on polymer nanofibers by electrospinning and their applications in nanocomposites." Composites Science and Technology **63**(15): 2223-2253.

Hummers, W. S. and R. E. Offeman (1958). "Preparation of graphitic oxide." Journal of the American Chemical Society **80**(6): 1339-1339.

Hussain, F., M. Hojjati, M. Okamoto and R. E. Gorga (2006). "Review article: Polymer-matrix nanocomposites, processing, manufacturing, and application: An overview." Journal of Composite Materials **40**(17): 1511-1575.

Jaeger, R., H. Schönherr and G. J. Vancso (1996). "Chain packing in electro-spun poly(ethylene oxide) visualized by atomic force microscopy." Macromolecules **29**(23): 7634-7636.

Jiao, L., L. Zhang, X. Wang, G. Diankov and H. Dai (2009). "Narrow graphene nanoribbons from carbon nanotubes." Nature **458**(7240): 877--880.

Johnston, D. F. (1955). "The structure of the $\pi $-band of graphite." Proceedings of the Royal Society of London. Series A. Mathematical and Physical Sciences **227**(1170): 349-358.

Jung, K.-H., W. Deng, D. W. Smith Jr and J. P. Ferraris (2012). "Carbon nanofiber electrodes for supercapacitors derived from new precursor polymer: Poly(acrylonitrile-co-vinylimidazole)." Electrochemistry Communications **23**: 149-152.

Kalaitzidou, K., H. Fukushima and L. T. Drzal (2007). "A new compounding method for exfoliated graphite--polypropylene nanocomposites with enhanced flexural properties and lower percolation threshold." Composites Science and Technology **67**(10): 2045--2051.

Kalayci, V. E., P. K. Patra, Y. K. Kim, S. C. Ugbolue and S. B. Warner (2005). "Charge consequences in electrospun polyacrylonitrile (pan) nanofibers." Polymer **46**(18): 7191-7200.

Kelly, B. T. (1981). "Physics of graphite." Applied Science **1**.

Kim, B.-H., C. H. Kim, K. S. Yang, A. Rahy and D. J. Yang (2012). "Electrospun vanadium pentoxide/carbon nanofiber composites for supercapacitor electrodes." Electrochimica Acta **83**: 335-340.

Kim, B.-H., K. Seung Yang and H.-G. Woo (2013). "Boron-nitrogen functional groups on porous nanocarbon fibers for electrochemical supercapacitors." Materials Letters **93**: 190-193.

Kim, B.-H., K. S. Yang, Y. H. Bang and S. R. Kim (2011). "Thermally induced porous carbon nanofibers for electrochemical capacitor electrodes from phenylsilane and polyacrylonitrile blend solutions." Materials Letters **65**(23–24): 3479-3481.

Kim, B.-H., K. S. Yang and J. P. Ferraris (2012). "Highly conductive, mesoporous carbon nanofiber web as electrode material for high-performance supercapacitors." Electrochimica Acta **75**: 325-331.

Kim, B.-H., K. S. Yang and H.-G. Woo (2011). "Thin, bendable electrodes consisting of porous carbon nanofibers via the electrospinning of polyacrylonitrile containing tetraethoxy orthosilicate for supercapacitor." Electrochemistry Communications **13**(10): 1042-1046.

Kim, B.-H., K. S. Yang, H.-G. Woo and K. Oshida (2011). "Supercapacitor performance of porous carbon nanofiber composites prepared by electrospinning polymethylhydrosiloxane (pmhs)/polyacrylonitrile (pan) blend solutions." Synthetic Metals **161**(13–14): 1211-1216.

Kim, C.-D., B.-K. Min and W.-S. Jung (2009). "Preparation of graphene sheets by the reduction of carbon monoxide." Carbon **47**(6): 1610--1612.

Kim, C., K. S. Yang, M. Kojima, K. Yoshida, Y. J. Kim, Y. A. Kim and M. Endo (2006). "Fabrication of electrospinning-derived carbon nanofiber webs for the anode material of lithium-ion secondary batteries." Advanced Functional Materials **16**(18): 2393-2397.

Kim, H., A. A. Abdala and C. W. Macosko (2010). "Graphene/polymer nanocomposites." Macromolecules **43**(16): 6515-6530.

Kim, H. and C. W. Macosko (2008). "Morphology and properties of polyester/exfoliated graphite nanocomposites." Macromolecules **41**(9): 3317-3327.

Kim, S. B., T. Inoue, A. Shimizu and S. Murase (2006). "The electromagnet design for 3-d superconducting actuator using hts bulk." Proceedings of the 18th International Symposium on Superconductivity (ISS 2005) Advances in Superconductivity XVIII Proceedings of the 18th International Symposium on Superconductivity (ISS 2005) **445-448**(0): 1119--1122.

Kim, S. Y., B.-H. Kim, K. S. Yang and K.-Y. Kim (2012). "The formation of silica nanoparticles on the polyacrylonitrile-based carbon nanofibers by graphene via electrospinning." Materials Letters **71**(0): 74-77.

Kim, S. Y., B.-H. Kim, K. S. Yang and K. Oshida (2012). "Supercapacitive properties of porous carbon nanofibers via the electrospinning of metal alkoxide-graphene in polyacrylonitrile." Materials Letters **87**: 157-161.

Ko, F. (2006). Nanofiber technology. Nanomaterials handbook, CRC Press.

Kolla, H. S., S. P. Surwade, X. Zhang, A. G. MacDiarmid and S. K. Manohar (2005). "Absolute molecular weight of polyaniline." Journal of the American Chemical Society **127**(48): 16770-16771.

Kosynkin, D. V., A. L. Higginbotham, A. Sinitskii, J. R. Lomeda, A. Dimiev, B. K. Price and J. M. Tour (2009). "Longitudinal unzipping of carbon nanotubes to form graphene nanoribbons." Nature **458**(7240): 872--876.

Krishnan, A. (1998). "Young's modulus of single-walled nanotubes." Physical Review B **58**(20): 14013--14019.

Kroto, H. W., J. R. Heath, S. C. O'Brien, R. F. Curl and R. E. Smalley (1985). "C60: Buckminsterfullerene." Nature **318**(6042): 162--163.

Kuila, T., S. Bose, C. E. Hong, M. E. Uddin, P. Khanra, N. H. Kim and J. H. Lee (2011). "Preparation of functionalized graphene/linear low density polyethylene composites by a solution mixing method." Carbon **49**(3): 1033--1037.

Kuilla, T., S. Bhadra, D. Yao, N. H. Kim, S. Bose and J. H. Lee (2010). "Recent advances in graphene based polymer composites." Progress in Polymer Science **35**(11): 1350-1375.

Larsen, G., R. Spretz and R. Velarde-Ortiz (2004). "Use of coaxial gas jackets to stabilize taylor cones of volatile solutions and to induce particle-to-fiber transitions." Advanced Materials **16**(2): 166-169.

Lee, C., X. Wei, J. W. Kysar and J. Hone (2008). "Measurement of the elastic properties and intrinsic strength of monolayer graphene." Science **321**(5887): 385-388.

Lee, W. D. and S. S. Im (2007). "Thermomechanical properties and crystallization behavior of layered double hydroxide/poly(ethylene terephthalate) nanocomposites prepared by in-situ polymerization." Journal of Polymer Science Part B: Polymer Physics **45**(1): 28--40.

Lerf, A., H. He, M. Forster and J. Klinowski (1998). "Structure of graphite oxide revisited‖." Journal of Physical Chemistry B **102**(23): 4477-4482.

Letheby, H. (1862). "Xxix.-on the production of a blue substance by the electrolysis of sulphate of aniline." Journal of the Chemical Society **15**: 161-163.

Li, D., A. Babel, S. A. Jenekhe and Y. Xia (2004). "Nanofibers of conjugated polymers prepared by electrospinning with a two-capillary spinneret." Advanced Materials **16**(22): 2062-2066.

Li, D. and Y. Xia (2004). "Direct fabrication of composite and ceramic hollow nanofibers by electrospinning." Nano Letters **4**(5): 933-938.

Li, D. and Y. Xia (2004). "Electrospinning of nanofibers: Reinventing the wheel?" Advanced Materials **16**(14): 1151-1170.

Li, F., Y. Zhao and Y. Song (2010). Core-shell nanofibers: Nano channel and capsule by coaxial electrospinning.

Li, N., Z. Wang, K. Zhao, Z. Shi, Z. Gu and S. Xu (2010). "Large scale synthesis of n-doped multi-layered graphene sheets by simple arc-discharge method." Carbon **48**(1): 255-259.

Li, X., W. Cai, J. An, S. Kim, J. Nah, D. Yang, R. Piner, A. Velamakanni, I. Jung, E. Tutuc, S. K. Banerjee, L. Colombo and R. S. Ruoff (2009). "Large-area synthesis of high-quality and uniform graphene films on copper foils." Science **324**(5932): 1312-1314.

Liang, J., Y. Huang, L. Zhang, Y. Wang, Y. Ma, T. Guo and Y. Chen (2009). "Molecular-level dispersion of graphene into poly(vinyl alcohol) and effective reinforcement of their nanocomposites." Advanced Functional Materials **19**(14): 2297--2302.

Lifeng, Z. and H. You-Lo (2006). "Nanoporous ultrahigh specific surface polyacrylonitrile fibres." Nanotechnology **17**(17): 4416.

Lu, W., M. Zu, J.-H. Byun, B.-S. Kim and T.-W. Chou (2012). "State of the art of carbon nanotube fibers: Opportunities and challenges." Advanced Materials **24**(14): 1805-1833.

Marcano, D. C., D. V. Kosynkin, J. M. Berlin, A. Sinitskii, Z. Sun, A. Slesarev, L. B. Alemany, W. Lu and J. M. Tour (2010). "Improved synthesis of graphene oxide." ACS Nano **4**(8): 4806--4814.

Mattausch, A. and O. Pankratov (2008). "Density functional study of graphene overlayers on sic." physica status solidi (b) **245**(7): 1425--1435.

Moniruzzaman, M. and K. I. Winey (2006). "Polymer nanocomposites containing carbon nanotubes." Macromolecules **39**(16): 5194-5205.

Novoselov, K. S., A. K. Geim, S. V. Morozov, D. Jiang, M. I. Katsnelson, I. V. Grigorieva, S. V. Dubonos and A. A. Firsov (2005). "Two-dimensional gas of massless dirac fermions in graphene." Nature **438**(7065): 197--200.

Novoselov, K. S., A. K. Geim, S. V. Morozov, D. Jiang, Y. Zhang, S. V. Dubonos, I. V. Grigorieva and A. A. Firsov (2004). "Electric field effect in atomically thin carbon films." Science **306**(5696): 666-669.

Novoselov, K. S. and A. H. C. Neto (2012). "Two-dimensional crystals-based heterostructures: Materials with tailored properties." Physica Scripta **2012**(T146): 014006.

Park, J.-Y. (2009). Band structure and electron transport physics of one-dimensional swnts. Carbon Nanotube Electronics, Springer US**:** 1-42.

Park, S. and R. Ruoff (2009). "Chemical methods for the production of graphenes." Nature Nanotechnology **4**(4): 217--224.

Peres, N. M. R. (2009). "The transport properties of graphene." Journal of Physics-Condensed Matter **21**(32): 323201.

Prasad, K. E., B. Das, U. Maitra, U. Ramamurty and C. N. R. Rao (2009). "Extraordinary synergy in the mechanical properties of polymer matrix composites reinforced with 2 nanocarbons." Proc Natl Acad Sci U S A **106**(32): 13186--13189.

Qin, X.-H., Y.-Q. Wan, J.-H. He, J. Zhang, J.-Y. Yu and S.-Y. Wang (2004). "Effect of licl on electrospinning of pan polymer solution: Theoretical analysis and experimental verification." Polymer **45**(18): 6409-6413.

Qu, H., S. Wei and Z. Guo (2013). "Coaxial electrospun nanostructures and their applications." Journal of Materials Chemistry A **1**(38): 11513-11528.

Rahaman, M. S. A., A. F. Ismail and A. Mustafa (2007). "A review of heat treatment on polyacrylonitrile fiber." Polymer Degradation and Stability **92**(8): 1421-1432.

Ramanathan, T., A. A. Abdala, S. Stankovich, D. A. Dikin, M. Herrera-Alonso, R. D. Piner, D. H. Adamson, H. C. Schniepp, X. Chen, R. S. Ruoff, S. T. Nguyen, I. A. Aksay, R. K. Prud'homme and L. C. Brinson (2008). "Functionalized graphene sheets for polymer nanocomposites." Nature Nanotechnology **3**(6): 327--331.

Reneker, D. H. and I. Chun (1996). "Nanometre diameter fibres of polymer, produced by electrospinning." Nanotechnology **7**(3): 216.

Rodriguez, N. M. (1993). "A review of catalytically grown carbon nanofibers." Journal of Materials Research **8**(12): 3233-3250.

Rollings, E., G. H. Gweon, S. Y. Zhou, B. S. Mun, J. L. McChesney, B. S. Hussain, A. V. Fedorov, P. N. First, W. A. de Heer and A. Lanzara (2006). "Synthesis and characterization of atomically thin graphite films on a silicon carbide substrate." Journal of Physics and Chemistry of Solids **67**(9-10): 2172-2177.

Salvetat, J.-P. (1999). "Elastic and shear moduli of single-walled carbon nanotube ropes." Physical Review Letters **82**(5): 944--947.

Schadler, L. S., S. K. Kumar, B. C. Benicewicz, S. L. Lewis and S. E. Harton (2007). "Designed interfaces in polymer nanocomposites: A fundamental viewpoint." Mrs Bulletin **32**(4): 335--340.

Schedin, F., A. K. Geim, S. V. Morozov, E. W. Hill, P. Blake, M. I. Katsnelson and K. S. Novoselov (2007). "Detection of individual gas molecules adsorbed on graphene." Nature Materials **6**(9): 652--655.

Shen, B., W. Zhai, C. Chen, D. Lu, J. Wang and W. Zheng (2011). "Melt blending in situ enhances the interaction between polystyrene and graphene through pi-pi stacking." Acs Applied Materials & Interfaces **3**(8): 3103--3109.

Shin, H.-J., K. K. Kim, A. Benayad, S.-M. Yoon, H. K. Park, I.-S. Jung, M. H. Jin, H.-K. Jeong, J. M. Kim, J.-Y. Choi and Y. H. Lee (2009). "Efficient reduction of graphite oxide by sodium borohydride and its effect on electrical conductance." Advanced Functional Materials **19**(12): 1987--1992.

Skotheim, T. A., R. L. Elsenbaumer and J. R. Reynolds (1998). Handbook of conducting polymers, M. Dekker.

Smith, A. W. and N. S. Rasor (1956). "Observed dependence of the low-temperature thermal and electrical conductivity of graphite on temperature, type, neutron irradiation, and bromination." Phys. Rev. **104**: 885--891.

Sprinkle, M., P. Soukiassian, W. A. de Heer, C. Berger and E. H. Conrad (2009). "Epitaxial graphene: The material for graphene electronics." physica status solidi (RRL) -- Rapid Research Letters **3**(6): A91--A94.

Stankovich, S., D. A. Dikin, G. H. B. Dommett, K. M. Kohlhaas, E. J. Zimney, E. A. Stach, R. D. Piner, S. T. Nguyen and R. S. Ruoff (2006). "Graphene-based composite materials." Nature **442**(7100): 282-286.

Stankovich, S., D. A. Dikin, R. D. Piner, K. A. Kohlhaas, A. Kleinhammes, Y. Jia, Y. Wu, S. T. Nguyen and R. S. Ruoff (2007). "Synthesis of graphene-based nanosheets via chemical reduction of exfoliated graphite oxide." Carbon **45**(7): 1558--1565.

Staudenmaier, L. (1898). "Verfahren zur darstellung der graphitsäure." Berichte der deutschen chemischen Gesellschaft **31**(2): 1481--1487.

Stenger-Smith, J. D. (1998). "Intrinsically electrically conducting polymers. Synthesis, characterization, and their applications." Progress in Polymer Science **23**(1): 57-79.

Stoller, M. D., S. Park, Y. Zhu, J. An and R. S. Ruoff (2008). "Graphene-based ultracapacitors." Nano Letters **8**(10): 3498-3502.

Sun, Z., E. Zussman, A. l. Yarin, J. h. Wendorff and A. Greiner (2003). "Compound core–shell polymer nanofibers by co-electrospinning." Advanced Materials **15**(22): 1929-1932.

Sutter, P. W., J.-I. Flege and E. A. Sutter (2008). "Epitaxial graphene on ruthenium." Nature Materials **7**(5): 406--411.

Syed, A. A. and M. K. Dinesan (1991). "Review: Polyaniline---a novel polymeric material." Talanta **38**(8): 815-837.

Tao, X. and T. Institute (2005). Wearable electronics and photonics, Woodhead.

Teng, C.-C., C.-C. M. Ma, C.-H. Lu, S.-Y. Yang, S.-H. Lee, M.-C. Hsiao, M.-Y. Yen, K.-C. Chiou and T.-M. Lee (2011). "Thermal conductivity and structure of non-covalent functionalized graphene/epoxy composites." Carbon **49**(15): 5107--5116.

Theron, A., E. Zussman and A. L. Yarin (2001). "Electrostatic field-assisted alignment of electrospun nanofibres." Nanotechnology **12**(3): 384.

Tibbetts, G. G., M. L. Lake, K. L. Strong and B. P. Rice (2007). "A review of the fabrication and properties of vapor-grown carbon nanofiber/polymer composites." Composites Science and Technology **67**(7–8): 1709-1718.

Tung, V. C., M. J. Allen, Y. Yang and R. B. Kaner (2009). "High-throughput solution processing of large-scale graphene." Nature Nanotechnology **4**(1): 25--29.

Verdejo, R., M. M. Bernal, L. J. Romasanta and M. A. Lopez-Manchado (2011). "Graphene filled polymer nanocomposites." Journal of Materials Chemistry **21**(10): 3301--3310.

Wallace, P. R. (1947). "The band theory of graphite." Phys. Rev. **71**: 622--634.

Wang, J., H. Hu, X. Wang, C. Xu, M. Zhang and X. Shang (2011). "Preparation and mechanical and electrical properties of graphene nanosheets-poly(methyl methacrylate) nanocomposites via in situ suspension polymerization." Journal of Applied Polymer Science **122**(3): 1866--1871.

Wang, X., H. You, F. Liu, M. Li, L. Wan, S. Li, Q. Li, Y. Xu, R. Tian, Z. Yu, D. Xiang and J. Cheng (2009). "Large-scale synthesis of few-layered graphene using cvd." Chemical Vapor Deposition **15**(1-3): 53--56.

Wang, Y., S. Serrano and J. J. Santiago-Avilés (2003). "Raman characterization of carbon nanofibers prepared using electrospinning." Synthetic Metals **138**(3): 423-427.

Wangxi, Z., L. Jie and W. Gang (2003). "Evolution of structure and properties of pan precursors during their conversion to carbon fibers." Carbon **41**(14): 2805-2812.

Wessling, B. (1998). "Dispersion as the link between basic research and commercial applications of conductive polymers (polyaniline)." Synthetic Metals **93**(2): 143--154.

Worsley, K. A., P. Ramesh, S. K. Mandal, S. Niyogi, M. E. Itkis and R. C. Haddon (2007). "Soluble graphene derived from graphite fluoride." Chemical Physics Letters **445**(1-3): 51-56.

Wu, M., Q. Wang, K. Li, Y. Wu and H. Liu (2012). "Optimization of stabilization conditions for electrospun polyacrylonitrile nanofibers." Polymer Degradation and Stability **97**(8): 1511-1519.

Yang, G. (2010). from http://www.physics.drexel.edu/~gyang/SOLID/lecture113010.pdf.

Yang, X., X. Dou, A. Rouhanipour, L. Zhi, H. J. Räder and K. Müllen (2008). "Two-dimensional graphene nanoribbons." Journal of the American Chemical Society **130**(13): 4216-4217.

Ye, L., X.-Y. Meng, X. Ji, Z.-M. Li and J.-H. Tang (2009). "Synthesis and characterization of expandable graphite--poly(methyl methacrylate) composite particles and their application to flame retardation of rigid polyurethane foams." Polymer Degradation and Stability **94**(6): 971-979.

Yoonessi, M. and J. R. Gaier (2010). "Highly conductive multifunctional graphene polycarbonate nanocomposites." ACS Nano **4**(12): 7211--7220.

Yu, A., P. Ramesh, M. E. Itkis, E. Bekyarova and R. C. Haddon (2007). "Graphite nanoplatelet-epoxy composite thermal interface materials." Journal of Physical Chemistry C **111**(21): 7565--7569.

Yu, J. H., S. V. Fridrikh and G. C. Rutledge (2004). "Production of submicrometer diameter fibers by two-fluid electrospinning." Advanced Materials **16**(17): 1562-1566.

Yun, Y. S., Y. H. Bae, D. H. Kim, J. Y. Lee, I.-J. Chin and H.-J. Jin (2011). "Reinforcing effects of adding alkylated graphene oxide to polypropylene." Carbon **49**(11): 3553--3559.

Zhang, H.-B., W.-G. Zheng, Q. Yan, Y. Yang, J.-W. Wang, Z.-H. Lu, G.-Y. Ji and Z.-Z. Yu (2010). "Electrically conductive polyethylene terephthalate/graphene nanocomposites prepared by melt compounding." Polymer **51**(5): 1191--1196.

Zhang, J., H. Yang, G. Shen, P. Cheng and S. Guo (2010). "Reduction of graphene oxide via l-ascorbic acid." Chemical communications (Cambridge, England) **46**(7): 1112-1114.

Zhang, L., A. Aboagye, A. Kelkar, C. Lai and H. Fong (2014). "A review: Carbon nanofibers from electrospun polyacrylonitrile and their applications." Journal of Materials Science **49**(2): 463-480.

Zhang, L. L. and X. S. Zhao (2009). "Carbon-based materials as supercapacitor electrodes." Chemical Society Reviews **38**(9): 2520-2531.

Zhang, W., J. Cui, C.-a. Tao, Y. Wu, Z. Li, L. Ma, Y. Wen and G. Li (2009). "A strategy for producing pure single-layer graphene sheets based on a confined self-assembly approach." Angewandte Chemie International Edition **48**(32): 5864--5868.

Zhang, Y., Z.-M. Huang, X. Xu, C. T. Lim and S. Ramakrishna (2004). "Preparation of core−shell structured pcl-r-gelatin bi-component nanofibers by coaxial electrospinning." Chemistry of Materials **16**(18): 3406-3409.

Zhao, X., Q. Zhang, D. Chen and P. Lu (2011). "Enhanced mechanical properties of graphene-based poly(vinyl alcohol) composites (vol 43, pg 2357, 2010)." Macromolecules **44**(7): 2392--2392.

Zheng, W., X. Lu and S.-C. Wong (2004). "Electrical and mechanical properties of expanded graphite-reinforced high-density polyethylene." Journal of Applied Polymer Science **91**(5): 2781--2788.

Zhi, L. and K. Mullen (2008). "A bottom-up approach from molecular nanographenes to unconventional carbon materials." Journal of Materials Chemistry **18**: 1472-1484.

Zhou, T., F. Chen, K. Liu, H. Deng, Q. Zhang, J. Feng and Q. Fu (2010). "A simple and efficient method to prepare graphene by reduction of graphite oxide with sodium hydrosulfite." Nanotechnology **22**(4): 045704.

Zhou, X., T. Wu, B. Hu, G. Yang and B. Han (2010). "Synthesis of graphene/polyaniline composite nanosheets mediated by polymerized ionic liquid." Chemical Communications **46**(21): 3663--3665.

Zhu, Y., S. Murali, M. D. Stoller, A. Velamakanni, R. D. Piner and R. S. Ruoff (2010). "Microwave assisted exfoliation and reduction of graphite oxide for ultracapacitors." Carbon **48**(7): 2118--2122.

Zussman, E., X. Chen, W. Ding, L. Calabri, D. A. Dikin, J. P. Quintana and R. S. Ruoff (2005). "Mechanical and structural characterization of electrospun pan-derived carbon nanofibers." Carbon **43**(10): 2175-2185.

CHAPTER 3 ORIGINALITY AND OBJECTIVES

3.1 Originality

Considerable research has been conducted on the usage of conductive polymer nanocomposites for electrical conductors and energy solutions application. However, the combined usage of graphene and electrospun fibers for these applications are very scarce as still there are great deal of complications in dispersion of graphene in the nanofibers. To the best of our knowledge there is no published work that has examined the polyaniline/functionalized graphene system (PANi/G) for these applications fabricated using single-nozzle electrospinning and that provided a through study on the effect of the addition of graphene on morphology, chemical microstructure and conductivity of the resulting nanofibers. Moreover, coaxial electrospinning technique is very promising for the preparation of nanofibers from polymers that are unspinnable but there is no published work on the fabrication of core-shell structured PANi/PMMA nanofibers with graphene nanosheets located on the surface by using this method.

Carbon nanofibers are very promising materials for energy storage solutions and in particular supercapacitors. However, their performance is very much dependent on the surface area of the final fibers. Also, they fall short for applications where high energy density is required. In this thesis, graphene was chosen to address both of these problems. In parallel a novel fabrication technique was developed by utilizing phase-separated solution of polyacrylonitrile and polyvinylpyrrolidone (PAN/PVP) to yield ultra-fine nanofibers which improved the performance

and capacitance of the supercapacitor considerably. To best of our knowledge no published work to this date has reported fabrication of supercapacitors from such a system.

3.2 Objectives

Taking into account the features of graphene and electrospun polymer nanofibers as discussed in the literature review (Chapter 2) and their potential application for sensors and supercapacitors, the main objective of this thesis was to study:

"Development of graphene-based polymer nanocomposites for electrical conductors and supercapacitors"

To achieve this main objective, this thesis was divided into two parts:

1) The first part investigates the fabrication of graphene-based polyaniline nanofibers using two approaches: i) Blend polyaniline with an easily electrospinnable polymer such as poly(ethylene oxide) (PEO). ii) Use coaxial electrospinning technique to produce core-shell structured polyaniline/poly(methyl methacrylate) (PANi/PMMA) and subsequently remove the shell layer by solvent etching to produce neat PANi nanofibers. The specific objectives of this work can be summarized as follows:

- Prepare graphene via chemical exfoliation methods using various characterization techniques to confirm the quality of produced graphene nanosheets.
- Stabilize graphene dispersion in organic media by noncovalent functionalization.
- Fabricate polyaniline nanofibers via single-nozzle electrospinning with highest possible graphene content through blending with PEO.

- Fabricate neat polyaniline/graphene nanofibers via coaxial electrospinning with PMMA as shell layer and its subsequent removal.
- Determine the optimized processing parameters which leads to successful electrospinning of graphene filled PANi/PEO and coaxial electrospinning of PANi/PMMA
- Investigate the morphology of nanofibers and confirm the presence and placement of graphene sheets in the nanofibers.
- Characterize the conductivity of nanofibers via four-point probe method.

2) The second part investigates the fabrication of graphene-based polymer nanocomposites for supercapacitor applications. To this extend, core–shell structured carbon nanofibers (CNFs) embedded with various amounts of noncovalently functionalized graphene were fabricated by single-nozzle electrospinning technique using phase-separated solution of polyacrylonitrile and polyvinylpyrrolidone (PAN/PVP) to yield ultrafine nanofibers.

The specific objectives of this work can be summarized as follows:

- Fabricate graphene-based carbon nanofibers from polyacrylonitrile precursor with various amount of graphene.
- Stabilize graphene dispersion in organic media by noncovalent functionalization with PVP.
- Determine the optimized processing parameters which leads to successful electrospun fibers.
- Investigate the morphology of nanofibers before and after carbonization and confirm the presence and placement of graphene sheets in the nanofibers before and after carbonization.

- Characterize the quality of carbon nanofibers and effect of addition of graphene using various techniques.
- Analyze the electrochemical performance of CNF/G for applications in supercapacitors.

CHAPTER 4 SUMMARY OF ARTICLES

The main achievements of this research are presented in the form of three scientific papers in the following three chapters:

Chapter 5 presents the results of the first paper: "*Fabrication of polyaniline/poly(ethylene oxide)/non-covalently functionalized graphene nanofibers via electrospinning"* that is published in the journal of Synthetic Metals (vol 200, 2015, 7-15). In this work, a procedure to fabricate graphene filled polyaniline/poly(ethylene oxide) (PANi/PEO) nanofibers is reported. The graphene nanosheets were well dispersed by noncovalent functionalization with 1-pyrenebutanoic acid, succinimidyl ester (PBASE). The functionalization of graphene with PBASE was investigated with Fourier transform infrared spectroscopy (FTIR). The morphology, chemical composition and conductivity of the PANi/PEO/G-PBASE nanofibers by scanning electron microscopy (SEM), transmission electron microscopy (TEM), X-ray photoelectron spectroscopy (XPS) and four-point probe conductivity meter is investigated.

Chapter 6 presents the results of the second paper: "*Core−shell structured graphene filled polyaniline/poly(methyl methacrylate) nanofibers by coaxial electrospinning"* that has been submitted to the Journal of Material Letters. In this work, we report the preparation of neat polyaniline nanofibers filled with highly dispersed as graphene nanosheets. The coaxial electrospinning process was used to produce core-shell structured fibers of a poly(methyl methacrylate) (shell) and a polyaniline (core) embedded with highly dispersed PBASE functionalized graphene nanosheets. The insulating shell was selectively removed by solvent etching. Scanning electron microscopy (SEM), transmission electron microscopy (TEM), and

electrical conductivity measurements by four-point probe setup were utilized to characterize morphology and conductivity of these nanofibers.

Chapter 7 presents the results of the third paper: "*High capacitance carbon nanofibers from polyacrylonitrile and polyvinylpyrrolidone-functionalized graphene by electrospinning"* that has been submitted to the Journal of Nanoscience and Nanotechnology. In this study, ultra-fine CNF/G nanofibers were produced via single nozzle electrospinning of phase-separated solution of polyacrylonitrile and polyvinylpyrrolidone (PAN/PVP) in N,N-dimethylformamide (DMF) solution dispersed with PVP-stabilized graphene nanosheets, followed by the calcination and carbonization processes. Utilizing this method to fabricate CNF/G nanofibers allowed obtaining very small fiber diameters. The morphology, microstructure and electrochemical performance of CNF/G nanofibers are characterized by scanning electron microscopy (SEM), transmission electron microscopy (TEM), X-ray photoelectron spectroscopy (XPS), Fourier transform infrared spectroscopy (FTIR), Brunauer-Emmett-Teller (BET), cyclic voltammetry (CV) and galvanostatic charge-discharge.

CHAPTER 5 ARTICLE 1: FABRICATION OF POLYANILINE/POLY(ETHYLENE OXIDE)/NON-COVALENTLY FUNCTIONALIZED GRAPHENE NANOFIBERS VIA ELECTROSPINNING

Ali Moayeri, Abdellah Ajji

Published in the Journal of Synthetic Metals vol. 200 (2015) 7–15

5.1 Abstract

Conducting nanofibers of polyaniline (PANi) doped with camphor-10-sulfonic acid (HCSA), blended with poly(ethylene oxide) (PEO), and filled with 1-pyrenebutanoic acid, succinimidyl ester functionalized graphene (G-PBASE) have been fabricated using electrospinning. Scanning electron microscopy (SEM), transmission electron microscopy (TEM), X-ray photoelectron spectroscopy (XPS), Fourier transforms infrared (FTIR) and thermal gravimetric analyzer (TGA) was utilized to characterize the PANi/PEO/G-PBASE fibers morphology and properties. The observations show that electrospun fibers are highly interconnected and possess a relatively smooth surface. The average diameter of fibers was 222 ± 60 nm. The electrical conductivity of PANi/PEO and PANi/PEO/G-PBASE at room temperature was also studied. The unique nanostructured composite of PANi/PEO/G-PBASE with small loading of G-PBASE (5 wt.% relative to PANi) showed two order of magnitude enhancement in the electrical conductivity and one order of magnitude enhancement in thermal stability in comparison to PANi/PEO nanofibers.

5.2 Introduction

Intrinsically conducting polymers (ICPs) have received a lot of attention due to their superior electrical properties (Bhattacharya and De 1996, Stenger-Smith 1998) and promising application in fields such as sensors, electronic nanodevices and energy storage (Das and Prusty 2012).

Polyaniline (PANi) is one of the most investigated ICPs because of its ease of synthesis, high conductivity, high environmental stability compared to other ICPs, and interesting redox chemistry (Wallace, Teasdale et al. 2002).

Electrospinning is a simple method to produce polymer nanofibers with controlled diameters ranging from nanometers to sub-micrometers (Reneker and Chun 1996, Huang, Zhang et al. 2003). In this process, ultrathin fibers are produced by the application of electrostatic force between a syringe filled with a polymer solution and a collector mounted at a fixed distance from the needle. The schematic outline of the electrospinning set up is shown in Figure 5-1.

The resulting non-woven porous mats possess a distinctly high surface area to volume ratio which, combined with the high electrical conductivity of intrinsically conductive polymers, will result in

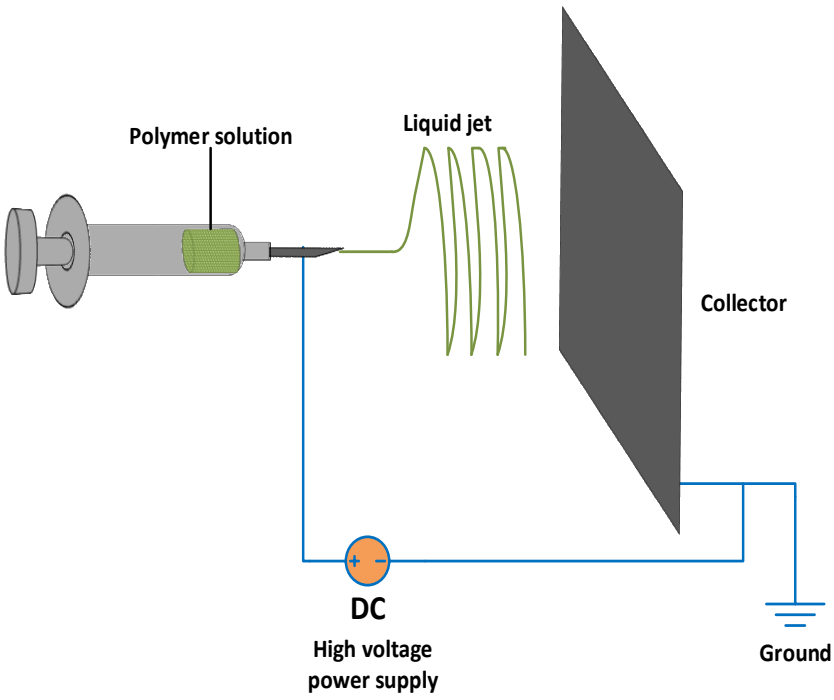

Figure 5-1: Schematic illustration of electrospinning process

conductive electrospun nanofibers having a promising future for applications in supercapacitors (Chaudhari, Sharma et al. 2013), sensors (Lin, Li et al. 2012) and solar cells (Peng, Zhu et al. 2012).

There are some limitations to PANi. The processing of PANi is daunting, mainly due to its rigid backbone which is related to its high level of conjugation (Ruiz, Gonzalo et al. 2013). Additionally, PANi is mostly available in low-molecular weights, which in turn affects the elasticity of its solutions for electrospinning (Zhang and Rutledge 2012). Moreover, PANi has poor solubility in common organic solvents but can be improved by introduction of a protonic acid into the PANi chains (e.g. doping with camphor-10-sulfonic acid (HCSA)), this further complicates it electrospinnability (Cao, Smith et al. 1992, Rao, Subrahmanya et al. 2003). One way to circumvent these problems, is by blending doped-PANi with an easily electrospinnable polymer such as poly(ethylene oxide) (PEO) (Norris, Shaker et al. 2000). However, the presence of an insulator polymer will decrease the fibers conductivity due to a reduction in the conducting component in the blend. A good strategy to compensate for PEO addition and to improve the overall electrical properties of the electrospun fibers blend is to incorporate carbon-based conductive nanofillers into the fibers. Recently, graphene, an atomically thick, two dimensional sheet composed of sp^2 carbon atoms arranged in a honeycomb crystal lattice (Li and Kaner 2008), has attracted a lot attention due to its outstanding properties such as extraordinary physical properties (high values of its Young's modulus (~ 1100 GPa) (Lee, Wei et al. 2008), fracture strength (125 GPa) (Lee, Wei et al. 2008)), high thermal conductivity (~5000 W m^{-1} K^{-1}) (Balandin, Ghosh et al. 2008), excellent mobility of charge carriers (200,000 cm^2 V^{-1} s^{-1}) (Bolotin, Sikes et al. 2008), high specific surface area (calculated value, 2630 m^2 g^{-1}) (Stoller, Park et al. 2008). Given the excel- lent electrical properties of graphene compared to other allotropes of carbon, it is possible to improve the

electronic properties of the polymer matrix by embedding it into a polymer matrix (Castro Neto, Guinea et al. 2009). Therefore, graphene was selected in order to enhance to the conductivity of electrospun PANi/PEO nanofibers.

However, graphene has a poor solubility in common organic solvents and it has a tendency to form agglomerates which can be attributed to its hydrophobic nature, the van der Waals inter- actions, and its strong π–π stacking (Xu, Bai et al. 2008). Therefore, these issues has to be addressed as dispersion of graphene in electrospinning solution is a pivotal step in the formation of nanofibers. Several covalent and noncovalent functionalization methods that can improve graphene solubility have been reported (Georgakilas, Otyepka et al. 2012). In the covalent functionalization, sp3 sites will be introduced on the graphene sheets that will permanently change its properties, and especially its electrical properties which is not desirable. In contrast, noncovalent functionalization through π–π interaction with an aromatic molecule improves the solubility of graphene without disturbing its electronic network (Subrahmanyam, Ghosh et al. 2009, Georgakilas, Otyepka et al. 2012). One of the aromatic molecules that can be used for noncovalent functionalization of graphene is 1-pyrenebutanoic acid, succinimidyl ester (PBASE) that can be attached to the basal plane of graphene via π–π stacking. Therefore, PBASE negative –COOH group can separate graphene sheets from each other through electrostatic repulsion and dispersing it in the solvent (Zhang, Gao et al. 2013).

In this article, a procedure to fabricate graphene filled PANi/PEO nanofibers will be reported and the morphology and conductivity of the PANi/PEO/G-PBASE nanofibers is investigated. The mass ratio of G-PBASE to PANi was predetermined to be maintained at 5 wt.% because firstly, it was observed that increasing the graphene content more than 5 wt.% promotes formation of the defects in the electrospun fibers due to changing solution properties and secondly, to have maximum

conductivity enhancement by inclusion of maximum graphene content possible. By taking into account the advantages of graphene and polyaniline, the development of electrospun nanocomposite of graphene-filled polyaniline offers further opportunities to improve the electrical characteristics of each of these materials.

5.3 Experimental methods

5.3.1 Materials

Graphite powder (<20 μm, synthetic), polyaniline (PANi, emeraldine base, M_w = 50,000 g mol^{-1}), camphor-10-sulfonic acid (HCSA, 98%), N,N-dimethylformamide (DMF, 99.8%), chloroform ($CHCl_3$, ≥99%), ethanol (CH_3CH_2OH, denatured), hydrochloric acid (HCl, 37%), sulfuric acid (H_2SO_4, 98%), hydrogen peroxide (H_2O_2, 30%), sodium nitrate ($NaNO_3$, ≥99.0%), hydrazine monohydrate (N_2H_4 , 98%) and 1-pyrenebutanoic acid, succinimidyl ester (PBASE) were all purchased from Sigma Aldrich. Polyethylene oxide (PEO, M_w = 600,000 g mol^{-1}) was purchased from Polysciences, Inc. All chemicals were reagent grade and were used as received. Deionized (DI) water (Millipore Milli-Q) was used for all the experiments (the structures of some of the chemicals used are depicted in Figure 5-2.

5.3.2 Characterization

SEM measurements were carried out on a field emission scanning electron microscope (JEOL JSM-7600TFE) at 5kV. Samples were cut from an electrospun mat on the aluminum foil and mounted on aluminum stubs that were coated by an ultrathin layer of gold for better conductivity prior to observation. SEM images were captured in resolution of 1280 × 1240 pixels. Fiber diameters were determined using Image Pro software 5.1. For each electrospun mat, 100 fibers were considered from different places on the sample to calculate the average diameter. The

dispersion of graphene in the prepared nanofibers was characterized by transmission electron microscopy (TEM, JEOL, JEM 2100F). For TEM observation, fibers were directly deposited onto a TEM copper grid with supporting carbon film (CF400-Cu, Electron Microscopy Sciences). Fourier transform infrared (FTIR) spectroscopy analysis was carried out using Perkin Elmer 65 FTIR-ATR instrument. A total of 128 scans were accumulated for the signal averaging of each IR spectral measurement with a 4 cm^{-1} resolution. The spectra of the samples were recorded over a wavenumber range of 4000–650 cm^{-1}. Thermo- gravimetric analysis was conducted under nitrogen atmosphere using Q5000 TGA (TA instruments, USA) in the temperature range of 30–900 °C, with a heating ramp of 10 °C/min. X-ray photoelectron spectroscopic (XPS) analysis was carried out on VG Scientific ESCALAB 3 MK II X-ray photoelectron spectrometer using a Mg Kα ˛ source (12 kV, 18 mA) to confirm the presence of graphene sheets in the nanofibers of PANi/PEO/G-PBASE. The survey scans were done at a pass energy of 100 eV and energy step size of 1.0 eV and the high resolution peaks were scanned at a 20 eV pass energy with an energy step of 0.05 eV. Thermo Scientific Advantage software was used for curve fitting and to calculate the relative atomic percent. Curve fitting of the C1s spectra was performed using a Gaussian–Lorentzian peak shape after performing a Shirley background correction. All presented spectra are charge corrected and energy referenced to C1s at 285 eV. The relative atomic percent is calculated using Equation 5-1 where A_1 represents the area of the peak for a given element and SF_1 is the sensitivity factor for that same element. Sensitivity factors from the Wagner table are used.

$$At.\% = \frac{\frac{A_1}{SF_1}}{\sum_n \left(\frac{A_n}{SF_n}\right)} \qquad 5\text{-}1$$

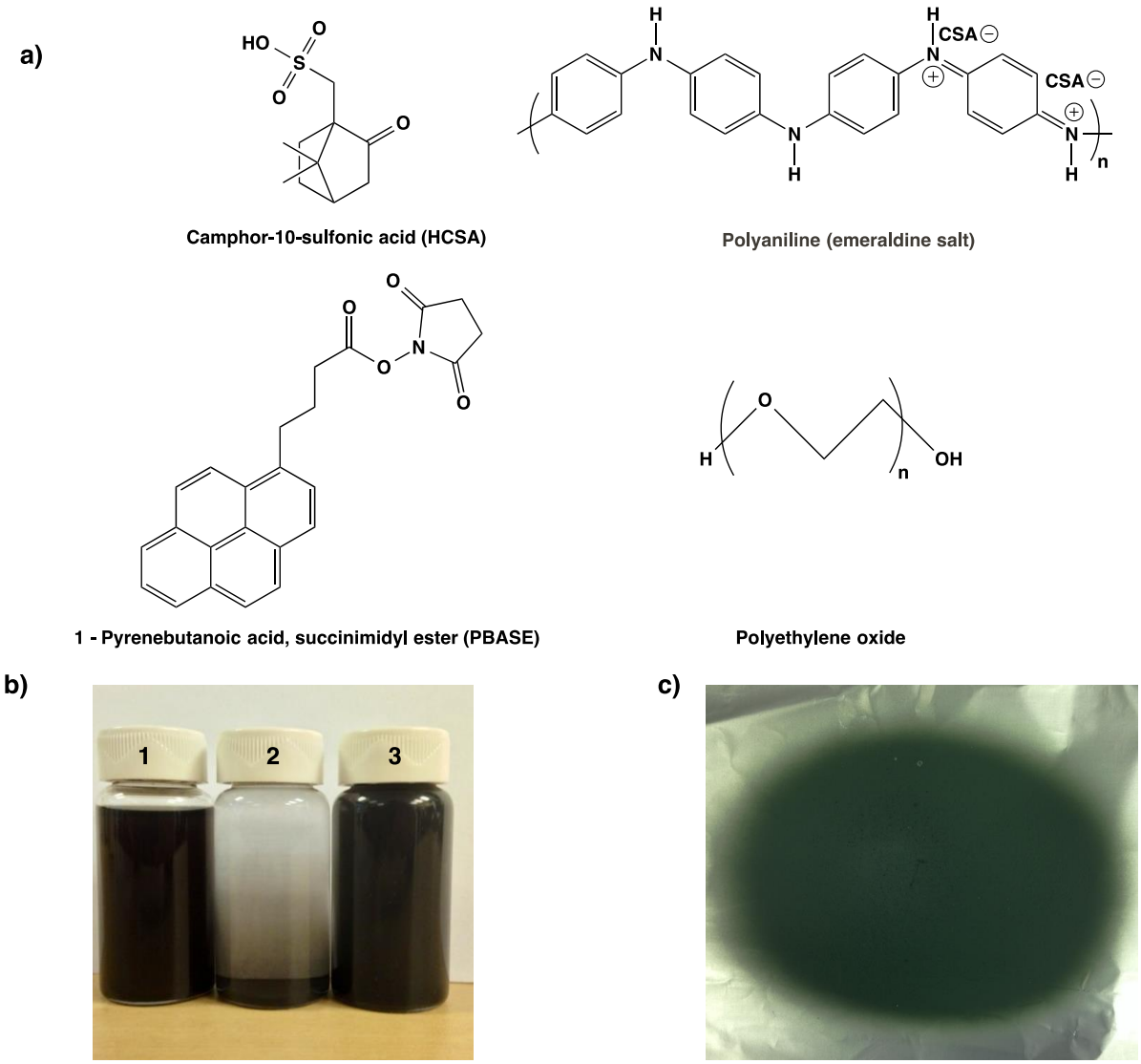

Figure 5-2: a) Chemical structures of camphor-10-sulfonic acid (HCSA), polyaniline (emeraldine salt), 1-pyrenebutanoic acid, succinimidyl ester (PBASE) and poly(ethylene oxide) (PEO) b) The dispersions of 1) GO 2) G 3) G-PBASE in 5:1 mixture of chloroform/DMF 10 days after ultrasonication c) Image of non-woven electrospun PANi/PEO/G-PBASE mat collected on an aluminium foil.

The electrical conductivities of the electrospun nanofiber were measured by four straight lines probe at room temperature connected to a Solarton SI 1260 Impedance/Gain-phase Analyzer equipped with Solarton 1470 battery test unit. The two outer probes are used for sourcing current

and the two inner probes are used for measuring the resulting voltage drop across the sample, the schematic of the four straight lines probe used is shown in Figure 5-3. Samples were cut in rectangular shapes (3cm × 1cm), the bias sweep of −1 to +1 V at the rate 10 mV/s was performed

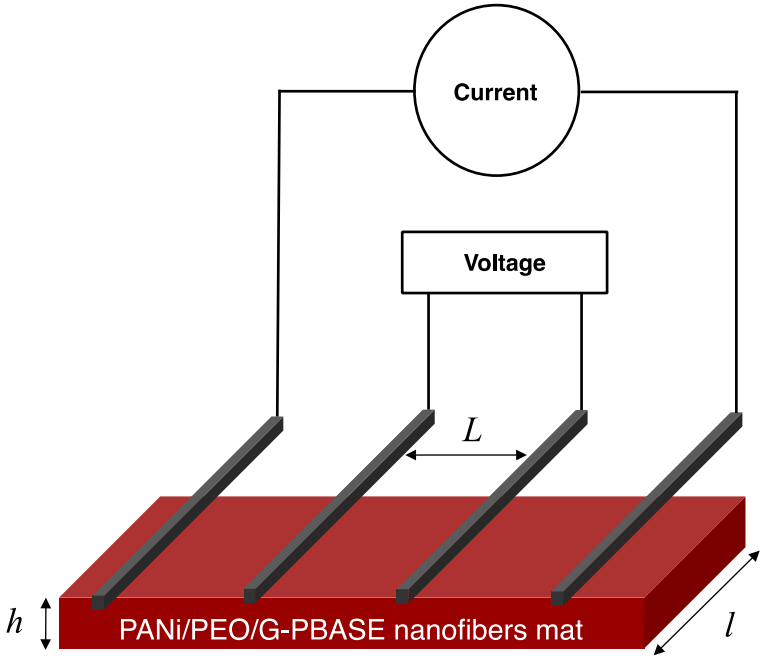

Figure 5-3: Schematic diagram for four-point probe used to measure the conductivity of PANi/PEO/G-PBASE mats.

on samples at room temperature and the current was measured using CorrWare software (Scribner Associates). The conductivity of the samples was calculated using 5-2, where is the conductivity, L is distance between probes, h is thickness of the sample, l is width of the sample, I is current passed through the outer probes, and V is voltage drop across the inner probes.

$$\sigma = \frac{L}{l \times h} \cdot \frac{I}{V} \qquad 5\text{-}2$$

5.3.3 Preparation of graphite oxide (GO)

Graphite oxide was synthesized from graphite by a modified Hummers method (Hummers and Offeman 1958). Briefly, graphite (6 g) and $NaNO_3$ (3 g) were mixed in 150 mL H_2SO_4 in 500 mL flask at 0 °C. The mixture was stirred 30 min before $KMnO_4$ (18 g) was slowly added over a period of 30 min while carefully controlling the temperature to remain below 20 °C. Then, the mixture was stirred at room temperature for 30 min after being kept at 0 °C for 2 h. Thereafter, 300 mL of DI water was slowly added to the mixture with vigorous agitation. The reaction temperature was rapidly increased to 98 °C with effervescence, and the color of the mixture changed to yellow. The diluted suspension was stirred overnight and afterwards the mixture was further treated with 300 mL 30% H_2O_2 solution to reduce residual permanganate to soluble manganese ions. Finally, the resulting suspension was filtered using Whatman Quantitative Filter Papers (Grade 50) and washed with 5% HCl. Then, the filtrate was redispersed in water and filtered and washed several times with DI water until the pH of the filtrate was neutral. Afterwards, the filtrate was dried under vacuum at 50 °C for 24 h and graphite oxide (GO) was obtained as a grey powder.

5.3.4 Reduction of graphite oxide (GO) to PBASE functionalized graphene

GO (1 mg) was dispersed in DMF (10 mL) by sonication (Fischer Scientific, FS110H) until clear, homogenous graphene oxide dispersion is obtained. PBASE-functionalized graphene (G-PBASE) was synthesized by reducing graphene oxide dispersion with hydrazine monohydrate in presence of PBASE. PBASE (1 mg) and hydrazine monohydrate (100 μL) were added to the graphene dispersion and heated to 80 °C under a water-cooled condenser for 24 h. The obtained dispersion

was mixed with ethanol (50mL) and centrifuged at 4500rpm for 1 h to obtain a black precipitate after pouring the supernatant away. The black precipitate was dried at room temperature in vacuum over-night to obtain G-PBASE. The same procedure was used in absence of PBASE, to reduce GO to graphene (G) for comparison.

5.3.5 Electrospinning solution preparation

PANi (10 mg) was mixed with HCSA (13 mg) and dissolved in chloroform (14.78 g) to dope the emeraldine base PANi. This solution was allowed to stir for 24h and subsequently filtered using Whatman Puradisk PTFE syringe filter (pore size, 0.45 μm) to remove the particulate matter. The as-synthesized G-PBASE (5mg) was dispersed in DMF (2.96 g) by sonication for 1 h. Then this solution was mixed with PANi solution and subsequently PEO (10 mg) was added to the solution and stirred for 24 h to form the electrospinning solution. For comparison, PANi/PEO solution was prepared in the same manner only without addition of G-PBASE. The composition of electrospun PANi/PEO/G-PBASE and PANi/PEO solutions is tabulated in Table 1.

Table 5-1: Composition of electrospun PANi/PEO/G-PBASE and PANi/PEO solutions.

PANi (mg)	**HCSA** (mg)	**G-PBASE** (g)	**Chloroform** (g)	**DMF** (g)	**Solution** (wt.%)	**PANi:PEO[a]** (wt.%)	**G:PANi[b]** (wt.%)
10	13	5	14.78	2.96	1.85%	50%	5
10	13	-	14.78	2.96	1.83%	50%	-

[a] PANi concentration to PEO (w/w).

[b] G-PBASE concentration to PANi (w/w).

5.3.6 Electrospinning setup and parameters

Electrospinning was performed using a horizontal set up containing a variable high DC voltage power supply (Gamma High Voltage Research, FL, USA) and a programmable micro-syringe pump (Harvard Apparatus, PHD 2000, USA). The electrospinning solution was poured into a 3 mL glass syringe with Luer–Lock connection to an 18-gauge blunt tip needle (Cadence Science, USA). The syringe was mounted with a grip on the micro-syringe pump and grounded by use of an alligator clip. The nanofibers were collected on an aluminum foil attached on a grounded metal collector. The optimized electrospinning parameters were: flow rate of 5 μL min^{-1}, applied voltage of 10 kV and needle-tip-to-collector distance of 10 cm. All experiments were conducted at room temperature and relative humidity of 2–5%.

5.4 Results and discussion

5.4.1 PBASE functionalized graphene

Graphene was functionalized via noncovalent π–π interactions with PBASE. The functionalized G-PBASE was able to be dispersed in 5:1 mixture of chloroform/DMF and no sedimentation was observed after 10 days where as neat graphene sedimented in the same solution as shown in Figure 5-2 (b). Fourier transform infrared (FTIR) spectroscopy was performed on the synthesized graphite oxide (GO), graphene (G) and PBASE functionalized graphene (G-PBASE) in order to verify the presence of fingerprint functional groups that should be present from the successful reduction of GO to G and non-covalent functionalization of G with PBASE. As depicted in Figure 5-4. The GO spectrum reveals vibration bands corresponding to C=O stretching at 1736 cm^{-1}, C–H stretching at 1219 cm^{-1}, and C–O stretching at 1041 cm^{-1} (Stankovich, Piner et al. 2006, Si and Samulski 2008). Also, the vibrations of the adsorbed water molecules or the skeletal vibrations of non-

oxidized graphitic domains can be observed at 1602 cm^{-1}. In the spectra of G obtained after chemical reduction of GO with hydrazine, some residual presence of bands at 1736, 1219, and 1011 cm^{-1} were detected which provides evidence of the presence of different types of oxygen functionalities on the GO and their decrease in intensity due to chemical reduction (Goncalves, Marques et al. 2009). In the spectrum of G-PBASE the presence of finger print peaks at 1115 cm^{-1} which is due to the stretching vibration of C–C(=O)–O bond of ester, confirms the successful noncovalent functionalization of graphene with PBASE through noncovalent π–π stacking.

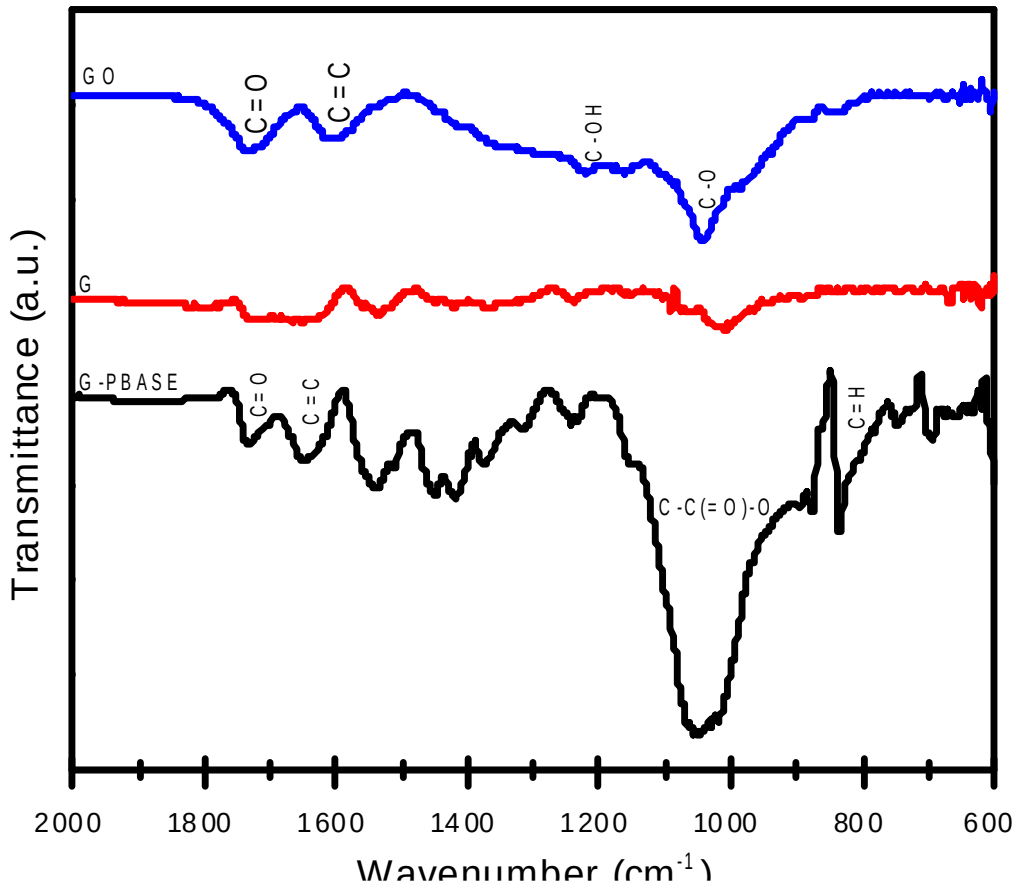

Figure 5-4: FTIR spectra of graphite oxide (GO), graphene (G) and PBASE functionalized graphene (G-PBASE).

Moreover, the peaks at 833 and 1651 cm^{-1} correspond to the out-of-plane vibration of the C–H bond and the C=C stretching vibration of the pyrene ring, respectively. Also, a sharp peak at 1731 cm^{-1} was observed that corresponds to a C=O stretching vibration, demonstrating the presence of the succinimidyl ester in PBASE (Jeong, Lee et al. 2009).

5.4.2 Morphology of electrospun nanofibers

Figure 5-5 shows representative SEM images and fiber diameter distribution of electrospun nanofibers from PANi/PEO solution containing 5 wt.% G-PBASE (wt.% to PANi). For comparison, SEM images of neat PANi/PEO is depicted in Figure 5-6. As illustrated in Figure 5-5 (a), the electrospun fibers form a highly interconnected web, the surfaces of fibers are relatively smooth and the fibers are randomly oriented. However, due to jet instabilities, some small amount of defects (beads) can be observed in Figure 5-5 (b) and (c) (Li and Xia 2004). The same characteristics was observed for PANi/PEO nanofibers, Figure 5-6 (a) to (c). As shown in Figure 5-5 (d), the fiber diameter distribution for PANi/PEO/G-PBASE lies in the range of 100–600 nm with an average diameter of 222 ± 60 nm, where as for PANi/PEO the fiber diameters are in the range of 100–500 nm with an an average diameter of 274 ± 76 nm. This decrease in the average fiber diameter of PANi/PEO/G-PBASE in comparison to PANi/PEO can be attributed to the presence of graphene sheets in the fibers, which give rise to the increased electrical conductivity.

Figure 5-7 (a)–(d) shows representative high-resolution TEM images of PANi/PEO/G-PBASE nanofibers. Figure 5-7 (a) and (b) illustrates that some of the incorporated G-PBASE are randomly embedded in the sidewall of PANi/PEO nanofibers. Moreover, Figure 5-7 (c) shows that individual

graphene sheets are randomly dispersed in the PANi/PEO matrix. Also shown in Figure 5-7 (c) is formation of branched fiber due to the ejection of smaller jets from the surface of the primary jets during the electrospinning process. The reason for this phenomena is the shift of balance between the electrical force and surface tension of the jet during the electrospinning process, which can make the shape of the jet to becomes unstable. This instability can decrease its local charge per

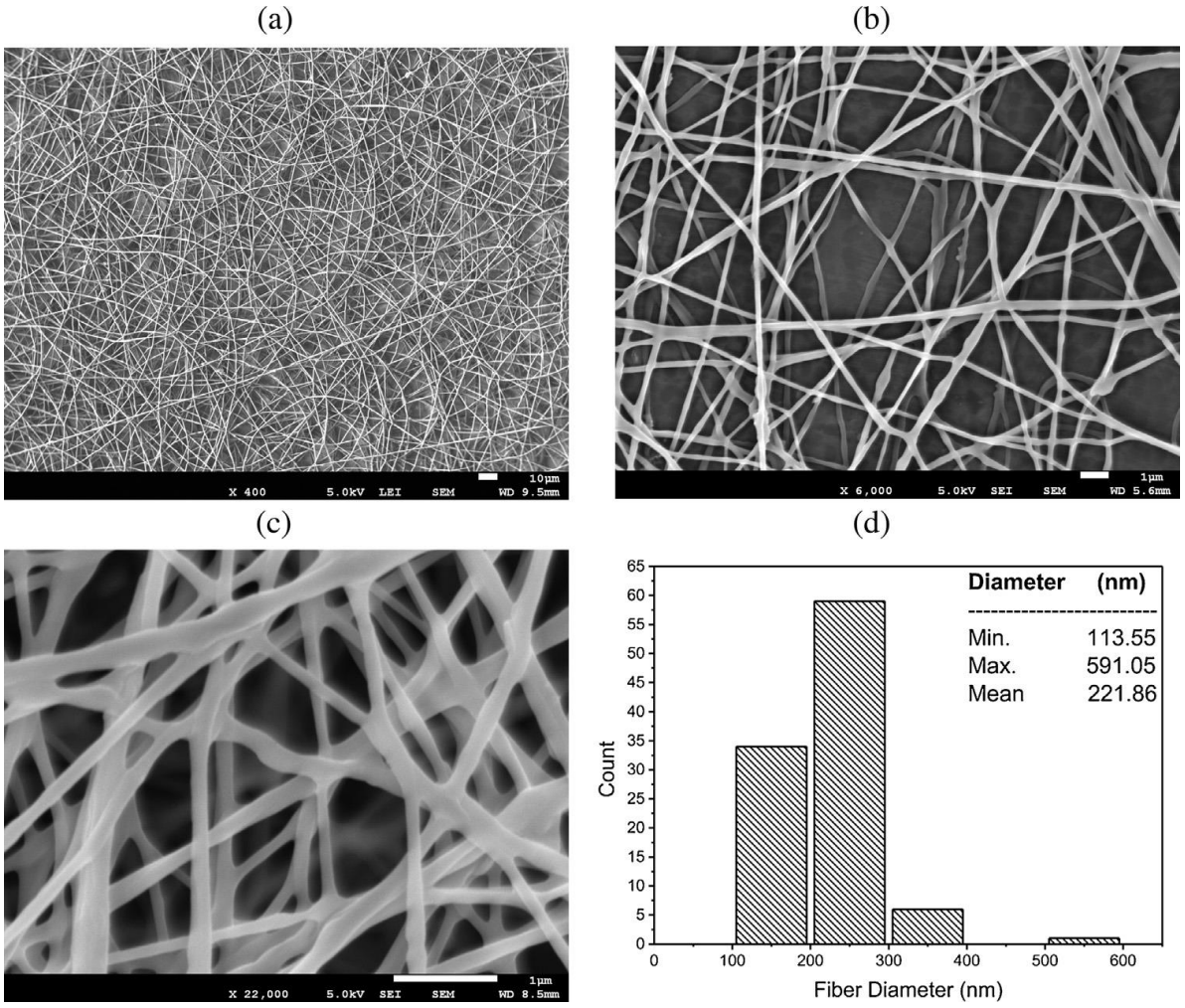

Figure 5-5: (a–c) SEM images of PANi/PEO/G-PBASE nanofibers at different magnification, (d) distribution of diameters of the nanofibers (PANi concentration to PEO = 50 wt.%, PEO concentration to PANi = 50 wt.% and G-PBASE concentration to PANi = 5 wt.%).

unit surface area by ejecting a smaller jet from the surface of primary jet (Ramakrishna 2005).

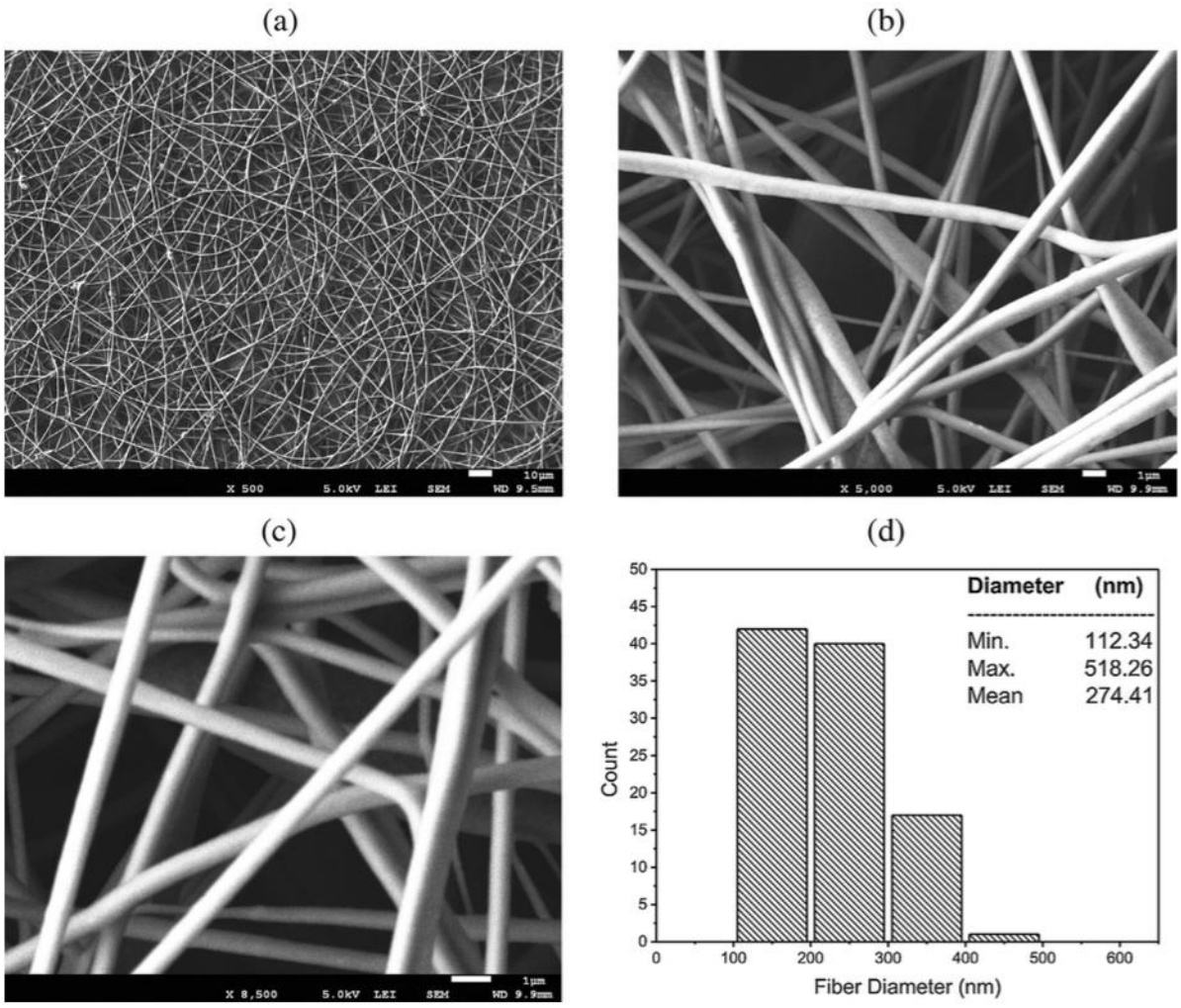

Figure 5-6: (a–c) SEM images of PANi/PEO nanofibers at different magnification, (d) distribution of diameters of the nanofibers (PANi concentration to PEO = 50 wt.%, PEO concentration to PANi = 50 wt.%).

The XPS was used to characterize the surface of PANi/PEO and PANi/PEO/G-PBASE nanofibers to further confirm the presence ofgraphene sheets in the nanofibers. XPS can provide an accurate composition of the surface. Figure 5-8 (a) and (b) shows the high-resolution XPS C1s spectra of PANi/PEO and PANi/PEO/G-PBASE respectively. As can be seen, the C1s spectra is decomposed into four peaks with the binding energy of 285.0eV (C=C and C-C), 285.9 eV (C-N), 286.6 eV (C-O), and 288.3 eV (C=O). The N1s spectra can be decomposed into two peaks with the binding

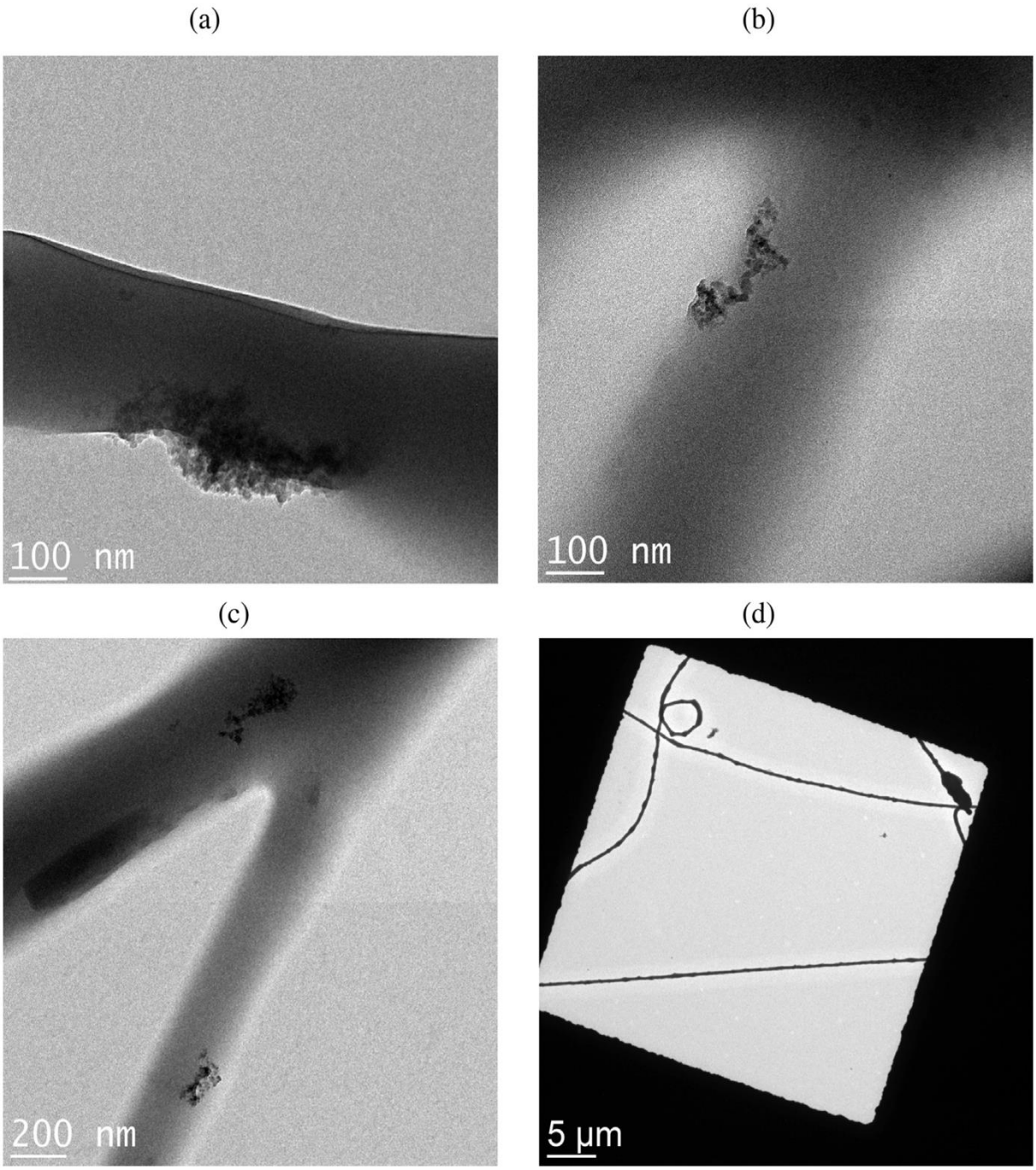

Figure 5-7: (a–c) High-resolution TEM images of PANi/PEO/G-PBASE nanofibers at different magnification, (a) shows an enlarged image of G-PBASE embedded in the sidewall of a PANi/PEO nanofiber (PANi concentration to PEO = 50wt.%, PEO concentration to PANi = 50wt.% and G-PBASE concentration to PANi = 5wt.%). (d) TEM image of PANi/PEO/G-PBASE nanofiber deposited on TEM copper grid with carbon support film.

energy of 399.5 eV (C-N) and 401.5eV (N^+). The relative atomic percent of each of these peaks are tabulated in Table 5-2.

Table 5-2: The relative atomic percent obtained from quantification of fitted peaks to high resolution C1s spectra of PANi/PEO and PANi/PEO/G-PBASE.

Chemical bond	**Binding energy (eV)**	**Relative atomic percent (%)**		**Sensitivity factor[a]**
		PANi/PEO	PANi/PEO/G-PBASE	
C=C and C-C	285.0	43.9	47.4	0.250
C-N	285.9	4.8	0.7	0.250
C-O	286.6	23.4	17.2	0.250
C=O	288.3	2.6	1.5	0.250

[a] Sensitivity factors from the Wagner table are used.

The results indicate that the ratio of C-O to C=C decreases significantly from 0.53 in PANi/PEO to 0.36 in PANi/PEO/G-PBASE. This decrease is due to the presence of graphene sheets in the PANi/PEO/G-PBASE which is expected to cause an increase in C=C groups with respect to the C-O groups which are characteristic of PEO. Similarly, the decrease in nitrogen content relative to C=C functional groups from 0.11 in PANi/PEO to 0.01 in PANi/PEO/G-PBASE confirms the addition of graphene sheets to the latter as this is expected to increase the content of C=C functional groups relative to the nitrogen characterizing the PANi content.

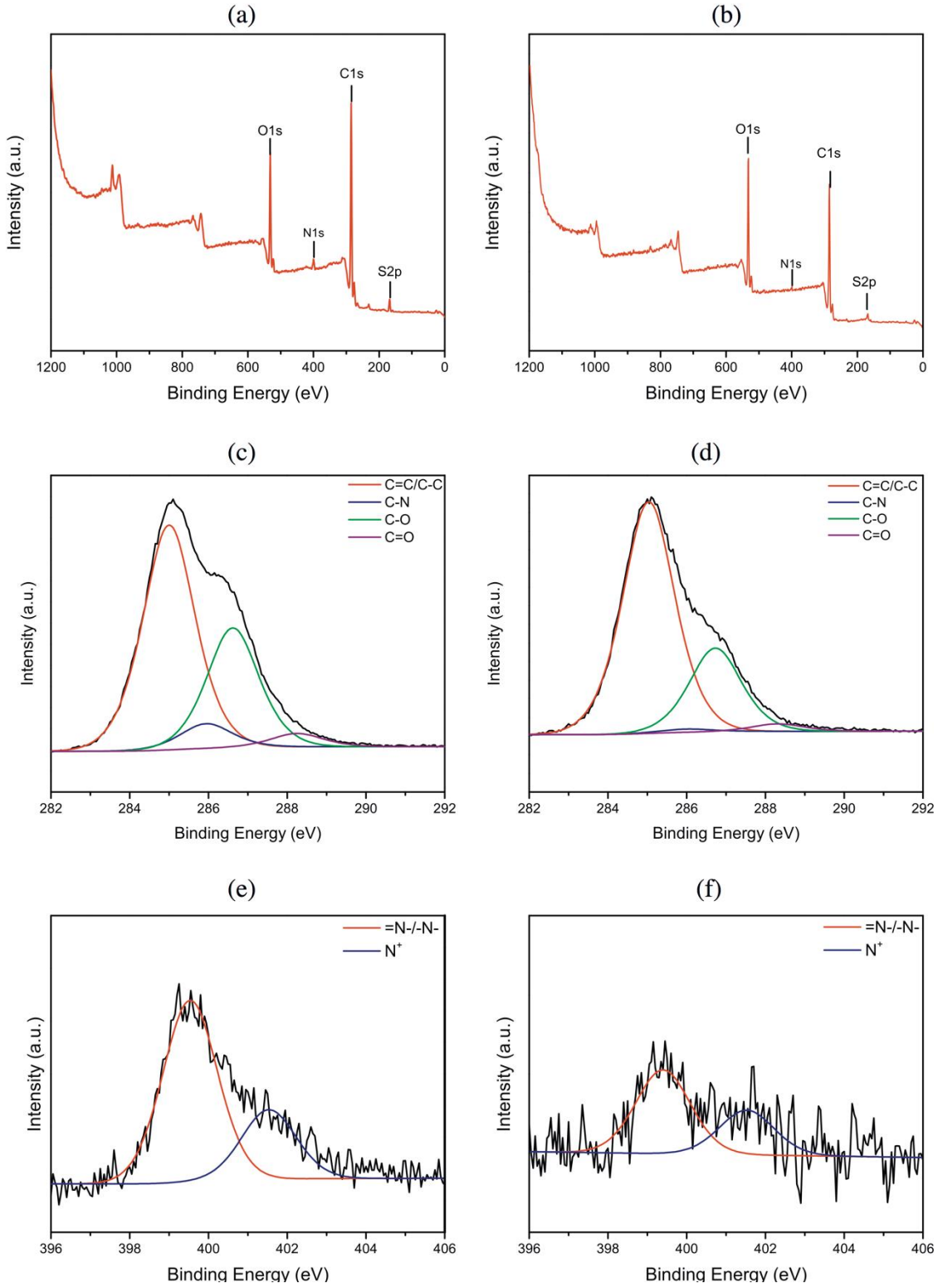

Figure 5-8: (a and b) Survey X-ray photoelectron spectra of PANi/PEO and PANi/PEO/G-PABSE, (c and d) high resolution C1s spectra of PANi/PEO and PANi/PEO/G-PABSE, (e and f) high resolution N1s spectra of PANi/PEO and PANi/PEO/G-PBASE.

5.4.3 Thermal stability

Thermal stability of electrospun PANi/PEO and PANi/PEO/G- PBASE nanofiber mats and bulk G and G-PBASE were measured using TGA in nitrogen atmosphere. Figure 5-9 (a) and (b) shows TGA thermographs and their first-order derivative curves of as spun PANi/PEO and PANi/PEO/G-PBASE, and bulk G and G-PBASE. For PANi/PEO nanofibers, the major weight loss occurs at ~285 °C. The incorporation of G-PBASE (5 wt.% to PANi) increases the onset decomposition temperature of PANi/PEO by 35 °C to ~321 °C. This shows that the incorporation of small amount of graphene in PANi/PEO improves its thermal stability, which can be attributed to the presence

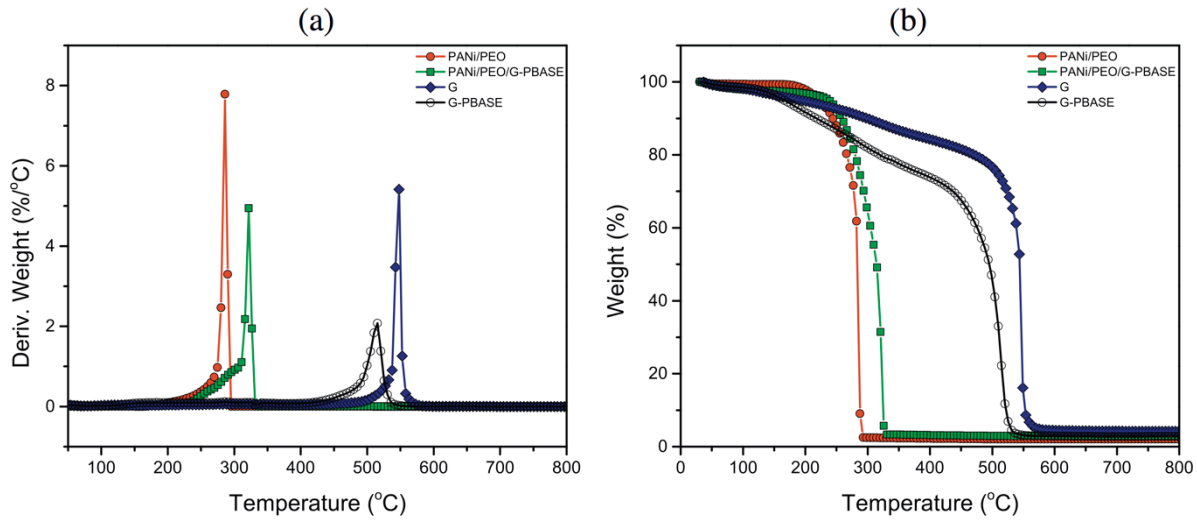

Figure 5-9: (a) TGA thermographs of as spun PANi/PEO and PANi/PEO/G-PBASE and bulk G and G-PBASE, (b) first-order derivative of TGA thermographs.

of interfacial bonding.

5.4.4 Electrical conductivity of nanofibers

Electrical conductivity of the as-prepared PANi/PEO and PANi/PEO/G-PBASE nanofibers mat with relatively same thickness (~200 μm) was measured using four-point probe at room temperature. Figure 5-10 (a) illustrates the I–V curves for PANi/PEO and PANi/PEO/G-PBASE nanofibers. The conducting nanofibers showed a linear ohmic behaviour at applied low voltages of

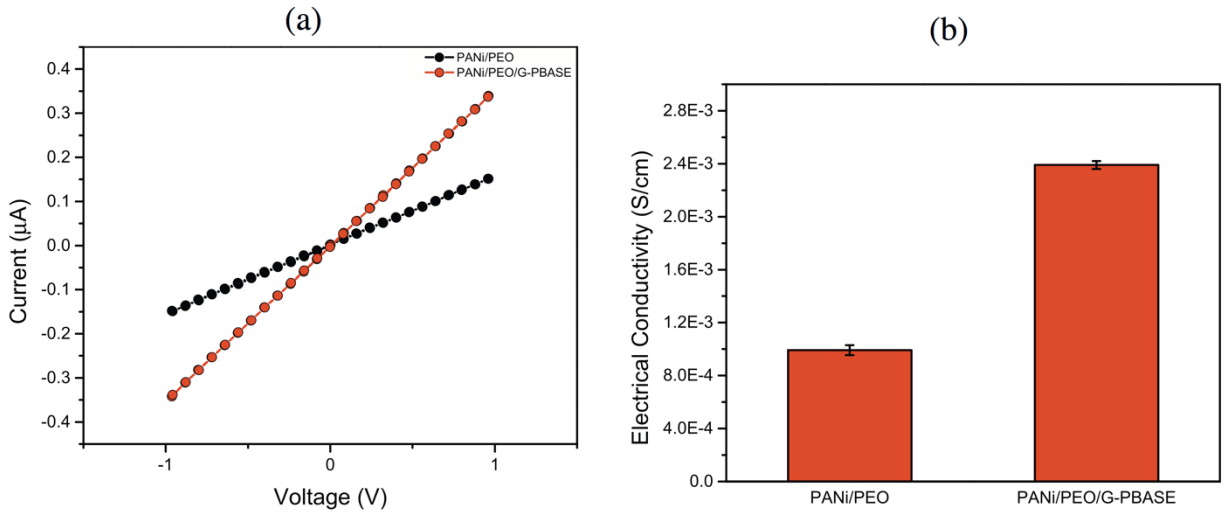

Figure 5-10: (a) I–V curves of PANi/PEO and PANi/PEO/G-PBASE nanofibers mat. (b) Electrical conductivity of PANi/PEO and PANi/PEO/G-PBASE nanofibers mat.

±1V. The I–V curves revealed that, for both nanocomposites, the current was in μA range and PANi/PEO/G-PBASE mats had current flow of more than two orders of magnitude higher than that of PANi/PEO. Figure 5-10 (b) shows the conductivity of PANi/PEO and PANi/PEO/G-PBASE nanofibers calculated from Equation 5-2 and their relative error bar. The electrical conductance for PANi/PEO/G-PBASE and PANi/PEO nanofibers was $2.39 \times 10^{-3} \pm 3.76 \times 10^{-5}$ S/cm and $9.92 \times 10^{-4} \pm 2.94 \times 10^{-4}$ S/cm respectively. As can be seen PANi/PEO/G-PBASE showed about 2.41 times higher conductivity in comparison to PANi/PEO.

5.5 Conclusion

Ultrafine electrospun nanofibers of PANi/PEO filled with G-PBASE were prepared by an electrospinning technique. The morphology of PANi/PEO/G-PBASE nanofibers revealed that the composite nanofibers had a diameter ranging between 160 and 280 nm, with a general uniform thickness along the nanofibers. The thermal degradation temperature of 5 wt.% PANi/PEO/G-PBASE nanofibers was increased to ~ 321 °C, more than one times in magnitudes higher than that of PANi/PEO samples. The electrical conductivity of 5 wt.% PANi/PEO/G-PBASE nanofibers at room temperature was more than 2 orders in magnitude higher than that of PANi/PEO samples. These results demonstrate that the addition of a small amount of G-PBASE to a PANi/PEO matrix can form a conducting network in well-dispersed nanofibers, thus increasing their electrical conductivity.

5.6 Acknowledgments

The authors gratefully acknowledge the financial support of NSERC (National Science and Engineering Research Council of Canada) and FRQNT (Fonds de recherche du Quebec – Nature et technologies). We are grateful to Dr. Josianne Lefebvre for her help with XPS analysis. We also thank Mr. Jean Philippe Masse for his help with TEM imaging.

5.7 References

Balandin, A. A., S. Ghosh, W. Bao, I. Calizo, D. Teweldebrhan, F. Miao and C. N. Lau (2008). "Superior thermal conductivity of single-layer graphene." Nano Letters **8**(3): 902-907.

Bhattacharya, A. and A. De (1996). "Conducting composites of polypyrrole and polyaniline a review." Progress in Solid State Chemistry **24**(3): 141-181.

Bolotin, K. I., K. J. Sikes, Z. Jiang, M. Klima, G. Fudenberg, J. Hone, P. Kim and H. L. Stormer (2008). "Ultrahigh electron mobility in suspended graphene." Solid State Communications **146**(9–10): 351-355.

Cao, Y., P. Smith and A. J. Heeger (1992). "Counter-ion induced processibility of conducting polyaniline and of conducting polyblends of polyaniline in bulk polymers." Synthetic Metals **48**(1): 91-97.

Castro Neto, A. H., F. Guinea, N. M. R. Peres, K. S. Novoselov and A. K. Geim (2009). "The electronic properties of graphene." Reviews of Modern Physics **81**(1): 109-162.

Chaudhari, S., Y. Sharma, P. S. Archana, R. Jose, S. Ramakrishna, S. Mhaisalkar and M. Srinivasan (2013). "Electrospun polyaniline nanofibers web electrodes for supercapacitors." Journal of Applied Polymer Science **129**(4): 1660-1668.

Das, T. K. and S. Prusty (2012). "Review on conducting polymers and their applications." Polymer-Plastics Technology and Engineering **51**(14): 1487-1500.

Georgakilas, V., M. Otyepka, A. B. Bourlinos, V. Chandra, N. Kim, K. C. Kemp, P. Hobza, R. Zboril and K. S. Kim (2012). "Functionalization of graphene: Covalent and non-covalent approaches, derivatives and applications." Chemical Reviews **112**(11): 6156-6214.

Goncalves, G., P. A. A. P. Marques, C. M. Granadeiro, H. I. S. Nogueira, M. K. Singh and J. Grácio (2009). "Surface modification of graphene nanosheets with gold nanoparticles: The role of oxygen moieties at graphene surface on gold nucleation and growth." Chemistry of Materials **21**(20): 4796-4802.

Huang, Z.-M., Y. Z. Zhang, M. Kotaki and S. Ramakrishna (2003). "A review on polymer nanofibers by electrospinning and their applications in nanocomposites." Composites Science and Technology **63**(15): 2223-2253.

Hummers, W. S. and R. E. Offeman (1958). "Preparation of graphitic oxide." Journal of the American Chemical Society **80**(6): 1339-1339.

Jeong, J., S. H. Lee, N. W. Song, C. S. Lee and B. H. Chung (2009). "Functionalization of fullerene nanowhiskers using pyrenebutanoic acid, succinimidyl ester in an aqueous solution." Carbon **47**(8): 2124-2127.

Lee, C., X. Wei, J. W. Kysar and J. Hone (2008). "Measurement of the elastic properties and intrinsic strength of monolayer graphene." Science **321**(5887): 385-388.

Li, D. and R. B. Kaner (2008). "Graphene-based materials." Science **320**(5880): 1170-1171.

Li, D. and Y. Xia (2004). "Electrospinning of nanofibers: Reinventing the wheel?" Advanced Materials **16**(14): 1151-1170.

Lin, Q., Y. Li and M. Yang (2012). "Polyaniline nanofiber humidity sensor prepared by electrospinning." Sensors and Actuators B: Chemical **161**(1): 967-972.

Norris, I. D., M. M. Shaker, F. K. Ko and A. G. MacDiarmid (2000). "Electrostatic fabrication of ultrafine conducting fibers: Polyaniline/polyethylene oxide blends." Synthetic Metals **114**(2): 109-114.

Peng, S., P. Zhu, Y. Wu, S. G. Mhaisalkar and S. Ramakrishna (2012). "Electrospun conductive polyaniline-polylactic acid composite nanofibers as counter electrodes for rigid and flexible dye-sensitized solar cells." RSC Advances **2**(2): 652-657.

Ramakrishna, S. (2005). An introduction to electrospinning and nanofibers, World Scientific.

Rao, P. S., S. Subrahmanya and D. N. Sathyanarayana (2003). "Synthesis by inverse emulsion pathway and characterization of conductive polyaniline–poly(ethylene-co-vinyl acetate) blends." Synthetic Metals **139**(2): 397-404.

Reneker, D. H. and I. Chun (1996). "Nanometre diameter fibres of polymer, produced by electrospinning." Nanotechnology **7**(3): 216.

Ruiz, J., B. Gonzalo, J. R. Dios, J. M. Laza, J. L. Vilas and L. M. León (2013). "Improving the processability of conductive polymers: The case of polyaniline." Advances in Polymer Technology **32**(S1): E180-E188.

Si, Y. and E. T. Samulski (2008). "Synthesis of water soluble graphene." Nano Letters **8**(6): 1679-1682.

Stankovich, S., R. D. Piner, S. T. Nguyen and R. S. Ruoff (2006). "Synthesis and exfoliation of isocyanate-treated graphene oxide nanoplatelets." Carbon **44**(15): 3342-3347.

Stenger-Smith, J. D. (1998). "Intrinsically electrically conducting polymers. Synthesis, characterization, and their applications." Progress in Polymer Science **23**(1): 57-79.

Stoller, M. D., S. Park, Y. Zhu, J. An and R. S. Ruoff (2008). "Graphene-based ultracapacitors." Nano Letters **8**(10): 3498-3502.

Subrahmanyam, K. S., A. Ghosh, A. Gomathi, A. Govindaraj and C. N. R. Rao (2009). "Covalent and noncovalent functionalization and solubilization of graphene." Nanoscience and Nanotechnology Letters **1**(1): 28-31.

Wallace, G. G., P. R. Teasdale, G. M. Spinks and L. A. P. Kane-Maguire (2002). Conductive electroactive polymers: Intelligent materials systems, second edition, CRC Press.

Xu, Y., H. Bai, G. Lu, C. Li and G. Shi (2008). "Flexible graphene films via the filtration of water-soluble noncovalent functionalized graphene sheets." Journal of the American Chemical Society **130**(18): 5856-5857.

Zhang, X., F. Gao, X. Cai, M. Zheng, F. Gao, S. Jiang and Q. Wang (2013). "Application of graphene–pyrenebutyric acid nanocomposite as probe oligonucleotide immobilization platform in a DNA biosensor." Materials Science and Engineering: C **33**(7): 3851-3857.

Zhang, Y. and G. C. Rutledge (2012). "Electrical conductivity of electrospun polyaniline and polyaniline-blend fibers and mats." Macromolecules **45**(10): 4238-4246.

CHAPTER 6 ARTICLE 2: CORE−SHELL STRUCTURED GRAPHENE FILLED POLYANILINE/POLY(METHYL METHACRYLATE) NANOFIBERS BY COAXIAL ELECTROSPINNING

Ali Moayeri, Abdellah Ajji

Accepted in Nanoscience and Nanotechnology Letters

6.1 Abstract

Core−shell structured Polyaniline/Poly(methyl methacrylate) **(**PANi/PMMA) nanofibers embedded with 1-pyrenebutanoic acid, succinimidyl ester functionalized graphene (G-PBASE) is produced using coaxial electrospinning. PANi/G-PBASE and PMMA solutions were used as core and shell layer respectively. The as-prepared PANi/G-PBASE/PMMA nanofibers possessed diameters in the range of 420 nm. Moreover, neat PANi/G-PBASE and PANi nanofibers were obtained by solvent etching of PMMA shell, which reduced the fiber diameter to 230 nm. The morphology of the nanofibers was investigated by scanning electron microscopy (SEM) and transmission electron microscopy (TEM). The core−shell structure and the existence of graphene sheets in the core layer were confirmed by TEM images and FTIR spectroscopy obtained before and after solvent etching of PMMA. The electrical conductivity of the fibers at room temperature were investigated by four-point probe method. The PANi/G-PBASE nanofibers exhibited electrical conductivity as high as of 30.25 S/cm which was 3 times higher than that of neat PANi nanofibers.

6.2 Introduction

Electrospinning is a simple method to produce nanofibers mats with diameters in the nanometer scale (Reneker and Chun 1996, Huang, Zhang et al. 2003). The technique is based on the application of an electrical field in a polymer solution, and it is considered one of the most efficient techniques to fabricate high performance nanofibers mats, with distinct advantages such as very high surface area to volume ratio and porosity (Li and Xia 2004, Greiner and Wendorff 2007).

Polyaniline (PANi) is one of the most researched intrinsically conductive polymers (ICPs) mainly due to its ease of synthesis and interesting doping mechanism (Bhattacharya and De 1996) with applications in solar cells, energy storage devices, gas sensors and light emitting diodes and etc. (Bhadra, Khastgir et al. 2009). It is however daunting to process PANi compared to most other polymers. As it is common among other ICPs, PANi has a fairly rigid backbone because of its high aromaticity and conjugation (Ruiz, Gonzalo et al. 2013). Additionally, PANi has poor solubility in common organic solvents although it can be improved by doping with a protonic acid such as camphor-10-sulfonic acid (HCSA) (Cao, Smith et al. 1992, Rao, Subrahmanya et al. 2003). Furthermore, PANi is available in low-molecular weights (5,000 to 100,000 Da) and do not possess the required elasticity needed for electrospinning (Zhang and Rutledge 2012). Thus, the aforementioned issues limits the electrospinability of PANi.

Blending PANi with materials that facilitate its processing such as an easily electrospinnable copolymers like poly(ethylene oxide) (PEO) is one approach to make PANi electrospinnable, as reported in our previous work (Moayeri and Ajji 2015). However, the presence of an insulator copolymer decreases the fibers conductivity due to dilution of the conducting polymer which is not desirable for applications where high conductivity is required.

The coaxial electrospinning method provides an alternative and effective way of fabricating neat PANi nanofibers. Coaxial electrospinning is an innovative electrospinning method that facilitates the fabrication of unspinable polymer nanofibers with unique core−shell structures (Sun, Zussman et al. 2003, Li and Xia 2004, Yu, Fridrikh et al. 2004). The coaxial spinneret is composed of a smaller capillary placed inside of a bigger capillary to make the coaxial setup. In this technique, two dissimilar solutions are spun simultaneously through the coaxial spinneret to produce the core−shell structured nanofibers with unspinable polymer at the core section (Qu, Wei et al. 2013).

Recently, graphene, a single-atom-thick two-dimensional sheet of sp^2-hybrized carbon atoms arranged in a honeycomb crystal structure, has attracted a lot of research interest and it is been considered as a "rising-star" carbon material (Stankovich, Dikin et al. 2006). Graphene has been intensively researched because of its remarkable properties such as high electrical (Bolotin, Sikes et al. 2008), thermal conductivities (Balandin, Ghosh et al. 2008), high mechanical strength (Lee, Wei et al. 2008) and large surface area (Stoller, Park et al. 2008). Given the excellent electrical conductivity and electron mobility at room temperature of graphene, a highly conductive graphene-based polymer nanocomposite may be obtained. In this work, we report the preparation of neat polyaniline nanofibers filled with highly dispersed as graphene sheets. The coaxial electrospinning process was used to produce core-shell structured fibers of a poly(methyl methacrylate) (shell) and a polyaniline (core) embedded with highly dispersed graphene nanosheets. The insulating shell was selectively removed by solvent etching. The schematics of this process is illustrated in Figure 6-1. Scanning electron microscopy (SEM), transmission electron microscopy (TEM), Fourier transform infrared (FTIR) spectroscopy and electrical conductivity measurements by four-point probe setup were utilized to characterize these nanofibers. The as-synthesized nanofibers have potential

applications in sensors for gas or pathogen detection due their high surface area, possibility of further functionalization for selective detection and electrical properties.

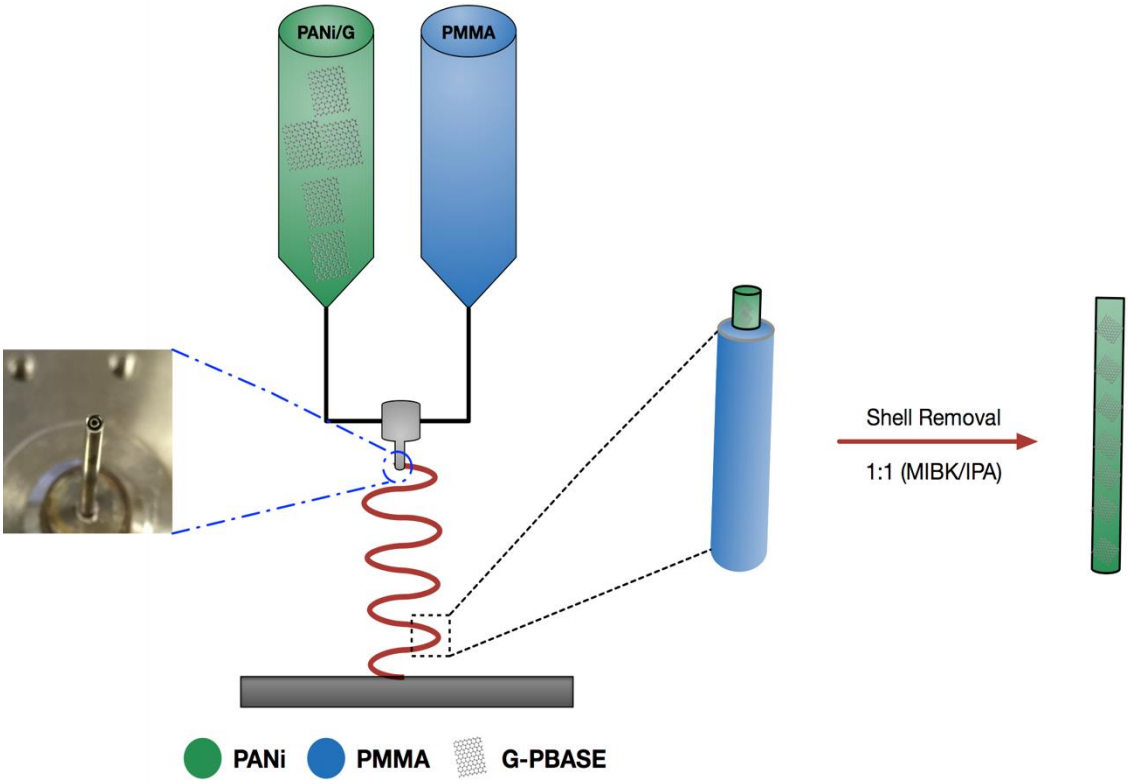

Figure 6-1: Schematic representation of the fabrication of PANi/G-PBASE/PMMA nanofibers by coaxial electrospinning and subsequent shell layer removal by 1:1 (v/v) mixture of MIBK/IPA for obtaining neat PANi/G-PBASE nanofibers.

6.3 Experimental

6.3.1 Materials

Graphite powder (<20 μm, synthetic), polyaniline (PANi, emeraldine base, M_w = 65,000 g mol^{-1}), poly(methyl methacrylate) (PMMA, M_w = 996,000 g mol^{-1}), 1-pyrenebutanoic acid, succinimidyl

ester (PBASE), camphor-10-sulfonic acid (HCSA, 98%), N,N-dimethylformamide (DMF, 99.8%), chloroform ($CHCl_3$, ≥99%), ethanol (CH_3CH_2OH, denatured), hydrochloric acid (HCl, 37%), sulfuric acid (H_2SO_4, 98%), hydrogen peroxide (H_2O_2, 30%), sodium nitrate ($NaNO_3$, ≥99.0%), hydrazine monohydrate (N_2H_4, 98%), methyl isobutyl ketone (MIBK), isopropyl alcohol (IPA, ≥99.5%) were all purchased from Sigma Aldrich. Osmium tetroxide (OsO_4) was purchased from Electron Microscopy Sciences. All chemicals were reagent grade and were used as received. Deionized (DI) water (Millipore Milli-Q) was used for all the experiments.

6.3.2 Characterization

SEM measurements were carried out on a field emission scanning electron microscope (JEOL JSM-7600TFE) at 5kV in LEI mode. Samples were cut from an electrospun mat on the aluminum foil and mounted on metal stubs using a double-sided adhesive tape. Prior to examination, the samples were vacuum-coated with gold sputtering layer to avoid charge accumulation. SEM images were captured in resolution of 1280 × 1240 pixels. Diameters and distributions of the electrospun nanofibers were analyzed from the SEM images by using Image J analysis software (Image J, National Institutes of Health, USA). For each electrospun mat, 100 fibers were considered from different locations on the sample to calculate the average diameter. The dispersion of graphene in the fibers and the core-shell structure was characterized by transmission electron microscopy (TEM, JEOL, JEM 2100F). For TEM observation, fibers were directly deposited onto a TEM copper grid with supporting carbon film (CF400-Cu, Electron Microscopy Sciences). TEM grids were stained with 20 μL of osmium tetroxide for 1 min to improve the contrast. Osmium tetroxide attacks the amide bond in polyaniline giving it a darker contrast compared to the PMMA. Fourier transform infrared (FTIR) spectroscopy analysis was carried out using Perkin Elmer 65

FTIR-ATR instrument. A total of 128 scans were accumulated for the signal averaging of each IR spectral measurement with a 4 cm^{-1} resolution. The spectra of the samples were recorded over a wavenumber range of 4000–650 cm^{-1}. The electrical conductivities of the electrospun nanofiber were measured by four straight lines probe at room temperature connected to a Solarton SI 1260 Impedance/Gain-phase Analyzer equipped with Solarton 1470 battery test unit. Samples were cut in 2 cm × 2 cm squares prior to measurements. The equipment was controlled with a custom coded LabView program with correction factor as a function of the ratio of thickness to probe tip spacing already implemented. Samples were cut in 2 cm × 2 cm squares prior to measurements.

6.4 Synthesis of PBASE-functionalized graphene

Graphite oxide (GO) was synthesized from graphite by a modified Hummers method (Hummers and Offeman 1958) as reported before (Moayeri and Ajji 2015). GO (1 mg) was dispersed in DMF (10 mL) by sonication until clear, homogenous graphene oxide dispersion is obtained. PBASE-functionalized graphene (G-PBASE) was synthesized by reducing graphene oxide dispersion with hydrazine monohydrate in presence of PBASE. PBASE (1 mg) and hydrazine monohydrate (100 μL) were added to the graphene dispersion and heated to 80 °C under a water-cooled condenser for 24 h. The obtained dispersion was mixed with ethanol (50mL) and centrifuged at 4500rpm for 1 h to obtain a black precipitate after pouring the supernatant away. The black precipitate was dried at room temperature in vacuum over-night to obtain G-PBASE.

6.5 Preparation of the Electrospinning solutions

PANi (220 mg) was mixed with HCSA (280 mg) and dissolved in chloroform (20 g) to dope the emeraldine base PANi. This solution was allowed to stir for 24 h and subsequently filtered using Whatman Puradisk PTFE syringe filter (pore size, 0.45 μm) to remove the considerable particulate matter. The as-synthesized G-PBASE (22 mg) was dispersed in DMF (4 g) by sonication for 1h and subsequently added to the PANi solution. The mass ratio of G-PBASE to PANi was predetermined to be maintained at 5 wt.% because firstly, it was observed that increasing the graphene content more than 5 wt.% promotes formation of the defects in the electrospun fibers due to changing solution properties and secondly, to have maximum conductivity enhancement by inclusion of maximum graphene content possible. For comparison, the same solution was prepared without G-PBASE. The stability of G-PBASE in the DMF is investigated in our previous work (Moayeri and Ajji 2015). PMMA solution was prepared at the concentration of 5% (w/w) by dissolving PMMA powder in DMF. Detailed contents of solutions are listed in Table 6-1.

Table 6-1: The electrospinning solutions contents

Sample	Solution	Conc. (wt%)	PANi (g)	HCSA (g)	G (g)	PBASE (g)	PMMA (g)	Chloroform (g)	DMF (g)	G:PANi[a)] (wt%)
PANi/PMMA	Core	2.24%	0.220	0.286				20	4	
	Shell	5.03%					1.06		20	
PANi/G-PBASE/PMMA	Core	2.06%	0.220	0.286	0.022	0.012		20	4	5.1%
	Shell	5.03%					1.06		20	

[a)] G concentration to PANi (w/w).

6.6 Electrospinning Setup and Processing Parameters

Coaxial electrospinning was performed using a horizontal setup containing a variable high DC voltage power supply (Gamma High Voltage Research, USA) and two programmable microsyringe pump (Harvard Apparatus, PHD 2000, USA). PANi or PANi/G-PBASE solutions (core) and PMMA solution (shell) were poured into two 10 mL glass syringe and mounted on each pumps. The syringes were connected by plastic tubing plastic tubing and Luer-Lock connections to the inlets of a coaxial spinneret (Linari Engineering, Pisa, Italy). The coaxial spinneret was comprised of a 21-gauge inner needle (i.d. 0.510 mm, o.d. 0.830 mm) concentrically mounted on a 15-gauge outer needle (i.d. 1.370 mm, o.d. 1.83 mm) and was was connected to the power supply by an alligator clip. The fibers were collected on an aluminum foil attached to a stationary collector screen situated at a certain distance from the tip of the needle.. The optimized electrospinning processing parameters were: flow rates of 0.3 mL hr^{-1} and 0.6 mL hr^{-1} for core and shell solutions respectively, applied voltage of 15 kV and needle-tip-to-collector distance of 15 cm. All experiments were conducted at room temperature and relative humidity of 2–5%. The reproducibility of mats was tested for 4 times.

6.6.1 Removal of PMMA from shell layer

The core-shell electrospun nanofibers of PANi/PMMA and PANi/G/PMMA were removed from the aluminum foil and submerged in a 1:1 (v/v %) mixture of methyl isobutyl ketone (MIBK)/ Isopropyl alcohol (IPA) (MIBK/IPA) for 2 h for removal of PMMA shell component. The shell removed nanofibers were then dried in vacuum oven at 50 °C for 24 h.

6.7 Results and discussion

6.7.1 Morphology

In this experimental study, neat PANi nanofibers embedded with graphene sheets (PANi/G-PBASE) were produced after removal shell segment by solvent etching. A 1:1 (v/v) mixture of methyl isobutyl ketone (MIBK)/isopropanol (IPA) (MIBK/IPA) was used for selective removal of the shell structure (PMMA).

The representative SEM micrographs of coaxial nanofibers of PANi/G-PBASE/PMMA, PANi/PMMA, and shell etched PANi and PANi/G-PBASE are shown in Figure 6-2 (a-d). As shown in Figure 6-2 (a) and (b) the surface of (a) PANi/PMMA and (b) PANi/G-PBASE/PMMA nanofibersare smooth and soft. Moreover, the electrospun fibers are randomly oriented and are highly interconnected. In Figure 6-2 (b) some of the graphene sheets can be observed. Figure 6-2 (c) and (d) illustrate SEM images of shell etched samples of (c) PANi and (d) PANi/G-PBASE respectively. As it is evident, the samples surface morphology became rougher after shell removal process and some the fibers network become broken. The average fiber diameter (AFD) of PANi/G-PBASE/PMMA and PANi/PMMA was in the range of 400 nm and 420 respectively. The slight decrease in the AFD because of graphene addition was expected due to reduction of electrospinning solution viscosity. As it is evident, the AFD of electrospun fibers decrease with the removal of PMMA to around 230 nm.

The characterization of as-prepared nanofibers by TEM provided accurate information about the structure and thickness of core-shell layers and the position of graphene sheets in the nanofibers. Figure 6-3 (a-d) shows representative TEM images of coaxial nanofibers of PANi/G-PBASE/PMMA and PANi/PMMA, and shell etched PANi and PANi/G-PBASE nanofibers.

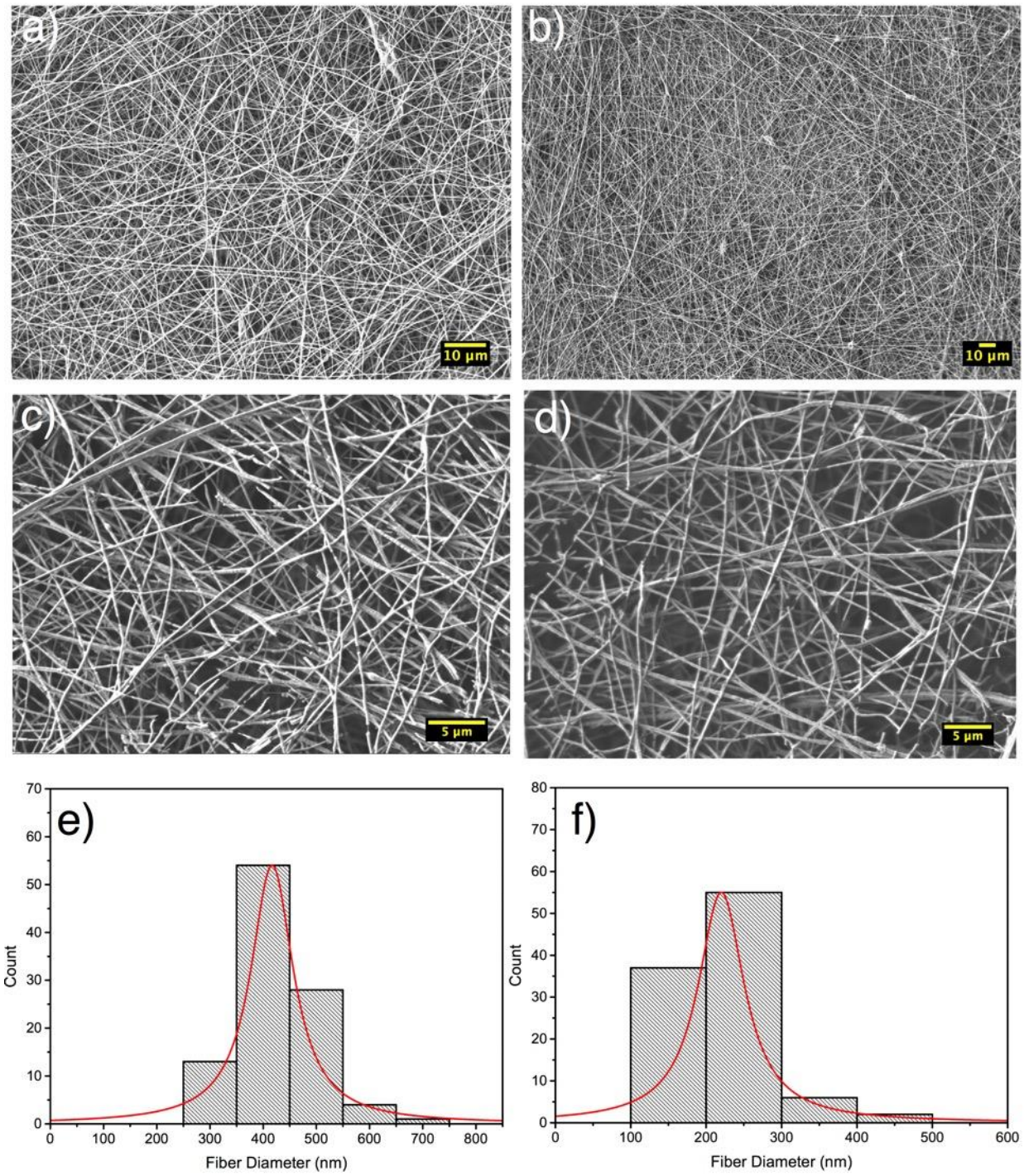

Figure 6-2: Representative SEM images of coaxial electrospun nanofibers of (a) PANi/PMMA, (b) PANi/G-PBASE/PMMA, and (c) PANi, (d) PANi/G-PBASE after removal of PMMA shell. Histograms of fiber diameter, distribution and average fiber diameter (AFD) of (e) PANI/G-PBASE/PMMA and (f) PANi/G-PBASE fibers.

The detailed morphology of the produced coaxial PANi/PMMA and PANi/G-PBASE/PMMA nanofibers is shown in a TEM micrograph in Figure 6-3 (a) and (b). The contrast which is created by electron beam diffraction represents the distinctive phases in the nanofibers. These dark and bright regions represent the core and shell of the nanofiber, respectively with PANi at core and PMMA at shell. Also, shown in Figure 6-3 (b) is the existence of the graphene sheet in the core layer of the nanofiber. Figure 6-3 (c) and (d) are representative TEM micrographs of PANi and

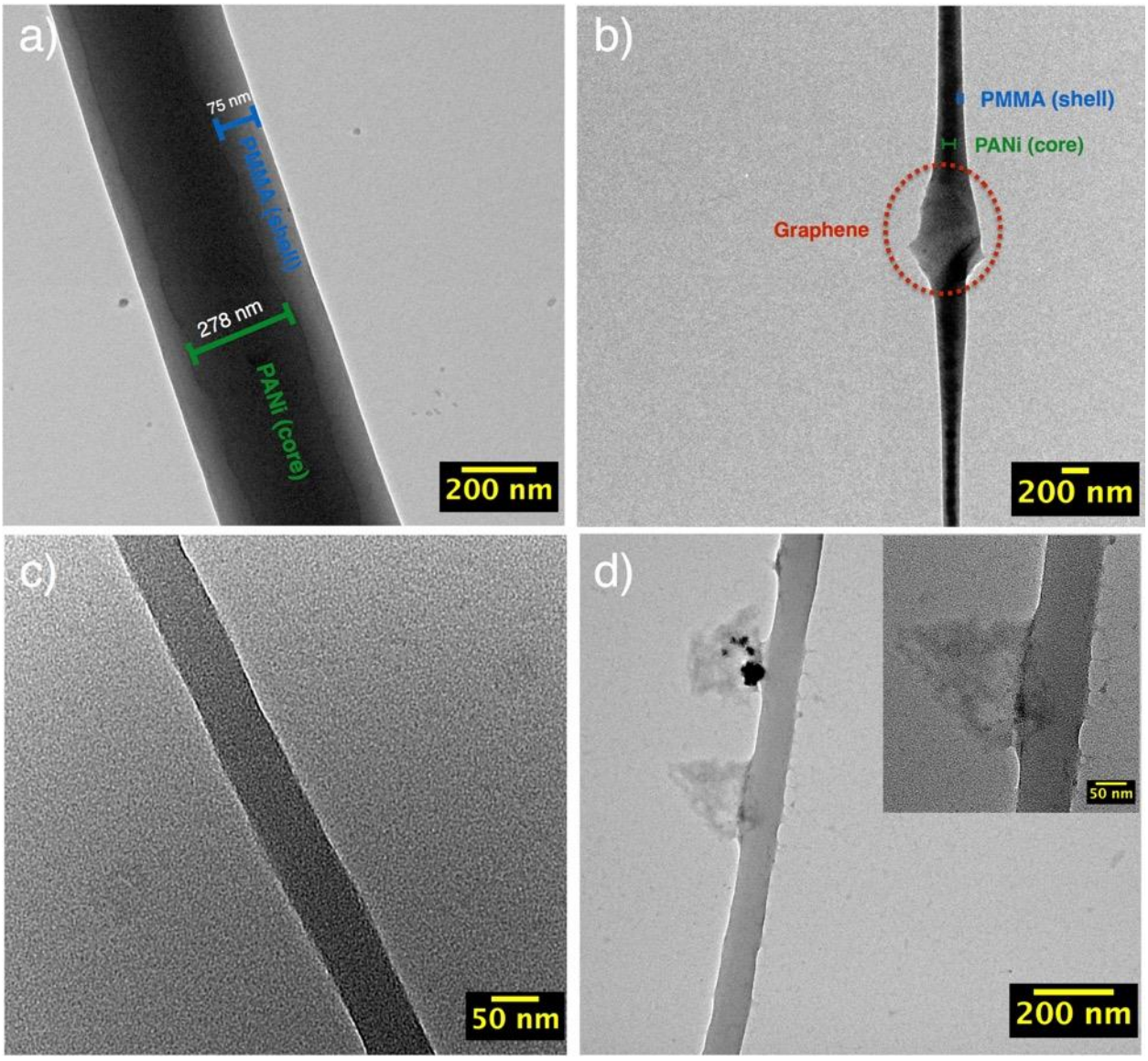

Figure 6-3: Representative TEM micrographs of electrospun (a) PANi/PMMA (b) PANi/PMMA/G, (c) PANi and (d) PANi/G after removal of PMMA shell with 1:1 (v/v) mixture of MIBK:IPA. The inset in (d) shows the higher resolution image of graphene sheet embedded in PANi.

PANi/G-PBASE after removal of PMMA shell. As it is evident, PMMA shell is removed and only the core layer is intact. As shown in Figure 6-3 (d), the graphene sheets are still present and connected to the core layer after the solvent etching process. The detailed morphology of the produced coaxial PANi/PMMA and PANi/G-PBASE/PMMA nanofibers is shown in a TEM micrograph in Figure 6-3 (a) and (b). The contrast which is created by electron beam diffraction represents the distinctive phases in the nanofibers. These dark and bright regions represent the core and shell of the nanofiber, respectively with PANi at core and PMMA at shell. Also, shown in Figure 6-3 (b) is the existence of the graphene sheet in the core layer of the nanofiber. Figure 6-3 (c) and (d) are representative TEM micrographs of PANi and PANi/G-PBASE after removal of PMMA shell. As it is evident, PMMA shell is removed and only the core layer is intact. As shown in Figure 6-3 (d), the graphene sheets are still present and connected to the core layer after the solvent etching process.

6.7.2 Chemical composition of nanofibers by FTIR

FTIR spectroscopy was used to confirm the material composition of core-shell structured PANi/G-PBASE/PMMA nanofibers before and removal of PMMA. As illustrated in Figure 6-4, the spectra associate to core-shell PANi/G-PBASE/PMMA reveals main vibrations that are characteristics of PMMA and the peaks attributed to PANi and G-PBASE was not detected due to strong presence of PMMA on the shell layer. The peaks at 1730 cm^{-1} due to C=O vibration stretching of the esters and the peak at 1147 cm^{-1} due to C–O–C vibration stretching of PMMA was observed {Mbese, 2014 #310}. After removal of PMMA, the resulting nanofiber spectrum revealed vibrations that are main characteristics of PANi. Namely, the bands at 1495 cm^{-1} and 1592 cm^{-1} corresponding to C=N and C=C stretching mode of vibration for the quinonoid and benzenoid units of PANi was

detected (Sudha, Kumar et al. 2013). In addition, in contrast to the featureless spectrum of graphene, the peak due to stretching vibration of C-C(=O)-O bond of ester for G-PBASE was observed at 824 cm^{-1} (Jeong, Lee et al. 2009). These fingerprint functional groups prove that PMMA shell layer was successfully removed and remnant is the PANi core layer and graphene sheets are intact, as also exhibited by TEM results.

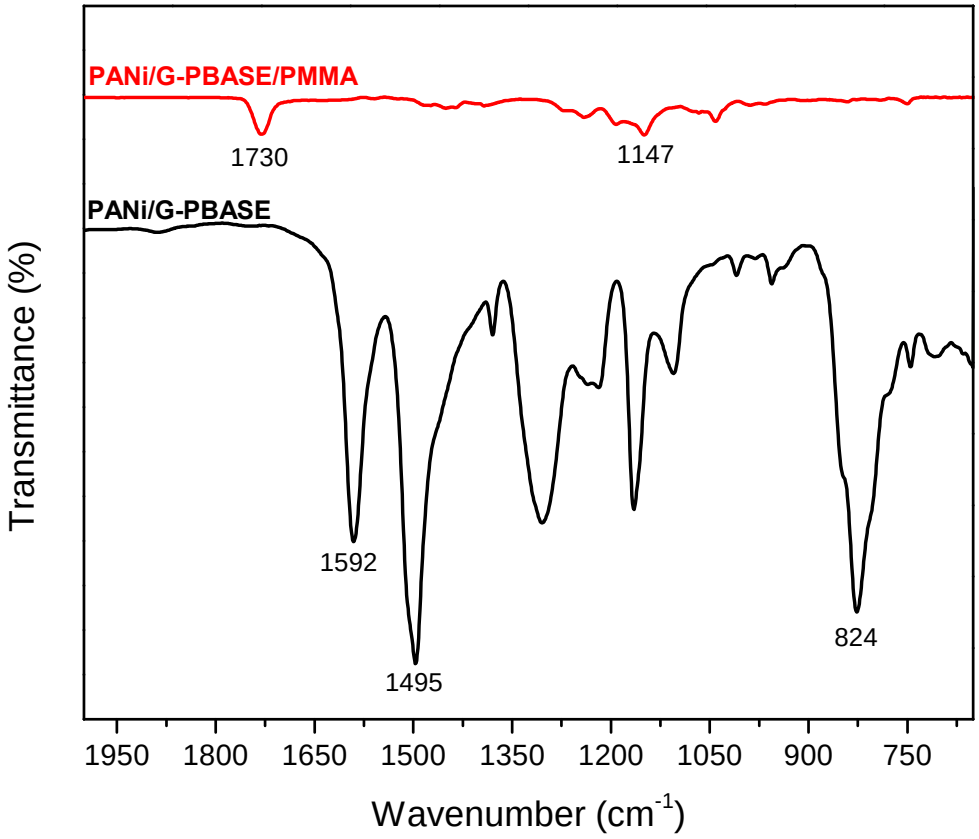

Figure 6-4 : FTIR spectra of core-shell structured PANi/G-PBASE/PMMA and PANi/G-PBASE.

6.7.3 Electrical conductivity of nanofibers

Electrical conductivity of the as-prepared nanofibers of PANi and PANi/G-PBASE with relatively same thickness (~200 μm) was measured using four-point probe at room temperature. The I-V curves for PANi and PANi/G-PBASE nanofibers is illustrated in the Figure 6-5. The conducting nanofibers showed a linear ohmic behavior at applied low voltages of ±1V. The I–V curves revealed that, for both nanofibers, the current was in A range and PANi/G-PBASE mats had current flow of more than three orders of magnitude higher than that of neat PANi.

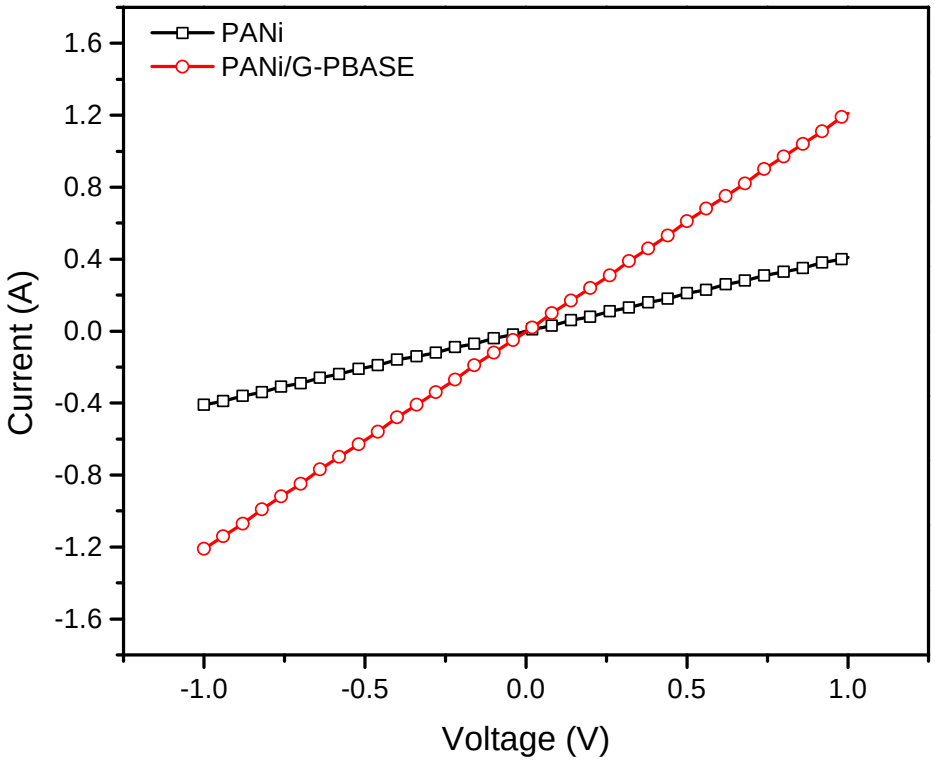

Figure 6-5: I–V curves of PANi and PANi/G-PBASE electrospun mat measured by four-point probe from -1 V to +1 V.

The conductivities of the nanofibers was calculated using the Equation , where σ is the conductivity, L is distance between the probes, h is the thickness of the sample, l is the width of the sample, I is current passed through the outer probes, and V is voltage drop across the inner probes.

$$\sigma = \frac{L}{l \times h} \cdot \frac{I}{V} \qquad 6\text{-}1$$

Utilizing the equation 1, the electrical conductivity for PANi and PANi/G-PBASE nanofibers was calculated $10.75 \pm 4.52 \times 10^{-7}$ S/cm and $30.25 \pm 2.83 \times 10^{-6}$ S/cm respectively. As an example for PANi/G-PBASE, the following values were used to calculate the conductivity: I=0.95 A**,** V=1.13 V, w=2 cm, L=0.5 cm and h= 0.00983 cm. As can be seen PANi/G-PBASE showed 3 times higher conductivity in comparison to neat PANi. These graphene filled nanofibers had significantly higher conductivity compared to fabrication method reported before[11] which exhibited conductivity in the range of 2.39×10^{-3} S/cm. However, the conductivity of as-synthesized nanofibers is still lower than that of PANi films or microfibers with conductivities as high as 600 S/cm[25] but as discussed the prepared PANi/G-PBASE nanofibers have properties that are advantageous for application in chemoresistive sensors.

6.8 Conclusion

Polyaniline is a polymer that is daunting to be electrospun. In this work we were able to produce core−shell structured PANi/PMMA embedded with 1-pyrenebutanoic acid, succinimidyl ester functionalized graphene (G-PBASE) nanofibers using coaxial electrospinning. The nanofibers had average fiber diameters in the range of 400 to 420. Core-shell structure of nanofibers and the

presence of graphene sheets was confirmed by TEM imaging. The PMMA shell layer was removed by solvent etching to obtain neat PANi and PANi/G-PBASE nanofibers, the occurrence of this process was verified by TEM imaging and reduced the AFD to 200 to 230 nm . The electrical conductivity of 5 wt.% PANi/G-PBASE nanofibers at room temperature was 3 times higher than that of neat PANi samples. These results demonstrate that the addition of a small amount of G-PBASE to a PANi matrix can form a conducting network in well-dispersed nanofibers, thus increasing their electrical conductivity.

6.9 Acknowledgments

The authors gratefully acknowledge the financial support of NSERC (National Science and Engineering Research Council of Canada) and FRQNT (Fonds de recherche du Quebec – Nature et technologies).

6.10 References

Balandin, A. A., S. Ghosh, W. Bao, I. Calizo, D. Teweldebrhan, F. Miao and C. N. Lau (2008). "Superior thermal conductivity of single-layer graphene." Nano Letters **8**(3): 902-907.

Bhadra, S., D. Khastgir, N. K. Singha and J. H. Lee (2009). "Progress in preparation, processing and applications of polyaniline." Progress in Polymer Science **34**(8): 783-810.

Bhattacharya, A. and A. De (1996). "Conducting composites of polypyrrole and polyaniline a review." Progress in Solid State Chemistry **24**(3): 141-181.

Bolotin, K. I., K. J. Sikes, Z. Jiang, M. Klima, G. Fudenberg, J. Hone, P. Kim and H. L. Stormer (2008). "Ultrahigh electron mobility in suspended graphene." Solid State Communications **146**(9–10): 351-355.

Cao, Y., P. Smith and A. J. Heeger (1992). "Counter-ion induced processibility of conducting polyaniline and of conducting polyblends of polyaniline in bulk polymers." Synthetic Metals **48**(1): 91-97.

Greiner, A. and J. H. Wendorff (2007). "Electrospinning: A fascinating method for the preparation of ultrathin fibers." Angewandte Chemie (International Ed. in English) **46**(30): 5670-5703.

Huang, Z.-M., Y. Z. Zhang, M. Kotaki and S. Ramakrishna (2003). "A review on polymer nanofibers by electrospinning and their applications in nanocomposites." Composites Science and Technology **63**(15): 2223-2253.

Hummers, W. S. and R. E. Offeman (1958). "Preparation of graphitic oxide." Journal of the American Chemical Society **80**(6): 1339-1339.

Jeong, J., S. H. Lee, N. W. Song, C. S. Lee and B. H. Chung (2009). "Functionalization of fullerene nanowhiskers using pyrenebutanoic acid, succinimidyl ester in an aqueous solution." Carbon **47**(8): 2124-2127.

Lee, C., X. Wei, J. W. Kysar and J. Hone (2008). "Measurement of the elastic properties and intrinsic strength of monolayer graphene." Science **321**(5887): 385-388.

Li, D. and Y. Xia (2004). "Direct fabrication of composite and ceramic hollow nanofibers by electrospinning." Nano Letters **4**(5): 933-938.

Li, D. and Y. Xia (2004). "Electrospinning of nanofibers: Reinventing the wheel?" Advanced Materials **16**(14): 1151-1170.

Moayeri, A. and A. Ajji (2015). "Fabrication of polyaniline/poly(ethylene oxide)/non-covalently functionalized graphene nanofibers via electrospinning." Synthetic Metals **200**: 7-15.

Qu, H., S. Wei and Z. Guo (2013). "Coaxial electrospun nanostructures and their applications." Journal of Materials Chemistry A **1**(38): 11513-11528.

Rao, P. S., S. Subrahmanya and D. N. Sathyanarayana (2003). "Synthesis by inverse emulsion pathway and characterization of conductive polyaniline–poly(ethylene-co-vinyl acetate) blends." Synthetic Metals **139**(2): 397-404.

Reneker, D. H. and I. Chun (1996). "Nanometre diameter fibres of polymer, produced by electrospinning." Nanotechnology **7**(3): 216.

Ruiz, J., B. Gonzalo, J. R. Dios, J. M. Laza, J. L. Vilas and L. M. León (2013). "Improving the processability of conductive polymers: The case of polyaniline." Advances in Polymer Technology **32**(S1): E180-E188.

Stankovich, S., D. A. Dikin, G. H. B. Dommett, K. M. Kohlhaas, E. J. Zimney, E. A. Stach, R. D. Piner, S. T. Nguyen and R. S. Ruoff (2006). "Graphene-based composite materials." Nature **442**(7100): 282-286.

Stoller, M. D., S. Park, Y. Zhu, J. An and R. S. Ruoff (2008). "Graphene-based ultracapacitors." Nano Letters **8**(10): 3498-3502.

Sudha, D. Kumar and M. Iwamoto (2013). "Investigation of the chiroptical behavior of optically active polyaniline synthesized from naturally occurring amino acids." Polym J **45**(2): 160-165.

Sun, Z., E. Zussman, A. l. Yarin, J. h. Wendorff and A. Greiner (2003). "Compound core–shell polymer nanofibers by co-electrospinning." Advanced Materials **15**(22): 1929-1932.

Yu, J. H., S. V. Fridrikh and G. C. Rutledge (2004). "Production of submicrometer diameter fibers by two-fluid electrospinning." Advanced Materials **16**(17): 1562-1566.

Zhang, Y. and G. C. Rutledge (2012). "Electrical conductivity of electrospun polyaniline and polyaniline-blend fibers and mats." Macromolecules **45**(10): 4238-4246.

CHAPTER 7 ARTICLE 3: HIGH CAPACITANCE CARBON NANOFIBERS FROM POLYACRYLONITRILE AND POLYVINYLPYRROLIDONE-FUNCTIONALIZED GRAPHENE BY ELECTROSPINNING

Ali Moayeri, Abdellah Ajji

Submitted to Journal of Nanoscience and Nanotechnology

7.1 Abstract

Core–shell structured carbon nanofibers embedded with various amounts of non-covalently functionalized graphene were fabricated by single-nozzle electrospinning technique using phase-separated solution of polyacrylonitrile and polyvinylpyrrolidone (PAN/PVP) in N,N-dimethylformamide (DMF). The concentration of graphene varied from 0 wt. % to 15 wt. % (relative to PAN). These core-shell structured electrospun nanofibers were first stabilized at 250 °C in air and consecutively carbonized at 850 °C in nitrogen atmosphere. The resulting ultra-fine fibers possessed average fiber diameters in the range of 60-80 nm. These nanofibers were characterized by scanning electron microscopy (SEM), transmission electron microscopy (TEM), Raman spectroscopy, x-ray photoelectron spectroscopy (XPS) and nitrogen adsorption at 77 K. The specific surface area and pore volume increased to 627 $m^2 g^{-1}$ and 0.35 $cm^3 g^{-1}$ respectively by embedding graphene nanosheets. The electrochemical performance of the CNF/G composites were investigated in 6M KOH electrolyte by cyclic voltammetry and galvanostatic charge/discharge. Electrochemical measurements of CNF/G nanofibers exhibited a maximum specific capacitance of 265 F g^{-1} after addition of 10 wt. % graphene nanosheets.

7.2 Introduction

Electrochemical supercapacitors are electrical energy storage devices that are utilized in wide variety of applications such as electric vehicles, hybrid electric vehicles and portable electronic devices due to having higher power density than lithium ion batteries and larger energy density in comparison to conventional capacitors. The advantages of these supercapacitors are their high power capabilities, fast charge propagation and charge-discharge processes, long cyclic life (more than 100,000 cycles) and very low maintenance requirement (Winter and Brodd 2004, Zhang, Zhou et al. 2010).

Electrospinning is a simple method to produce polymer nanofibers with controlled diameters ranging from nanometers to sub-micrometers (Reneker and Chun 1996, Huang, Zhang et al. 2003). In this process, fibers are produced by the application of an electrostatic force between a syringe filled with a polymer solution and a collector mounted at a fixed distance from the needle. The microstructure and morphology of electrospun nanofibers are dependent on various parameters in the electrospinning process, such as solution properties (i.e. polymer molecular weight, viscosity, conductivity), process parameters (i.e. needle to collector distance, flow rate, applied potential), and ambient conditions (i.e. temperature, humidity).

In recent years, there has been an extensive research on the fabrication of polyacrylonitrile (PAN) based carbon nanofibers (CNFs) as a great candidate for electrode material of energy storage devices mainly due to CNFs high surface area and chemical resistance (Kim and Yang 2003, Gu, Ren et al. 2005, Kalayci, Patra et al. 2005, He, Wan et al. 2008, Ra, Raymundo-Piñero et al. 2009, Zhang, Aboagye et al. 2014). However, the low conductivity of CNFs has limited their power densities and hindered their potential usage in application where high power densities are sought after (Shaijumon, Ou et al. 2008).

Recently, graphene, an atomically thick, two dimensional sheet composed of sp^2 carbon atoms arranged in a honeycomb crystal lattice (Li and Kaner 2008), has attracted a lot of attention due to its outstanding properties such as extraordinary physical properties (high values of its Young's modulus (~1,100 GPa), fracture strength (125 GPa) (Lee, Wei et al. 2008), high thermal conductivity ~5,000 $W\ m^{-1}K^{-1}$) (Balandin, Ghosh et al. 2008), excellent mobility of charge carriers (200,000 $cm^2\ V^{-1}\ s^{-1}$) (Bolotin, Sikes et al. 2008), and high specific surface area (calculated value, 2,630 $m^2\ g^{-1}$) (Stoller, Park et al. 2008). These nanosheets have demonstrated attractive properties as a new family of carbon nanomaterials for use in electro- chemical energy generation and storage applications (Brownson, Kampouris et al. 2011). Thus, given the high surface area and electrical conductivity of graphene, which is an essential characteristic of an electrode material for energy production and storage, it is an attractive material for applications in energy storage systems and provides the possibility of improving the power density of CNFs by embedding graphene nanosheets into the precursor polymer matrix (Castro Neto, Guinea et al. 2009).

However, graphene has a poor solubility in common organic solvents and has a tendency to form agglomerates that can be attributed to its hydrophobic nature, the van der Waals interactions and its strong $\pi - \pi$ stacking (Xu, Bai et al. 2008). Therefore, this issue has to be addressed as its dispersion in the electrospinning solution is a pivotal step in the formation of nanofibers with well dispersed graphene. Several covalent and noncovalent functionalization methods that can improve graphene solubility have been reported (Georgakilas, Otyepka et al. 2012). In the covalent functionalization, sp^3 sites will be introduced on the graphene sheets that will permanently change its properties, especially its electrical properties, which is not desirable. In contrast, noncovalent functionalization improves the solubility of graphene without disturbing much its electronic

network (Subrahmanyam, Ghosh et al. 2009, Georgakilas, Otyepka et al. 2012). One of the structures that can be used for stabilization of graphene is polyvinylpyrrolidone (PVP). PVP is known to noncovalently functionalize the graphene surface and stabilize graphene dispersions against aggregation (Bourlinos, Georgakilas et al. 2009, Wajid, Das et al. 2012). Also, the PVP backbone can undergo $\pi - \pi$ stacking and enhance interfacial bonding in polymer nanocomposites (Bao, Zhang et al. 2010).

In this study, ultra-fine CNF/G nanofibers were produced via single nozzle electrospinning of phase-separated solution of polyacrylonitrile and polyvinylpyrrolidone (PAN/PVP) in N,N-dimethylformamide (DMF) solution dispersed with PVP-stabilized graphene nanosheets, followed by the calcination and carbonization processes. The schematic of the overall procedure is illustrated in Figure 7-1. Utilizing this method to fabricate CNF/G nanofibers allowed obtaining very small fiber diameters. The morphology, microstructure and electrochemical performance of CNF/G nanofibers are characterized.

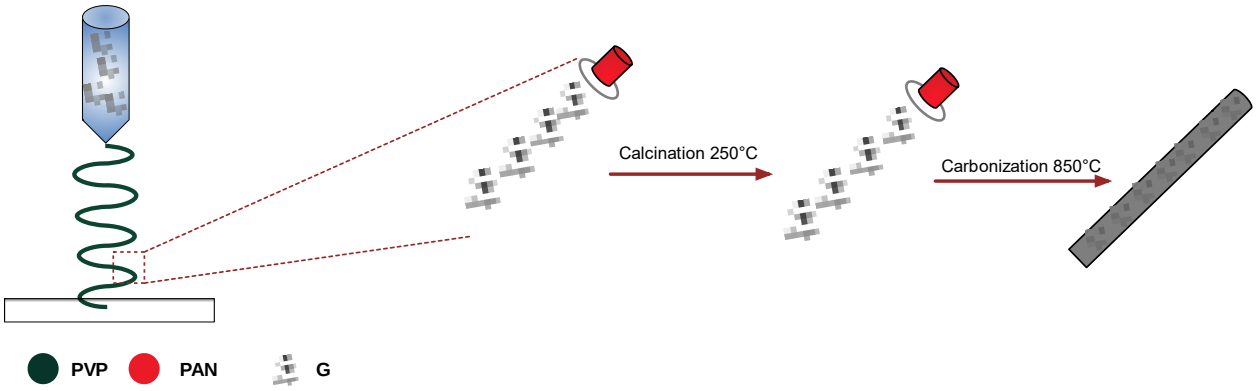

Figure 7-1: Schematic illustration of fabrication of CNF/G nanofibers by single nozzle electro-spinning using phase-separated solution of polyacrylonitrile and polyvinylpyrrolidone (PAN/PVP) in N,N-dimethylformamide (DMF) solution dispersed with various amount of PVP-stabilized graphene nanosheets (0 to 15 wt. %).

7.3 Experimental methods

7.3.1 Materials

Graphite powder (<20μm, synthetic), polyacrylonitrile (PAN, M_w = 150,000 $gmol^{-1}$), polyvinylpyrrolidone (PVP, M_w = 1,300,000 g mol^{-1}), N,N-dimethylformamide (DMF, 99.8%), ethanol (CH_3CH_2OH, denatured), hydrochloric acid (HCl, 37%), sulfuric acid (H_2SO_4, 98%), hydrogen peroxide (H_2O_2, 30%), sodium nitrate ($NaNO_3$, ≥ 99.0%) and hydrazine monohydrate (N_2H_4, 98%) were all purchased from Sigma Aldrich. All chemicals were reagent grade and were used as received. Deionized (DI) water (Millipore Milli-Q) was used for all the experiments.

7.3.2 Characterization

7.3.2.1 Electrospinning solution characterization

The electrical conductivity and viscosity of electrospinning solutions were measured by a pH/conductivity meter (Fischer Scientific, accumet AB200) and a vibrating viscometer (A&D Japan, VC-10) at 25 °C, respectively. The measurements were repeated 3 times and the average values are reported in Table 7-1.

7.3.2.2 Scanning electron microscope (SEM)

SEM measurements were carried out on a field emission scanning electron microscope (JEOL JSM-7600TFE) equipped with an Oxford Instruments energy dispersive X-ray spectroscopy (EDX) at 5kV in LEI mode. Samples were cut from electrospun mats on an aluminum foil and mounted on metal stubs using a double-sided carbon tape. Prior to observation, the samples were vacuum- coated with gold sputtering layer. SEM images were captured in the resolution of 1280 × 1240 pixels. Diameters and distributions of the electrospun nanofibers were analyzed from the

SEM images by using Image J analysis software (Image J, National Institutes of Health, USA). For each electrospun mat, 100 fibers were considered from different locations on the sample to calculate the average fiber diameter (AFD). Results are expressed as mean ± standard deviation.

7.3.2.3 Transmission electron microscopy (TEM)

The dispersion of graphene in the fibers and the core-shell structure was characterized by transmission electron microscopy (TEM, JEOL, JEM 2100F). For TEM observation, PAN fibers were directly deposited onto a TEM copper grid with supporting carbon film (CF400-Cu, Electron Microscopy Sciences) while carbonized fibers were first dispersed in ethanol and then deposited on the TEM grid.

7.3.2.4 Fourier transform infrared (FTIR)

Fourier transform infrared (FTIR) spectroscopy analysis was carried out using Perkin Elmer 65 FTIR-ATR instrument in order to confirm functionalization of graphene with polyvinylpyrrolidone as well as confirm the presence of its fingerprint functional groups on graphene. A total of 128 scans were accumulated for the signal averaging of each IR spectral measurement with a 4 cm^{-1} resolution with H_2O and CO_2 correction. The spectra of the samples were recorded over a wavenumber range of 4000-650 cm^{-1}.

7.3.2.5 Raman spectroscopy

Raman spectroscopy was carried out on a Renishaw spectrometer with a He–Ne laser as the excitation source that produced a monochromatic red light of 514 nm wavelength on the sample surface to investigate the chemical microstructure of the as-prepared CNF/G nanofibers and quantify the ordered and disordered structures of the carbon.

7.3.2.6 X-Ray photoelectron spectroscopy (XPS)

X-ray photoelectron spectroscopic (XPS) analysis was carried out on VG Scientific ESCALAB 3 MK II X-ray photoelectron spectrometer using a Mg Kα source (12kV, 18mA) to characterize the surface chemistry of the electrospun mats. Survey spectra were taken to identify the chemical species on the sample surface. The survey scans were done at a pass energy of 100 eV and energy step size of 1.0 eV. Thermo Scientific Advantage software was used for curve fitting and to calculate the relative atomic percent. All presented spectra are charge corrected and energy referenced to C1s at 285 eV. The relative atomic percent is calculated using Equation 7-1, where A_1 represents the area of the peak for a given element and SF_1 is the sensitivity factor for that same element. Sensitivity factors from the Wagner table are used.

$$At.\% = \frac{\frac{A_1}{SF_1}}{\sum_n \left(\frac{A_n}{SF_n}\right)} \qquad 7\text{-}1$$

7.3.2.7 Specific Surface Area Measurement

The Brunauer-Emmett-Teller (BET) method was utilized to calculate the specific surface area of each sample. The specific surface area and pore structure were obtained by nitrogen adsorption/desorption at 77 K utilizing (Quantachrome Autosorb-1, USA). Before the adsorption measurements, samples were degassed at 300 °C under vacuum.

7.3.2.8 Electrochemical measurements

All the electrochemical measurements were performed using a three electrode cell setup (VC-2 voltammetry cell, BASi) with platinum wire counter electrode and a Ag/AgCl reference electrode in 6M KOH aqueous electrolyte, which was deoxygenated with highly purified nitrogen for 30 mins prior to measurements. Working electrode was prepared by pressing 2.0 cm^2 of CNF/G mats in a stainless steel wire cloth (Alfa Aesar, type 304) as the current collector. All measurements were carried out on a Solarton SI 1260 Impedance/Gain-phase Analyzer equipped with Solarton 1470 battery test unit and analyzed using CorrWare software (Scribner Associates). Cyclic voltammetry (CV) and galvanostatic charge-discharge are used to evaluate the capacitive performance of the CNF/G samples. The weight of samples were measured before the measurements were performed.

7.3.3 Preparation of Graphite Oxide (GO)

Graphite oxide was synthesized from graphite by a modified Hummers method (Hummers and Offeman 1958) as reported before (Moayeri and Ajji 2015). Briefly, graphite (6 g) and $NaNO_3$ (3 g) were mixed in 150 mL H2SO4 in 500 mL flask at 0 °C. The mixture was stirred 30 min before $KMnO_4$ (18 g) was slowly added over a period of 30 min while carefully controlling the temperature to remain below 20 °C. Then, the mixture was stirred at room temperature for 30 min after being kept at 0 °C for 2 h. Thereafter, 300 mL of DI water was slowly added to the mixture with vigorous agitation. The reaction temperature was rapidly increased to 98 °C with effervescence, and the color of the mixture changed to yellow. The diluted suspension was stirred overnight and afterwards the mixture was further treated with 300 mL 30% H_2O_2 solution to reduce residual permanganate to soluble manganese ions. Finally, the resulting suspension was filtered using Whatman Quantitative Filter Papers (Grade 50) and washed with 5% HCl. Then, the filtrate

was redispersed in water and filtered and washed several times with DI water until the pH of the filtrate was neutral. Afterwards, the filtrate was dried under vacuum at 50 °C for 24 h and graphite oxide (GO) was obtained as a grey powder.

7.3.4 Reduction of graphite oxide (GO) to graphene (G)

GO (1 mg) was dispersed in DMF (10 mL) by sonication (Fischer Scientific, FS110H) until clear, homogenous graphene oxide dispersion is obtained. Reduced graphene oxide (G) was obtained by reducing graphene oxide dispersion with hydrazine monohydrate. Hydrazine monohydrate (100 μL) were added to the graphene dispersion and heated to 80 °C under a water-cooled condenser for 24 h. The obtained dispersion was mixed with ethanol (50 mL) and centrifuged at 4500 rpm for 1 h to obtain a black precipitate after pouring the supernatant away. The black precipitate was dried at room temperature in vacuum over-night to obtain G.

7.3.5 Electrospinning Solution Preparation

The electrospinning solutions were prepared by mixing 1 g of PVP with various amount of G in DMF solution. These solutions were stirred at room temperature for 2 h and then ultrasonicated for 1 h to ensure good dispersion of G in DMF and stabilization with PVP. Thereafter, 1 g of PAN was added to these solutions and the solutions were stirred at 90 °C for 24 h for complete dissolution of PAN. For comparison, the same solution was prepared without addition of G. The detailed contents of solutions are presented in the Table 7-1.

Table 7-1: Composition of electrospun PAN/PVP/G solutions and their solutions respective conductivity and viscosity.

Sample	Conc. (wt. %)	PAN (g)	PVP (g)	G (g)	DMF (g)	G:PAN[a] (wt. %)	Conductivity (μS/cm)	Viscosity (Pa.s)
PAN/PVP/G0	9.52	1.0	1.0	0	19.0	0	64.8 ± 0.7	122.2
PAN/PVP/G5	9.74	1.0	1.0	0.05	19.0	5	73.4 ± 0.3	142.5
PAN/PVP/G10	9.95	1.0	1.0	0.10	19.0	10	80.4 ± 0.1	156.1
PAN/PVP/G15	10.17	1.0	1.0	0.15	19.0	15	85.4 ± 0.1	164.5

[a] G concentration relative to PAN (w/w).

7.3.6 Electrospinning Setup and Parameters

Electrospinning was performed using a horizontal set up containing a variable high DC voltage power supply (Gamma High Voltage Research, FL, USA) and a programmable micro-syringe pump (Harvard Apparatus, PHD 2000, USA). The electrospinning solution was poured into a 3 mL glass syringe with Luer-Lock connection to an 18-gauge blunt tip needle (Cadence Science, USA). The syringe was mounted with a grip on the micro-syringe pump and grounded by use of an alligator clip. The nanofibers were collected on an aluminum foil attached on a grounded metal collector. The optimized electrospinning parameters were: flow rate of 0.5 mL/hr, applied voltage of 10 kV and needle-tip-to-collector distance of 10 cm. All experiments were conducted at room temperature and relative humidity of 2 to 5%. For all experiments 5 mL of solution were electrospun to keep the thickness of all the samples the same. The samples were dried in an oven at 80 °C for 24 h prior to nanofibers carbonization.

7.3.7 Carbonization of nanofibers

The calcination and carbonization of the as-prepared PAN/PVP/G nanofibers mats were performed in a tubular quartz furnace (MTI Corporation, GSL-1300-40X). The electrospun mats were first heated up at a rate of 1 °C/min to 250 °C in the air and maintained at that temperature for 1h for the purpose of stabilization of fiber structure. Thereafter, the nanofibers were carbonized in nitrogen atmosphere as the temperature was increased from 250 to 850 °C with the rate of 5 °C min^{-1} and kept at that temperature for 2 h.

7.4 Results and Discussion

7.4.1 Graphene stabilization with polyvinylpyrrolidone (PVP)

In order to create high dispersion of graphene in the DMF solution, PVP was used to stabilize graphene. PVP attaches to the basal plane of graphene sheet via noncovalent $\pi - \pi$ interactions and prevents the graphene sheets reaggregation sterically (Wajid, Das et al. 2012). As shown in the inset of Figure 7-2, the PVP functionalized graphene was successfully dispersed in DMF and no sedimentation was observed after 15 days whereas neat graphene sedimented in the same solution. Fourier transform infrared (FTIR) spectroscopy was performed on graphene and PVP functionalized graphene (G/PVP) in order to verify the presence of fingerprint functional groups that should be present from the successful noncovalent functionalization of graphene with PVP. In the spectra of graphene obtained after chemical reduction of GO with hydrazine, some residual presence of bands at 1736 and 1011 cm^{-1} were detected which provides evidence of the presence of different types of oxygen functionalities on the GO and their decrease in intensity due to chemical reduction (Goncalves, Marques et al. 2009). Also shown is C−C and C−C bands of

graphene located at 1569 and 1216 cm^{-1}. The G/PVP spectrum not only shows the characteristic peaks of graphene corresponding to C−C and C−C but also reveals vibrations that are characteristic peaks of PVP. These peaks are located at 1290 and 1660 cm^{-1} and are attributed to the stretching mode of −C−N and conjugated carbonyl groups respectively (Borodko, Habas et al. 2006). The presence of these new peaks in G/PVP spectrum indicates the presence of PVP component and interactions between PVP and graphene.

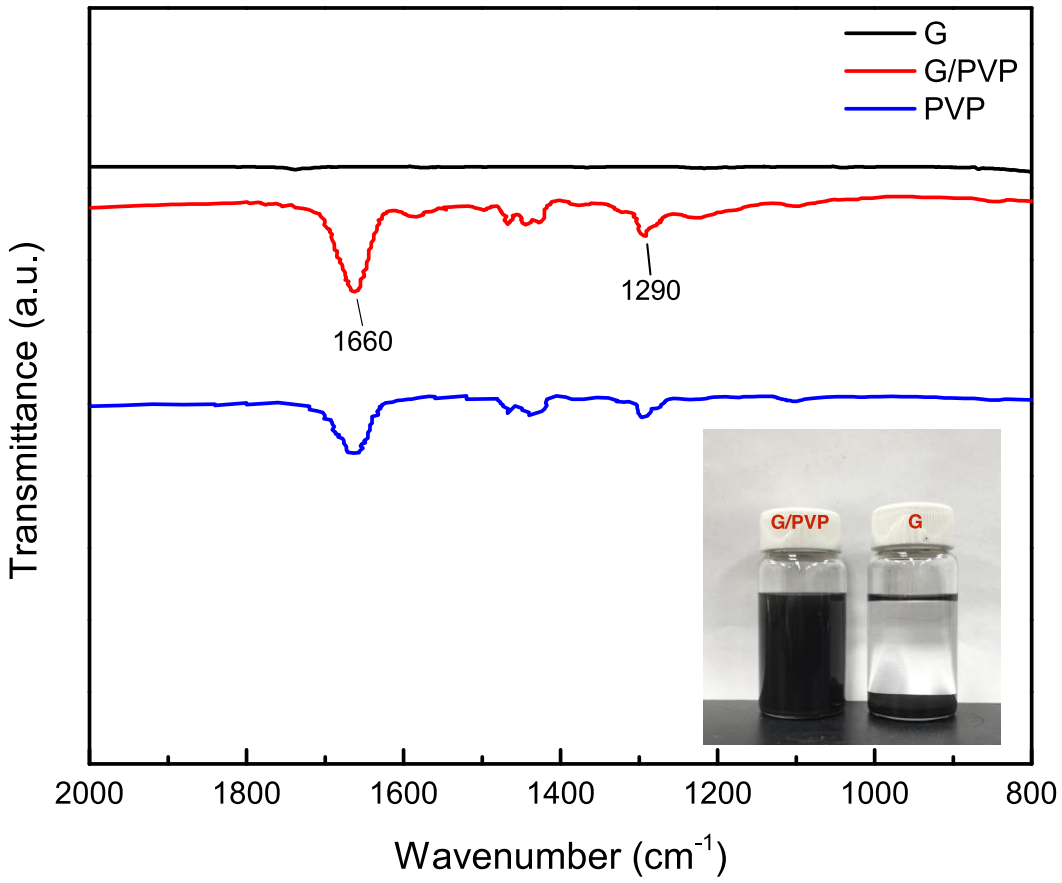

Figure 7-2: Fourier transform infrared (FTIR) spectra of G, G/PVP and PVP. The inset shows the stabilization of G/PVP and G powders dispersed by ultrasonication in DMF after 15 days.

7.4.2 Morphology and microstructure characterization

The morphology of the nanofibers was analyzed by scanning electron microscopy (SEM) and transmission electron microscopy (TEM). Figure 7-3 shows representative SEM images of carbonized PAN/PVP/G (CNF/G) fibers containing various amount of graphene. As can be seen, all electrospun fibers form a fibrous morphology and highly interwoven network structure.

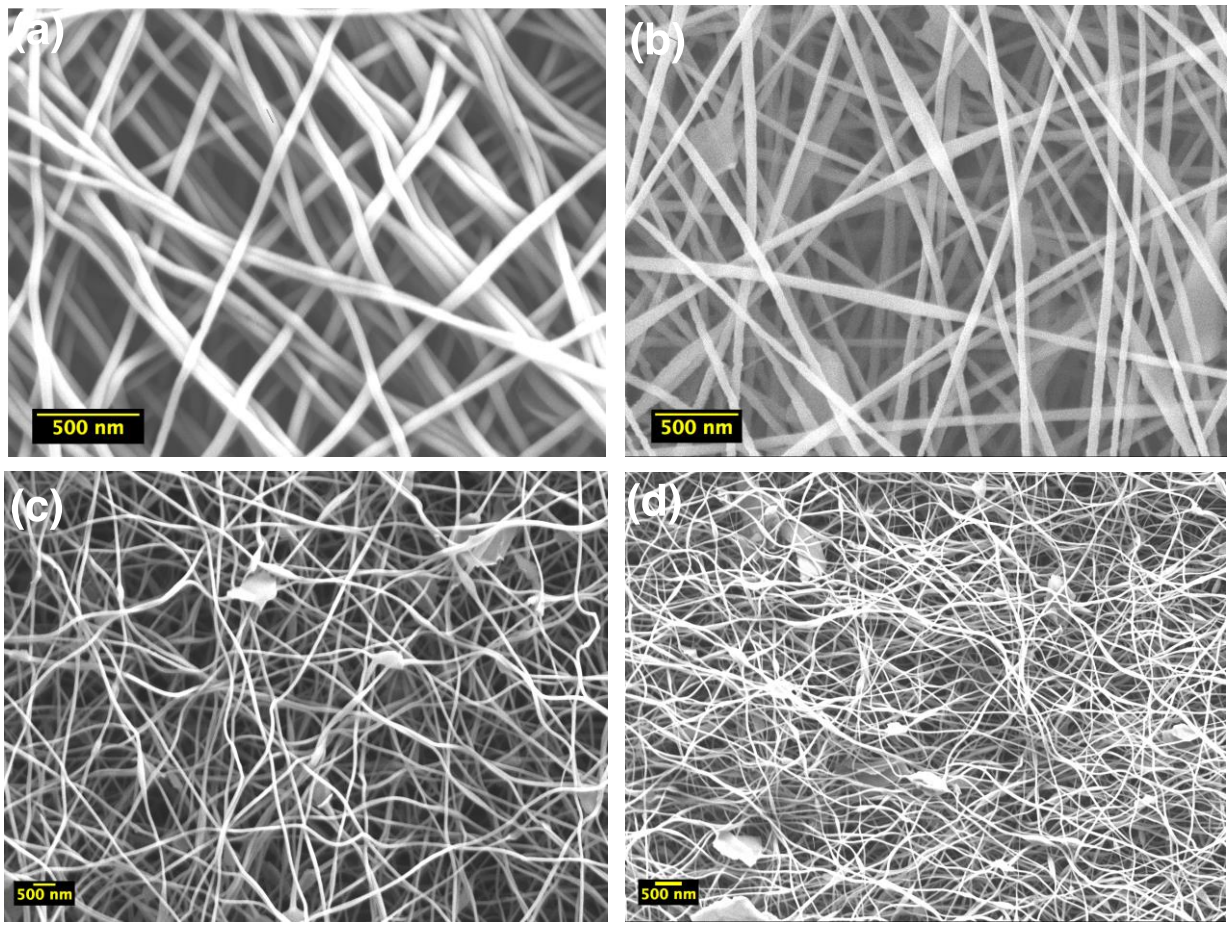

Figure 7-3: SEM micrographs of electrospun (a) CNF/G0, (b) CNF/G5, (c) CNF/G10, (d) CNF/G15 (scale bar = 500nm). The number after G denotes weight percent of G relative to PAN.

Also, the surfaces of fibers are relatively smooth and the fibers are randomly oriented. Because of higher amount of graphene in Figure 7-3 (c) and (d) (10 wt% and 15 wt%), graphene sheets are more visible. This may be due to the larger size of some of the sheets in comparison to fiber diameter since they cannot be completely enclosed by the fibers. Moreover, as evident in Figure 7-3 (c) and (d), by increasing the amount of graphene, defects in the form of beads are introduced in the fibers because of the jet instabilities.

Figure 7-4 shows the representative elemental mapping of an individual CNF/G nanofiber and its respective EDX spectra. The EDX spectra shows that the nanofiber is composed primarily of C, N and O with 95 wt.%, 3 wt.% and 2 wt.% content respectively.

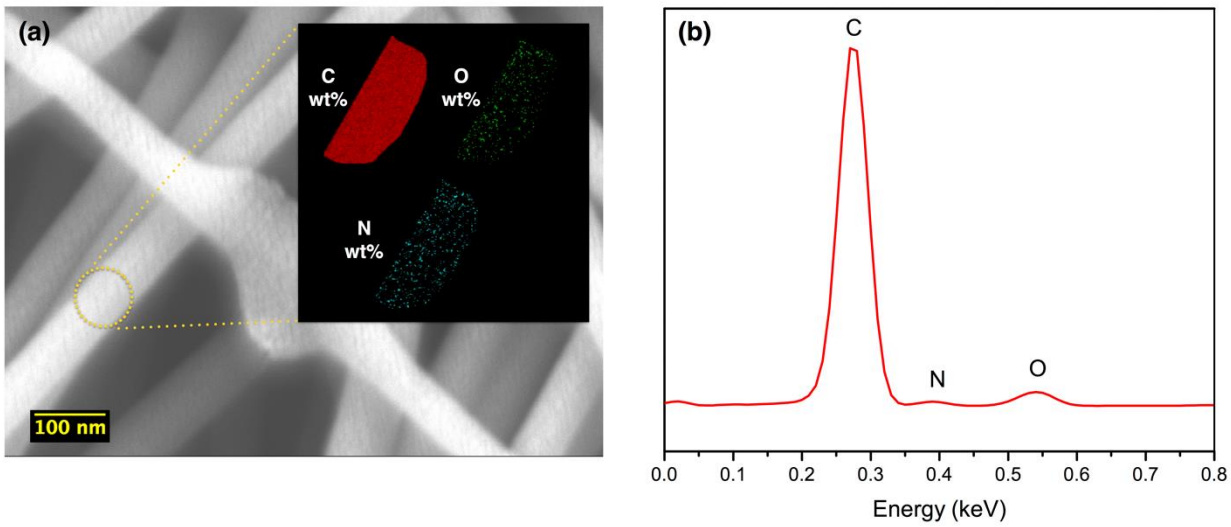

Figure 7-4: : (a) Representative elemental mapping of CNF/G fiber containing 5% graphene and (b) its corresponding EDX spectra.

Figure 7-5 presents representative TEM micrographs of PAN/PVP/G and CNF/G nanofibers. Figure 7-5 (a) and (b) show the core-shell structure of the nanofibers with PAN at the core and PVP in the shell, which is due to the incompatibility of the two polymers in the electrospun solution, which resulted in formation of bicomponent fiber. In addition, graphene flakes are evident in these micrographs. Figure 7-5 (c) and (d) are representative TEM micrographs of CNF/G. As shown, the

graphene sheet is still present and connected to the nanofiber after the carbonization process and its morphology did not change after the carbonization.

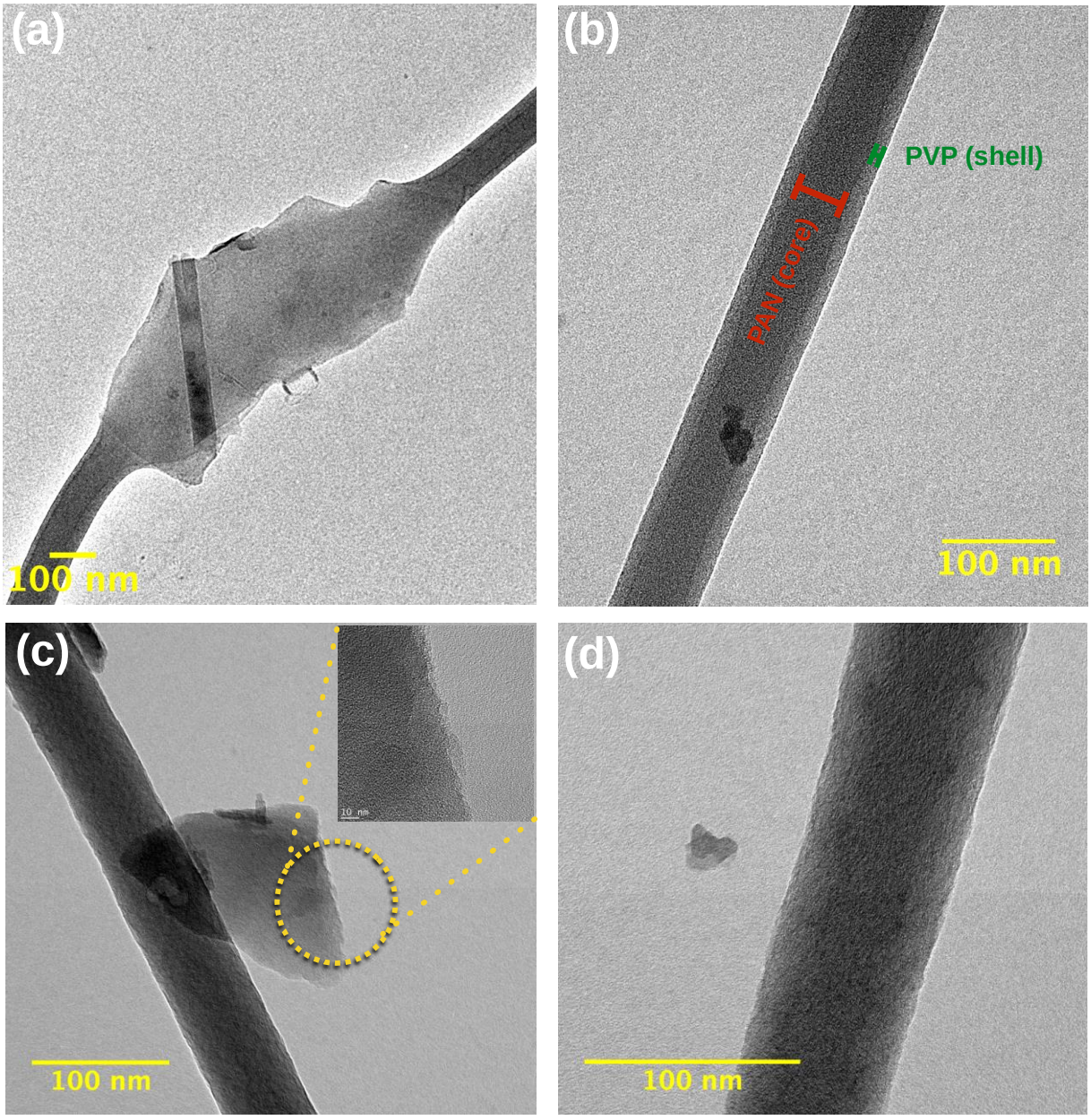

Figure 7-5: Representative TEM micrographs of electrospun (a) and (b) PAN/PVP/G, (c) and (d) CNF/G (scale bar = 100nm). The inset in (c) shows the edge of graphene sheet.

Figure 7-6 shows the histograms of fiber diameters, distribution and average fiber diameter (AFD) of (a) PAN/PVP/G fiber mats, before carbonization, and (b) CNF/G after carbonization. As can be seen, the average fiber diameters of PAN/PVP/G nanofibers are in the range of 190 to 250 nm and the AFD increases as the graphene concentration is increased from 0% to 15%.

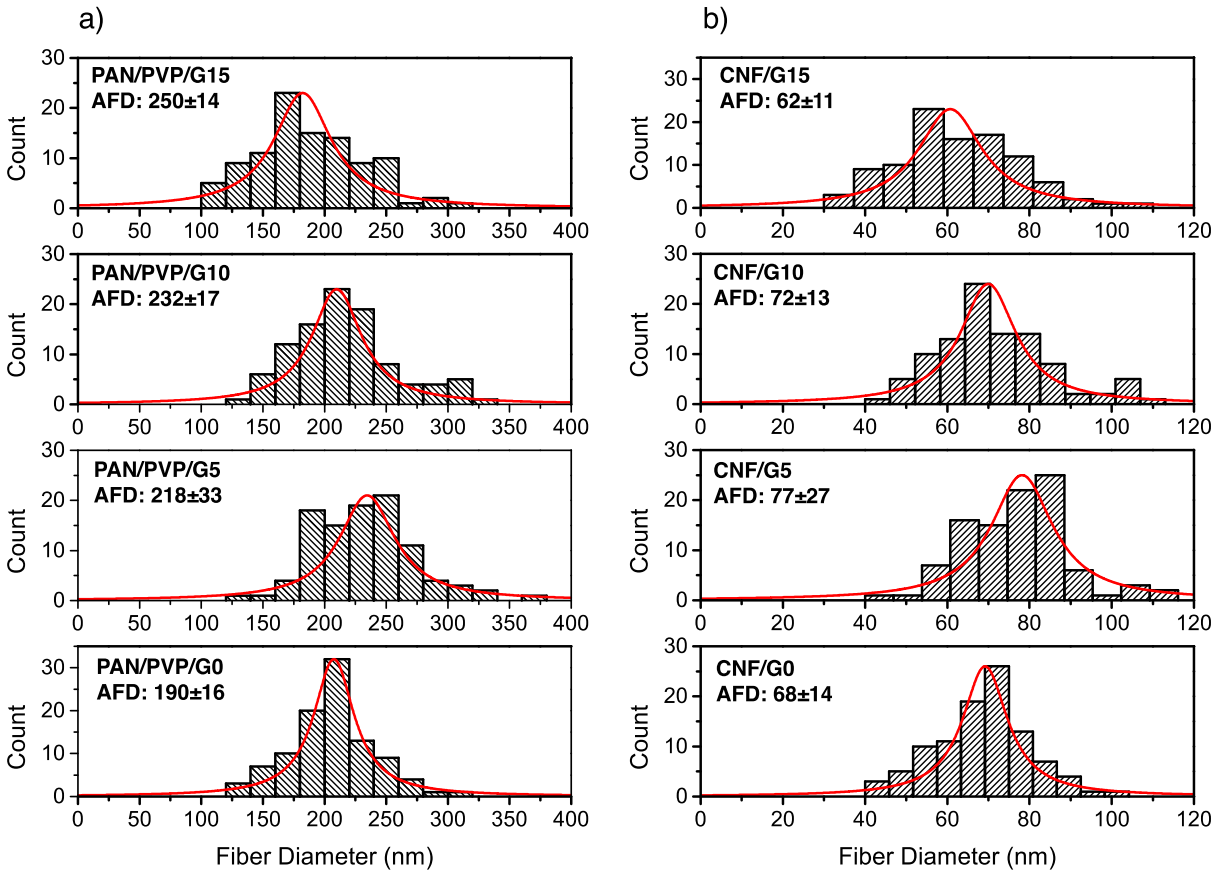

Figure 7-6: Histograms of fiber diameter, distribution and average fiber diameter (AFD) of (a) PAN/PVP/G fibers (before carbonization) and (b) CNF/G (after carbonization). The number after G denotes weight percent of G relative to PAN.

This can be attributed to the increase in viscosity of solution as graphene concentration increases, as presented in Table 7-1, resulting in fibers with higher AFD. After carbonization of PAN/PVP/G samples, the AFD decreased significantly (Figure 7-6 (b)) and the AFD of these fibers reached 60-

80 nm. The reason for this significant decrease in AFD is due to the addition of PVP. In the carbonization process, the PAN (core) is converted into CNF whereas the PVP (shell) is decomposed without leaving any ash, thus causing significant reduction in the fiber diameter. Therefore, by employing this technique ultra-fine CNFs are obtained.

The chemical microstructure of the as-prepared CNF/G nanofibers was characterized by Raman spectroscopy. Figure 7-7 illustrates the Raman spectra of CNF/G nanofibers containing various amount of graphene (0% to 15%).

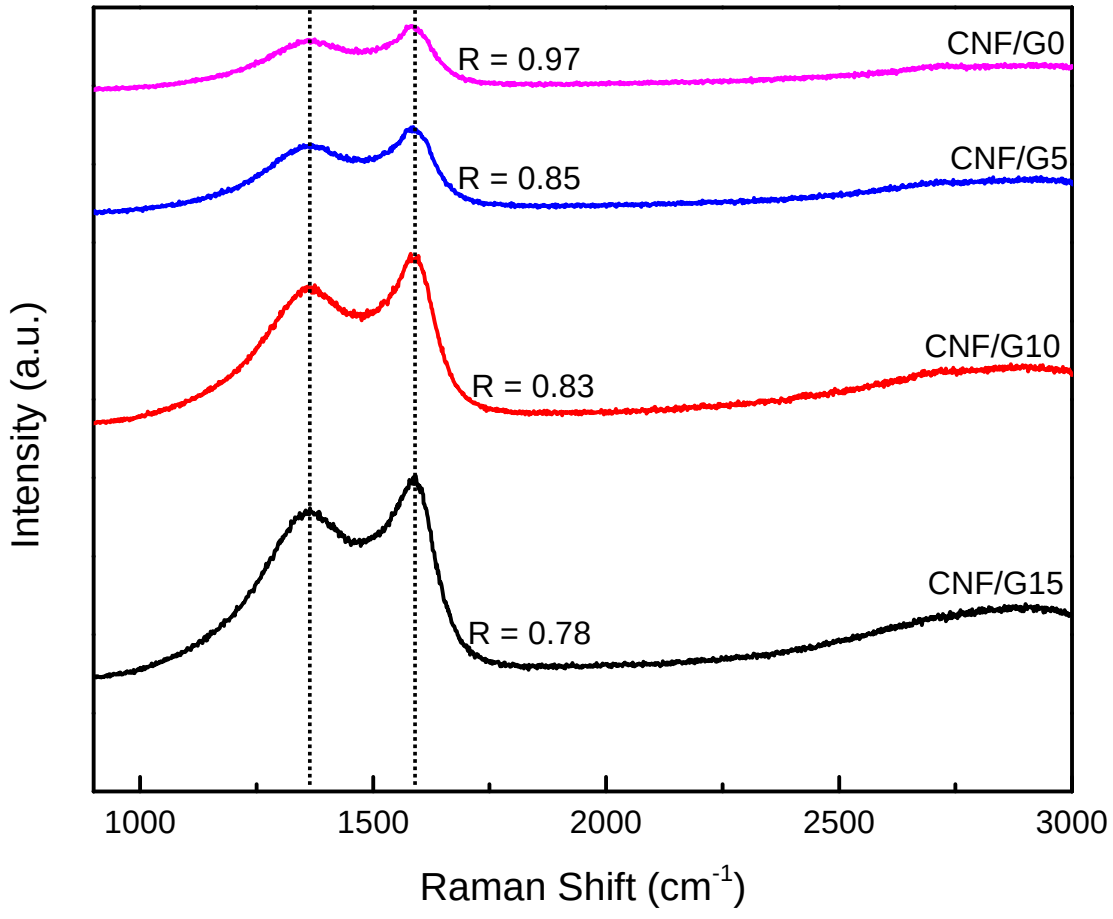

Figure 7-7: Raman spectra of CNF/G15, CNF/G10 , CNF/G5 and CNF/G0 samples, respectively. R is the intensity ratio of the D peak (1350 cm^{-1}) to the G peak (1580 cm^{-1}), which represents the amount of ordered graphite crystallites in the CNFs.

The Raman spectra is dominated by two main peaks around 1350 cm^{-1} and 1580 cm^{-1} which are attributed to the D and G band respectively (Kim, Park et al. 2004). D band is due to the disordered structures of carbon and G to the ordered graphitized structures of carbon. The ratio of D band to G band intensities (I_D/I_G) is referred to as the intensity ratio (R). This ratio decreases as the amount of defects is reduced or the amount of graphitized structures is increased. As illustrated in Figure 7-7, the R value is decreased from 0.97 for CNF/G0 sample to 0.78 for CNF/G15 sample. This indicates that the samples with higher amount of graphene have more ordered graphite structure.

The chemical composition of the CNFs was compared with pristine CNF (i.e. CNF/G0) by X-ray photoelectron spectroscopy (XPS). Figure 7-8 shows the survey spectra of CNF/G samples between 200 and 600 eV with C1s (~ 285.9 eV), O1s (~ 533.6 eV) and N1s (~ 401.2 eV) peaks.

The carbon, oxygen and nitrogen content of CNF/G samples are presented in Table 7-2 by using Equation 7-1 above. The CNF/G samples had carbon, oxygen and nitrogen content of between 84-90%, 3-10% and 2-6% respectively. During the stabilization process of PAN/G, the CH_2 and CN groups reduce to C−C, C−N and −C−H groups due to elimination, aromatization and cyclization reactions and form a ladder structure. Then, in the subsequent high temperature carbonization process, non- carbon atoms will be kept out to yield a turbostatic structure. However, some residual O and N atoms can be left after these processes (Rahaman, Ismail et al. 2007). The nitrogen content was relatively high for CNF/G0 to CNF/G10 samples. It was shown that the carbon materials enriched with nitrogen exhibit higher capacitance behavior (Lota, Grzyb et al. 2005).

N_2 adsorption-desorption measurements were performed at 77K according to the Brunauer-Emmett-Teller (BET) method to characterize the specific surface area and the pore-size distribution of the different CNF/G samples. As Figure 7-9 (a) shows, all isotherms exhibit type I behavior according to the IUPAC classification, which is characteristics of highly microporous materials.

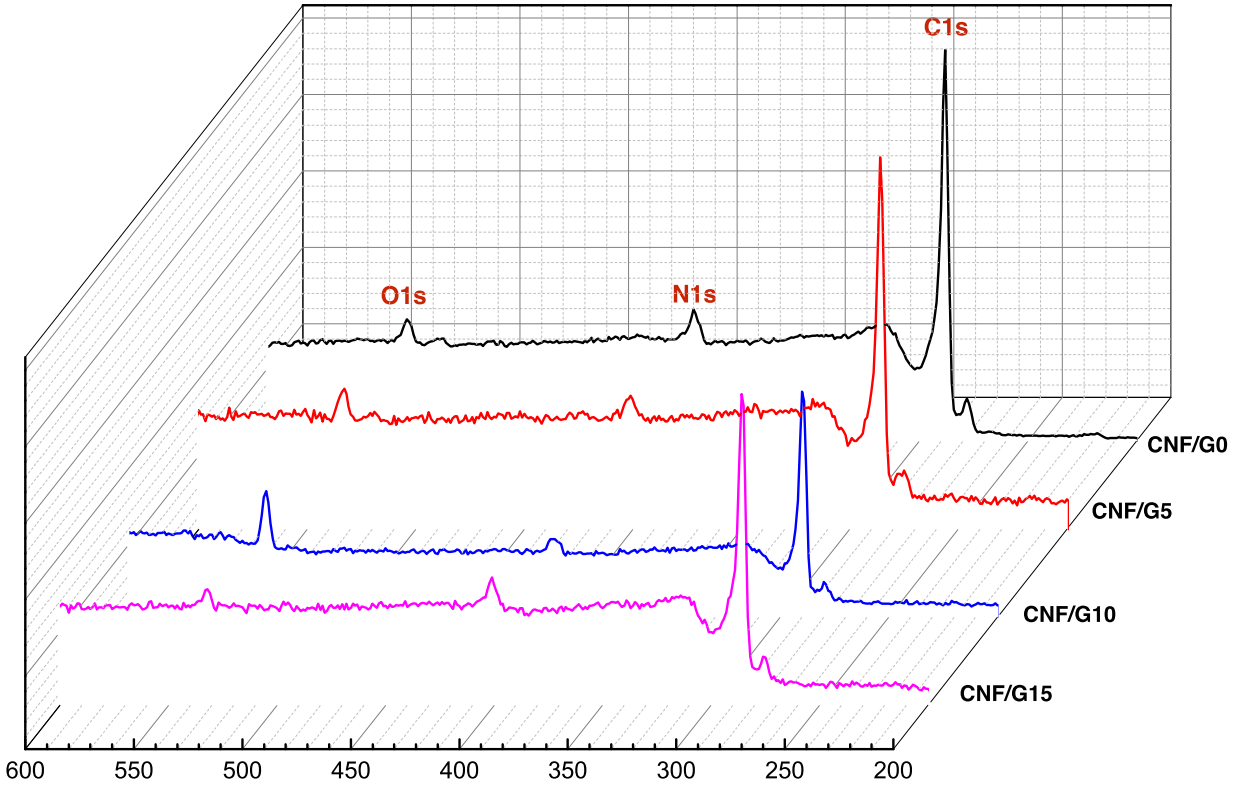

Figure 7-8: X-ray photoelectron survey spectrum of CNF/G0 to CNF/G15 showing C1s (~285.9 eV), O1s (~533.6 eV) and N1s (~401.2 eV) peaks.

Table 7-2: Elemental composition and pore structural characterization of the CNF/G samples

Sample	C (At. %)	O (At. %)	N (At. %)	S_{BET}[a] ($m^2\ g^{-1}$)	V_t[b] ($cm^3\ g^{-1}$)	APW[c] (nm)
CNF/G0	90.3	3.1	6.6	337	0.15	1.47
CNF/G5	89.0	5.1	5.9	571	0.24	1.54
CNF/G10	84.2	10.0	5.8	627	0.35	1.61
CNF/G15	89.8	8.0	2.0	472	0.18	1.67

[a] S_{BET} : specific surface area of CNF/G samples calculated by the BET method.

[b] V_t: total pore volume.[c] APW: average pore width calculated by the BET method.

The pore-size distribution of samples was calculated using the density functional theory (DFT) method. The pore structural parameters are listed in Table 7-2. The specific surface area, and pore volume (V*t*) increased by increasing the graphene content up to 10 wt%. However after 10 wt% they decreased as the graphene concentration got higher. This can be justified by the fact that at higher graphene concentrations the graphene sheets can agglomerate which can block the pore structures produced in the carbonization process and resulting in the lower specific surface area and pore volume.

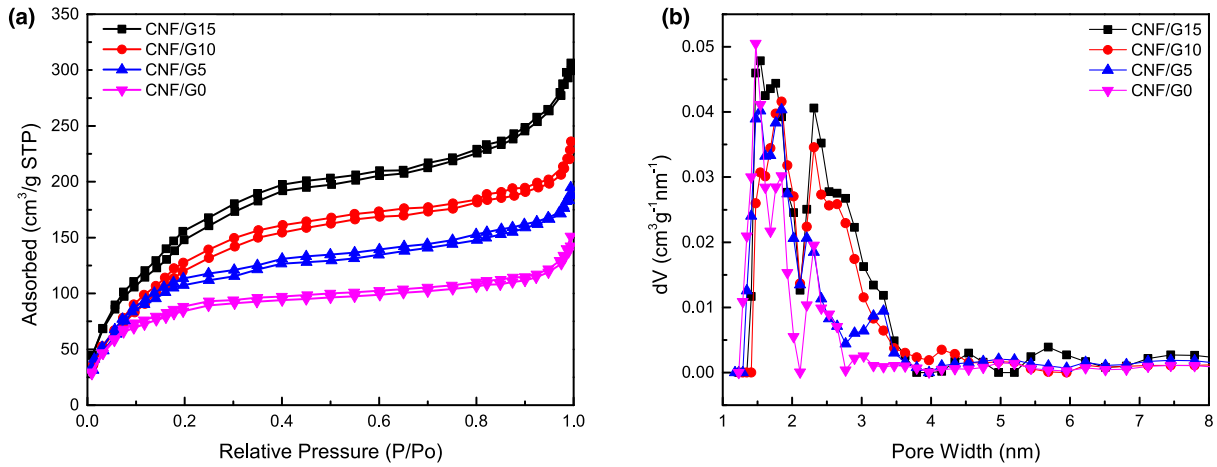

Figure 7-9: (a) Nitrogen adsorption-desorption isotherms and (b) pore size distributions determined by DFT calculations for CNF/G nanofibers containing 0% to 15% graphene content.

As depicted in Figure 7-9 (b), the pore size distributions of the various CNF/G nanofibers were mostly between 25 nm with average pore width (APW) of 1.47 to 1.67 nm. There- fore, the CNF/G nanofibers possess a mesoporous structure and no microporous structure was observed. This

phenomenon can be explained by the decomposition of the PVP-shell layer that leaves behind an ultrafine CNF/G nanofibers with a mesoporous structure.

7.4.3 Electrochemical characterization

The electrochemical properties of CNF/G nanofibers were investigated using a three-electrode cell setup in 6M KOH electrolyte solution. Cyclic voltammetry (CV) was used to evaluate the electrochemical performance of CNF/G samples. Figure 7-10 (a) shows the CV curves of different CNF/G samples measured at a scan rate of 10 mV s^{-1} in the range 0 to 0.8V at room temperature. CVs exhibit a rectangular and symmetric shape, which indicates the ideal electric double-layer capacitor behavior. As illustrated, CV area of the samples with G is significantly higher than that of neat CNF, which indicates that samples with graphene have higher capacitance. However, this trend was only observed from CNF/G0 to CNF/G10, as CNF/G15 showed a lower current from CNF/G10. This can be explained by the XPS and BET results presented earlier.

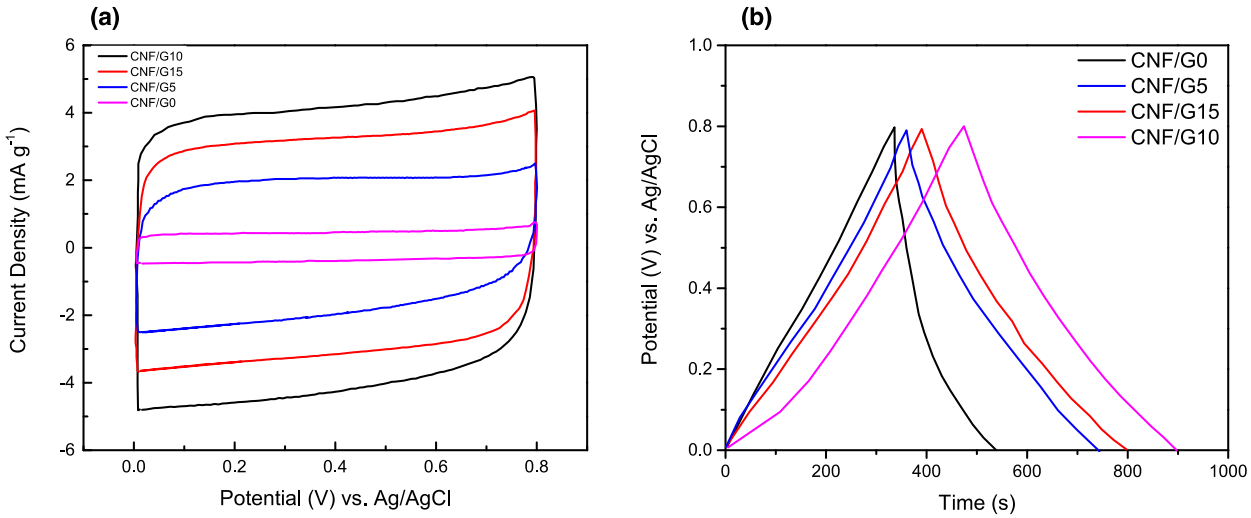

Figure 7-10: (a) cyclicvoltammetry of CNF/G nanofibers at scan rate of 10 mV s^{-1} (b) Galvanostatic charging/discharging curves of CNF/G samples at a specific current of 0.5 A g^{-1}.

The CNF/G samples had higher level of nitrogen for samples with 0 wt% to 10 wt% graphene and it is shown that the higher nitrogen content results in the better capacitance behavior. Moreover, based on BET results, the specific surface area and pore volume had an increasing trend from CNF/G0 to CNF/G10 samples and then decreased for CNF/G15 sample, which can further support the results obtained from electrochemical tests. This is due to the fact that the larger pore volume and surface area are favorable for ion diffusion with high speed at high loading current density and allows the efficient utilization of specific surface area (Li, Jiang et al. 2011). Therefore, CNF/G15 exhibited a lower capacitance behavior than CNF/G10 because of having lower specific surface area and pore volume, even though its graphene content was increased.

As plotted in Figure 7-10 (b), the specific capacitances of the CNF/G samples were determined by galvanostatic charging/discharging measurements at the constant current density of 1 mA g^{-1} in the potential range from 0 to 0.8 V. The average specific capacitance (C) is calculated by using Equation 7-2 where I and Δt denote applied current and discharge time respectively. ΔV is the potential difference during the discharge process and m is the total mass of the CNF/G sample used as the active electrode.

$$C = \frac{I \times \Delta t}{\Delta V \times m} \qquad 7\text{-}2$$

The specific capacitances of CNF/G0, CNF/G5, CNF/G10 and CNF/G15 calculated using equation 2 were 126 F g^{-1}, 240 F g^{-1}, 265 F g^{-1} and 246 F g^{-1} respectively. CNF/G10 exhibited the highest capacitance among the CNF/G samples. Moreover, by incorporation of graphene in CNFs, the specific capacitance was increased by 2 times in the case of CNF/G10. However, as was evident

from the smaller CV curve area of CNF/G15 than CNF/G10, the specific capacitances of CNG/G15 was lower than that of CNF/G10.

7.5 Conclusion

In summary, carbon nanofibers embedded with different amounts of polymer stabilized graphene were fabricated using single nozzle electrospinning of phase separated solutions of PVP/PAN. Subsequently, the core-shell structured PAN/PVP/G nanofibers were thermally treated to obtain ultrafine carbon nanofibers. These nanofibers possessed small diameters in the range of 60-80 nm due to the decomposition of PVP and carbonization process. It was shown that by increasing the embedded graphene content from 0% to 10% the specific surface area of the nanofibers increased from 337 to 627 $m^2\ g^{-1}$ and the total pore volume was increased from 0.15 to 0.35 $cm^3\ g^{-1}$. Also, addition of highly conductive graphene sheets increased the specific capacitance of nanofibers by more than 2 times from 126 to 265 $F\ g^{-1}$. These CNF/G nanofibers with high specific capacitance are ideal candidates for application in high-capacitance electric double-layer capacitor.

7.6 Acknowledgments

The authors gratefully acknowledge the financial support of NSERC (National Science and Engineering Research Council of Canada) and FRQNT (Fonds de recherche du Quebec Nature et technologies). We are grateful to Dr. Gwenaël Chamoulaud for his help with the electrochemical measurements. We also thank Ms. Nicole MacDonald for her help with the TEM imaging.

7.7 References

Balandin, A. A., S. Ghosh, W. Bao, I. Calizo, D. Teweldebrhan, F. Miao and C. N. Lau (2008). "Superior thermal conductivity of single-layer graphene." Nano Letters **8**(3): 902-907.

Bao, Q., H. Zhang, J.-x. Yang, S. Wang, D. Y. Tang, R. Jose, S. Ramakrishna, C. T. Lim and K. P. Loh (2010). "Graphene--polymer nanofiber membrane for ultrafast photonics." Advanced Functional Materials **20**(5): 782--791.

Bolotin, K. I., K. J. Sikes, Z. Jiang, M. Klima, G. Fudenberg, J. Hone, P. Kim and H. L. Stormer (2008). "Ultrahigh electron mobility in suspended graphene." Solid State Communications **146**(9–10): 351-355.

Borodko, Y., S. E. Habas, M. Koebel, P. Yang, H. Frei and G. A. Somorjai (2006). "Probing the interaction of poly(vinylpyrrolidone) with platinum nanocrystals by uv−raman and ftir." Journal of Physical Chemistry B **110**(46): 23052-23059.

Bourlinos, A. B., V. Georgakilas, R. Zboril, T. A. Steriotis, A. K. Stubos and C. Trapalis (2009). "Aqueous-phase exfoliation of graphite in the presence of polyvinylpyrrolidone for the production of water-soluble graphenes." Solid State Communications **149**(47--48): 2172--2176.

Brownson, D. A. C., D. K. Kampouris and C. E. Banks (2011). "An overview of graphene in energy production and storage applications." Journal of Power Sources **196**(11): 4873-4885.

Castro Neto, A. H., F. Guinea, N. M. R. Peres, K. S. Novoselov and A. K. Geim (2009). "The electronic properties of graphene." Reviews of Modern Physics **81**(1): 109-162.

Georgakilas, V., M. Otyepka, A. B. Bourlinos, V. Chandra, N. Kim, K. C. Kemp, P. Hobza, R. Zboril and K. S. Kim (2012). "Functionalization of graphene: Covalent and non-covalent approaches, derivatives and applications." Chemical Reviews **112**(11): 6156-6214.

Goncalves, G., P. A. A. P. Marques, C. M. Granadeiro, H. I. S. Nogueira, M. K. Singh and J. Grácio (2009). "Surface modification of graphene nanosheets with gold nanoparticles: The role of oxygen moieties at graphene surface on gold nucleation and growth." Chemistry of Materials **21**(20): 4796-4802.

Gu, S. Y., J. Ren and G. J. Vancso (2005). "Process optimization and empirical modeling for electrospun polyacrylonitrile (pan) nanofiber precursor of carbon nanofibers." European Polymer Journal **41**(11): 2559-2568.

He, J.-H., Y.-Q. Wan and J.-Y. Yu (2008). "Effect of concentration on electrospun polyacrylonitrile (pan) nanofibers." Fibers and Polymers **9**(2): 140-142.

Huang, Z.-M., Y. Z. Zhang, M. Kotaki and S. Ramakrishna (2003). "A review on polymer nanofibers by electrospinning and their applications in nanocomposites." Composites Science and Technology **63**(15): 2223-2253.

Hummers, W. S. and R. E. Offeman (1958). "Preparation of graphitic oxide." Journal of the American Chemical Society **80**(6): 1339-1339.

Kalayci, V. E., P. K. Patra, Y. K. Kim, S. C. Ugbolue and S. B. Warner (2005). "Charge consequences in electrospun polyacrylonitrile (pan) nanofibers." Polymer **46**(18): 7191-7200.

Kim, C., S.-H. Park, J.-I. Cho, D.-Y. Lee, T.-J. Park, W.-J. Lee and K.-S. Yang (2004). "Raman spectroscopic evaluation of polyacrylonitrile-based carbon nanofibers prepared by electrospinning." Journal of Raman Spectroscopy **35**(11): 928--933.

Kim, C. and K. S. Yang (2003). "Electrochemical properties of carbon nanofiber web as an electrode for supercapacitor prepared by electrospinning." Applied Physics Letters **83**(6): 1216-1218.

Lee, C., X. Wei, J. W. Kysar and J. Hone (2008). "Measurement of the elastic properties and intrinsic strength of monolayer graphene." Science **321**(5887): 385-388.

Li, D. and R. B. Kaner (2008). "Graphene-based materials." Science **320**(5880): 1170-1171.

Li, Q., R. Jiang, Y. Dou, Z. Wu, T. Huang, D. Feng, J. Yang, A. Yu and D. Zhao (2011). "Synthesis of mesoporous carbon spheres with a hierarchical pore structure for the electrochemical double-layer capacitor." Carbon **49**(4): 1248--1257.

Lota, G., B. Grzyb, H. Machnikowska, J. Machnikowski and E. Frackowiak (2005). "Effect of nitrogen in carbon electrode on the supercapacitor performance." Chemical Physics Letters **404**(1--3): 53--58.

Moayeri, A. and A. Ajji (2015). "Fabrication of polyaniline/poly(ethylene oxide)/non-covalently functionalized graphene nanofibers via electrospinning." Synthetic Metals **200**: 7-15.

Ra, E. J., E. Raymundo-Piñero, Y. H. Lee and F. Béguin (2009). "High power supercapacitors using polyacrylonitrile-based carbon nanofiber paper." Carbon **47**(13): 2984--2992.

Rahaman, M. S. A., A. F. Ismail and A. Mustafa (2007). "A review of heat treatment on polyacrylonitrile fiber." Polymer Degradation and Stability **92**(8): 1421--1432.

Reneker, D. H. and I. Chun (1996). "Nanometre diameter fibres of polymer, produced by electrospinning." Nanotechnology **7**(3): 216.

Shaijumon, M. M., F. S. Ou, L. Ci and P. M. Ajayan (2008). "Synthesis of hybrid nanowire arrays and their application as high power supercapacitor electrodes." Chem. Commun.: 2373-2375.

Stoller, M. D., S. Park, Y. Zhu, J. An and R. S. Ruoff (2008). "Graphene-based ultracapacitors." Nano Letters **8**(10): 3498-3502.

Subrahmanyam, K. S., A. Ghosh, A. Gomathi, A. Govindaraj and C. N. R. Rao (2009). "Covalent and noncovalent functionalization and solubilization of graphene." Nanoscience and Nanotechnology Letters **1**(1): 28-31.

Wajid, A. S., S. Das, F. Irin, H. S. T. Ahmed, J. L. Shelburne, D. Parviz, R. J. Fullerton, A. F. Jankowski, R. C. Hedden and M. J. Green (2012). "Polymer-stabilized graphene dispersions at high concentrations in organic solvents for composite production." Carbon **50**(2): 526-534.

Winter, M. and R. J. Brodd (2004). "What are batteries, fuel cells, and supercapacitors?" Chemical Reviews **104**(10): 4245--4270.

Xu, Y., H. Bai, G. Lu, C. Li and G. Shi (2008). "Flexible graphene films via the filtration of water-soluble noncovalent functionalized graphene sheets." Journal of the American Chemical Society **130**(18): 5856-5857.

Zhang, L., A. Aboagye, A. Kelkar, C. Lai and H. Fong (2014). "A review: Carbon nanofibers from electrospun polyacrylonitrile and their applications." Journal of Materials Science **49**(2): 463-480.

Zhang, L. L., R. Zhou and X. S. Zhao (2010). "Graphene-based materials as supercapacitor electrodes." Journal of Materials Chemistry **20**: 5983-5992.

CHAPTER 8 GENERAL DISCUSSION

Considerable research has been conducted on the usage of conductive polymer nanocomposites for electrical conductors and energy solutions application. However, the combined usage of graphene and electrospun fibers for these applications are very scarce as there is still great deal of complications in dispersion of graphene in the nanofibers. Dispersion of graphene in the initial solution before electrospinning is one of the most important factors for producing nanofibers that have good graphene dispersion and directly effects the performance of the final product.

The first part of this works aimed at electrospinning of PANi nanofibers and with highly dispersed graphene nanosheets in the nanofibers. In order to stabilize graphene dispersion in the electrospinning solution, graphene nanosheets were noncovalently functionalized with PBASE, which will prevent the graphene sheets aggregation. The successful functionalization of graphene with PBASE was confirmed by detection of fingerprint functional groups due to the stretching vibration of C–C(=O)–O bond of ester of PBASE on graphene. Subsequently PEO was added as copolymer to the electrospinning solution to improve PANi's processability. Afterwards, the solution containing PANi/PEO/G-PBASE was electrospun to obtain highly interconnected fibers with average fiber diameter in the range of 220 nm. The presence of graphene sheets in the PANi/PEO nanofibers were confirmed by TEM imaging and XPS elemental analysis. XPS results indicate that the ratio of C-O to C=C decreases significantly from 0.53 in PANi/PEO to 0.36 with addition of graphene in PANi/PEO/G-PBASE. This decrease is due to the presence of graphene sheets in the PANi/PEO/G-PBASE which is expected to cause an increase in C=C groups with respect to the C-O groups which are characteristic of PEO. Similarly, the decrease in nitrogen content relative to C=C functional groups from 0.11 in PANi/PEO to 0.01 in PANi/PEO/G-PBASE

confirms the addition of graphene sheets to the latter as this is expected to increase the content of C=C functional groups relative to the nitrogen characterizing the PANi content. Finally, to understand the effect of addition of graphene on thermal and electrical performance of PANi/PEO nanofibers, TGA and four-point probe. The addition of graphene increased the the onset decomposition temperature by 35 °C to ~321 °C. Similarly, conductivity increased by 2.41 times and reached ~ 2.39×10^{-3} S/Cm.

In the second part of this work, core-shell structured PANi/PMMA nanofibers embedded with G-PBASE were prepared through coaxial electrospinning setup. The advantage of this technique over pervious blending technique is that the shell layer can be subsequently removed via solvent etching, opening the possibility of obtaining neat PANi fibers. In addition, since the insulator copolymer used for blending technique is not present, the final nanofibers will have higher conductivity. To fabricate those nanofibers, a coaxial electrospinning technique was employed and core-shell structured PANi/PMMA nanofibers embedded G-PBASE were produced, in which PMMA is located at the shell layer and PANi at the core layer. The produced core-shell structured fibers exhibited interconnected structure and possessed diameters in the range of 420 nm. Afterwards, PMMA shell-layer was removed with mixture of MIBK/IPA to obtain neat PANi nanofibers with diameters in the range of 230 nm. TEM imaging were performed to confirm the core-shell structure of PANi/G-PBASE/PMMA nanofibers and the removal of PMMA shell layer. Also, the presence of graphene sheets in the nanofibers were analyzed by TEM. Finally, the four-point probe method was used to investigate the conductivity of neat PANi and PANi/G-PBASE. Result shown that the electrical conductivity of PANi/G-PBASE nanofibers is ~ 30.25 S/cm which is 3 times higher than that of PANi nanofibers. Interestingly, the electrical conductivity of neat PANi/G-PBASE

nanofibers are more than 12,000 times higher than fibers produced from blended PANi/PEO/G-PBASE. The prepared PANi/graphene nanofibers by blending and coaxial technique can have potential applications as chemoresitive sensor for gas or pathogen detection.

In the third part of this work, novel electrospinning technique is used to produce ultrafine carbon nanofibers (CNFs) embedded with graphene. First, core–shell structured polyacrylonitrile and polyvinylpyrrolidone (PAN/PVP) nanofibers embedded with various amounts of PVP-functionalized graphene (G/PVP), 0 wt% to 15 wt%, were fabricated by single-nozzle electrospinning technique of phase-separated solution with diameters in the range of 190 to 250 nm. PVP is known to noncovalently functionalize the graphene surface and stabilize graphene dispersions against aggregation. Also, PVP and PAN form a phase-separated solution in DMF due to incompatibility of the two polymers in the electrospun solution, which can be exploited to produce core-shell structured nanofibers. FTIR spectroscopy was performed on G/PVP in order to verify the presence of fingerprint functional groups that should be present from the successful noncovalent functionalization of graphene with PVP. Afterwards, PAN/PVP/G nanofibers were first stabilized at 250 °C in the air and consecutively carbonized at 850 °C in the nitrogen atmosphere. In the carbonization process, the PAN (core) is converted into CNF whereas the PVP (shell) is decomposed without leaving any ash, thus causing significant reduction in the fiber diameter to 60-80 nm. Graphene sheets remain intact during the carbonization process which was confirmed by TEM imaging. The chemical microstructure of the CNF/G nanofibers was characterized by Raman spectroscopy. It was illustrated that as the graphene increases, the intensity ratio (R) decreases since the amount of defects is reduced and the amount of graphitized structures is increased. N_2 adsorption-desorption measurements were performed at 77K according to the Brunauer-Emmett-Teller (BET) method to characterize the specific surface area and the pore-size

distribution. Also, the pore-size distribution of samples was calculated using the density functional theory (DFT) method. Results exhibited that by increasing the graphene content from 0% to 10% the specific surface area of the nanofibers increased from 337 to 627 m^2 g^{-1} and the total pore volume was increased from 0.15 to 0.35 cm^3 g^{-1}. Finally, the electrochemical properties of CNF/G nanofibers were investigated using a three-electrode cell setup in 6M KOH electrolyte solution. As reported the addition of graphene sheets increased the specific capacitance of nanofibers by more than 2 times from 126 to 265 F g^{-1}. These CNF/G nanofibers with high specific capacitance are ideal candidates for application in high-capacitance electric double-layer capacitor.

CHAPTER 9 CONCLUSION AND RECOMMENDATIONS

9.1 Conclusions

In the first part of this thesis, graphene-based polyaniline nanofibers were fabricated using two strategies: 1) blending with easily electrospinnable polymeric solution of poly(ethylene oxide) (PEO) and 2) coaxial electrospinning with poly(methyl methacrylate) (PMMA) as shell segment. In the both cases the morphology, micro structure and conductivity of fibers were studied. The following conclusions are drawn from this work:

1) Electrospun polyaniline/polyethylene oxide (PANi/PEO) nanofibers embedded with 5 wt% PBASE functionalized graphene (G-PBASE) can be obtained with diameters in the range of 160-280 nm from DMF solution.

2) PBASE attaches to graphene nanosheets through noncovalent π-π bonding and prevents the graphene sheet aggregation.

3) The thermal stability of PANi/PEO/G-PBASE nanofibers increased by 35°C after addition of graphene in comparison with neat PANi/PEO.

4) PANi/PEO/G-PBASE nanofibers exhibited 2 times higher electrical conductivity (~2.39×10^{-3} S/cm) than that of neat PANi/PEO (~9.92×10^{-4} S/cm) nanofibers due to addition of graphene.

5) Core-shell structured PANi/PMMA nanofibers embedded with 5 wt% PBASE functionalized graphene (G-PBASE) prepared by a coaxial electrospinning process, with PMMA as the shell component and PANi/G-PBASE as the core segment. The fibers had diameters in the range of 400-420 nm.

6) Neat PANi/G-PBASE nanofibers obtained after removal of PMMA shell layer with IPA/MIBK solution. The average fiber diameter decreased to 200-230 nm after shell removal.

7) Electrical conductivity of PANi/G-PBASE (30.25 S/cm) was 3 times higher than that PANi nanofibers (~ 10.75 S/cm).

In the second part of this thesis, core-shell structured carbon nanofibers embedded with various amounts of non-covalently functionalized graphene were fabricated by single-nozzle electrospinning technique using phase-separated solution of polyacrylonitrile and polyvinylpyrrolidone (PAN/PVP) in N,N-dimethylformamide (DMF).

1) Defect free nanofibers of 190-250 nm can be obtained from single-nozzle electrospinning technique using phase-separated solution of PAN/PVP in N,N-dimethylformamide (DMF) in the presence of a small amount of graphene (5 wt%).

2) PVP stabilized graphene nanosheets through $\pi - \pi$ stacking and avoided their aggregation.

3) Ultra-thin carbon nanofibers (CNFs), 60-80 nm, obtained after that core-shell structured PAN/PVP/G nanofibers were thermally treated in the nitrogen atmosphere.

4) BET anaylsis shown that by increasing the embedded graphene content from 0% to 10% the specific surface area of the nanofibers increased from 337 to 627 $m^2\ g^{-1}$ and the total pore volume was increased from 0.15 to 0.35 $cm^3\ g^{-1}$.

5) Addition of highly conductive graphene sheets increased the specific capacitance of nanofibers by more than 2 times from 126 to 265 $F\ g^{-1}$.

9.2 Recommendations

The following aspects are recommended for more exploration in future work:

1) Investigate the effect of PANi doping level on the electrospinability and conductivity of the final nanofibers.

2) Determine the minimum molecular weight and concentration of PEO in PANi/PEO blend the leads to stable electrospinning conditions.

3) Study usage of other ICPs in this system such as poly(3,4-ethylenedioxythiophene (PEDOT) or polypyrrole (Ppy).

4) Study functionalization of graphene for selective gas detection such as with amines (i.e. (ethylenediamine (EDA), diethylenetriamine (DETA), and triethylene tetramine (TETA)).

5) Explore the application of graphene-based PANi nanofibers as chemoresistive gas sensor and measure its sensitivity, response time, recovery rate and selectivity.

6) Investigate functionalization of graphene for pathogen detection such as with bacteria antibodies (i.e. E. Coli antibodies)

7) Study the application of graphene-based PANi nanofibers for biosensors in pathogen detection.

8) Investigate the application of as-synthesized CNF/G nanofibers for counter electrode of dye sensitized solar cells and Li-ion batteries.

8) Study the effect of combined addition of multi-wall carbon nanotubes and graphene to CNFs and its electrochemical performance.

BIBLIOGRAPHY

Balandin, A. A., S. Ghosh, W. Bao, I. Calizo, D. Teweldebrhan, F. Miao and C. N. Lau (2008). "Superior thermal conductivity of single-layer graphene." Nano Letters **8**(3): 902-907.

Bao, Q., H. Zhang, J.-x. Yang, S. Wang, D. Y. Tang, R. Jose, S. Ramakrishna, C. T. Lim and K. P. Loh (2010). "Graphene--polymer nanofiber membrane for ultrafast photonics." Advanced Functional Materials **20**(5): 782--791.

Baumgarten, P. K. (1971). "Electrostatic spinning of acrylic microfibers." Journal of Colloid and Interface Science **36**(1): 71--79.

Behabtu, N., J. R. Lomeda, M. J. Green, A. L. Higginbotham, A. Sinitskii, D. V. Kosynkin, D. Tsentalovich, A. N. G. Parra-Vasquez, J. Schmidt, E. Kesselman, Y. Cohen, Y. Talmon, J. M. Tour and M. Pasquali (2010). "Spontaneous high-concentration dispersions and liquid crystals of graphene." Nature Nano **5**(6): 406--411.

Bhadra, S., D. Khastgir, N. K. Singha and J. H. Lee (2009). "Progress in preparation, processing and applications of polyaniline." Progress in Polymer Science **34**(8): 783-810.

Bhattacharya, A. and A. De (1996). "Conducting composites of polypyrrole and polyaniline a review." Progress in Solid State Chemistry **24**(3): 141-181.

Bognitzki, M., W. Czado, T. Frese, A. Schaper, M. Hellwig, M. Steinhart, A. Greiner and J. H. Wendorff (2001). "Nanostructured fibers via electrospinning." Advanced Materials **13**(1): 70--72.

Bolotin, K. I., K. J. Sikes, Z. Jiang, M. Klima, G. Fudenberg, J. Hone, P. Kim and H. L. Stormer (2008). "Ultrahigh electron mobility in suspended graphene." Solid State Communications **146**(9–10): 351-355.

Borodko, Y., S. E. Habas, M. Koebel, P. Yang, H. Frei and G. A. Somorjai (2006). "Probing the interaction of poly(vinylpyrrolidone) with platinum nanocrystals by uv−raman and ftir." Journal of Physical Chemistry B **110**(46): 23052-23059.

Bourlinos, A. B., V. Georgakilas, R. Zboril, T. A. Steriotis and A. K. Stubos (2009). "Liquid-phase exfoliation of graphite towards solubilized graphenes." Small **5**(16): 1841--1845.

Bourlinos, A. B., V. Georgakilas, R. Zboril, T. A. Steriotis, A. K. Stubos and C. Trapalis (2009). "Aqueous-phase exfoliation of graphite in the presence of polyvinylpyrrolidone for the production of water-soluble graphenes." Solid State Communications **149**(47--48): 2172--2176.

Brodie, B. C. (1859). "On the atomic weight of graphite." Philosophical Transactions of the Royal Society of London **149**: 249-259.

Brownson, D. A. C., D. K. Kampouris and C. E. Banks (2011). "An overview of graphene in energy production and storage applications." Journal of Power Sources **196**(11): 4873-4885.

Bruce, P. G., B. Scrosati and J.-M. Tarascon (2008). "Nanomaterials for rechargeable lithium batteries." Angewandte Chemie International Edition **47**(16): 2930-2946.

Cao, Y., P. Smith and A. J. Heeger (1992). "Counter-ion induced processibility of conducting polyaniline and of conducting polyblends of polyaniline in bulk polymers." Synthetic Metals **48**(1): 91-97.

Carissan, Y. and W. Klopper (2006). "Growing graphene sheets from reactions with methyl radicals: A quantum chemical study." ChemPhysChem **7**(8): 1770--1778.

Castro Neto, A. H., F. Guinea, N. M. R. Peres, K. S. Novoselov and A. K. Geim (2009). "The electronic properties of graphene." Reviews of Modern Physics **81**(1): 109-162.

Chae, S. J., F. Güneş, K. K. Kim, E. S. Kim, G. H. Han, S. M. Kim, H.-J. Shin, S.-M. Yoon, J.-Y. Choi, M. H. Park, C. W. Yang, D. Pribat and Y. H. Lee (2009). "Synthesis of large-area graphene layers on poly-nickel substrate by chemical vapor deposition: Wrinkle formation." Advanced Materials **21**(22): 2328--2333.

Chaudhari, S., Y. Sharma, P. S. Archana, R. Jose, S. Ramakrishna, S. Mhaisalkar and M. Srinivasan (2013). "Electrospun polyaniline nanofibers web electrodes for supercapacitors." Journal of Applied Polymer Science **129**(4): 1660-1668.

Chen, G., C. Wu, W. Weng, D. Wu and W. Yan (2003). "Preparation of polystyrene/graphite nanosheet composite." Polymer **44**(6): 1781--1784.

Chen, S. J., G. C. Berry and D. J. Plazek (1995). "Moderately concentrated-solutions of polystyrene .6. Gel formation in carbon-disulfide." Macromolecules **28**(19): 6539--6550.

Das, T. K. and S. Prusty (2012). "Review on conducting polymers and their applications." Polymer-Plastics Technology and Engineering **51**(14): 1487-1500.

Dasari, A., Z.-Z. Yu and Y.-W. Mai (2009). "Electrically conductive and super-tough polyamide-based nanocomposites." Polymer **50**(16): 4112--4121.

de Heer, W. A., C. Berger, X. Wu, P. N. First, E. H. Conrad, X. Li, T. Li, M. Sprinkle, J. Hass, M. L. Sadowski, M. Potemski and G. Martinez (2007). "Epitaxial graphene." Exploring graphene Recent research advances **143**(1-2): 92--100.

Demczyk, B. G., Y. M. Wang, J. Cumings, M. Hetman, W. Han, A. Zettl and R. O. Ritchie (2002). "Direct mechanical measurement of the tensile strength and elastic modulus of multiwalled carbon nanotubes." Materials Science and Engineering: A **334**(1--2): 173--178.

Di, C.-a., D. Wei, G. Yu, Y. Liu, Y. Guo and D. Zhu (2008). "Patterned graphene as source/drain electrodes for bottom-contact organic field-effect transistors." Advanced Materials **20**(17): 3289--3293.

Díaz, J. E., A. Barrero, M. Márquez and I. G. Loscertales (2006). "Controlled encapsulation of hydrophobic liquids in hydrophilic polymer nanofibers by co-electrospinning." Advanced Functional Materials **16**(16): 2110-2116.

Doshi, J. and D. H. Reneker (1995). "Electrospinning process and applications of electrospun fibers." Selected papers from the special technical session "Electrostatics in Polymer Processing and Charge Monitoring", 1993 IEEE Industry Applications Society Meeting **35**(2--3): 151--160.

Du, J. and H.-M. Cheng (2012). "The fabrication, properties, and uses of graphene/polymer composites." Macromolecular Chemistry and Physics **213**(10-11): 1060--1077.

Eizenberg, M. and J. M. Blakely (1979). "Carbon monolayer phase condensation on ni(111)." Surface Science **82**(1): 228-236.

Elahi, M. F., W. Lu, G. Guoping and F. Khan (2013). "Core-shell fibers for biomedical applications-a review." J Bioengineer & Biomedical Sci 3: 121. doi.

Fang, X. and D. H. Reneker (1997). "DNA fibers by electrospinning." Journal of Macromolecular Science, Part B **36**(2): 169-173.

Feng, L., N. Xie and J. Zhong (2014). "Carbon nanofibers and their composites: A review of synthesizing, properties and applications." Materials **7**(5): 3919-3945.

Fong, H. and D. H. Reneker (1999). "Elastomeric nanofibers of styrene--butadiene--styrene triblock copolymer." Journal of Polymer Science Part B: Polymer Physics **37**(24): 3488--3493.

Galal, A., N. F. Atta and H. K. Hassan (2012). "Graphene supported-pt-m (m = ru or pd) for electrocatalytic methanol oxidation." International Journal of Electrochemical Science **7**(1): 768--784.

Geim, A. K. (2009). "Graphene: Status and prospects." Science **324**(5934): 1530--1534.

Georgakilas, V., M. Otyepka, A. B. Bourlinos, V. Chandra, N. Kim, K. C. Kemp, P. Hobza, R. Zboril and K. S. Kim (2012). "Functionalization of graphene: Covalent and non-covalent approaches, derivatives and applications." Chemical Reviews **112**(11): 6156-6214.

Goncalves, G., P. A. A. P. Marques, C. M. Granadeiro, H. I. S. Nogueira, M. K. Singh and J. Grácio (2009). "Surface modification of graphene nanosheets with gold nanoparticles: The role of oxygen moieties at graphene surface on gold nucleation and growth." Chemistry of Materials **21**(20): 4796-4802.

Greiner, A. and J. H. Wendorff (2007). "Electrospinning: A fascinating method for the preparation of ultrathin fibers." Angewandte Chemie (International Ed. in English) **46**(30): 5670-5703.

Gu, S. Y., J. Ren and G. J. Vancso (2005). "Process optimization and empirical modeling for electrospun polyacrylonitrile (pan) nanofiber precursor of carbon nanofibers." European Polymer Journal **41**(11): 2559-2568.

Haynes, A. S. (2008). Electrospun conducting polymer composites for chemo-resistive environmental and health monitoring applications, State University of New York at Stony Brook.

He, H., J. Klinowski, M. Forster and A. Lerf (1998). "A new structural model for graphite oxide." Chemical Physics Letters **287**(1-2): 53-56.

He, J.-H., Y.-Q. Wan and J.-Y. Yu (2008). "Effect of concentration on electrospun polyacrylonitrile (pan) nanofibers." Fibers and Polymers **9**(2): 140-142.

Hernandez, Y., V. Nicolosi, M. Lotya, F. M. Blighe, Z. Sun, S. De, M. T, B. Holland, M. Byrne, Y. K. Gun'Ko, J. J. Boland, P. Niraj, G. Duesberg, S. Krishnamurthy, R. Goodhue, J. Hutchison, V. Scardaci, A. C. Ferrari and J. N. Coleman (2008). "High-yield production of graphene by liquid-phase exfoliation of graphite." Nature Nano **3**(9): 563--568.

Hirsch, A. (2009). "Unzipping carbon nanotubes: A peeling method for the formation of graphene nanoribbons." Angewandte Chemie International Edition **48**(36): 6594--6596.

Hohman, M. M., M. Shin, G. Rutledge and M. P. Brenner (2001). "Electrospinning and electrically forced jets. I. Stability theory." Physics of Fluids (1994-present) **13**(8): 2201-2220.

Hou, H., J. J. Ge, J. Zeng, Q. Li, D. H. Reneker, A. Greiner and S. Z. D. Cheng (2005). "Electrospun polyacrylonitrile nanofibers containing a high concentration of well-aligned multiwall carbon nanotubes." Chemistry of Materials **17**(5): 967-973.

Huang, J.-C. (2002). "Carbon black filled conducting polymers and polymer blends." Advances in Polymer Technology **21**(4): 299--313.

Huang, X., X. Qi, F. Boey and H. Zhang (2012). "Graphene-based composites." Chemical Society Reviews **41**(2): 666--686.

Huang, Z.-M., Y. Z. Zhang, M. Kotaki and S. Ramakrishna (2003). "A review on polymer nanofibers by electrospinning and their applications in nanocomposites." Composites Science and Technology **63**(15): 2223-2253.

Hummers, W. S. and R. E. Offeman (1958). "Preparation of graphitic oxide." Journal of the American Chemical Society **80**(6): 1339-1339.

Hussain, F., M. Hojjati, M. Okamoto and R. E. Gorga (2006). "Review article: Polymer-matrix nanocomposites, processing, manufacturing, and application: An overview." Journal of Composite Materials **40**(17): 1511-1575.

Jaeger, R., H. Schönherr and G. J. Vancso (1996). "Chain packing in electro-spun poly(ethylene oxide) visualized by atomic force microscopy." Macromolecules **29**(23): 7634-7636.

Jeong, J., S. H. Lee, N. W. Song, C. S. Lee and B. H. Chung (2009). "Functionalization of fullerene nanowhiskers using pyrenebutanoic acid, succinimidyl ester in an aqueous solution." Carbon **47**(8): 2124-2127.

Jiao, L., L. Zhang, X. Wang, G. Diankov and H. Dai (2009). "Narrow graphene nanoribbons from carbon nanotubes." Nature **458**(7240): 877--880.

Johnston, D. F. (1955). "The structure of the $\pi $-band of graphite." Proceedings of the Royal Society of London. Series A. Mathematical and Physical Sciences **227**(1170): 349-358.

Jung, K.-H., W. Deng, D. W. Smith Jr and J. P. Ferraris (2012). "Carbon nanofiber electrodes for supercapacitors derived from new precursor polymer: Poly(acrylonitrile-co-vinylimidazole)." Electrochemistry Communications **23**: 149-152.

Kalaitzidou, K., H. Fukushima and L. T. Drzal (2007). "A new compounding method for exfoliated graphite--polypropylene nanocomposites with enhanced flexural properties and lower percolation threshold." Composites Science and Technology **67**(10): 2045--2051.

Kalayci, V. E., P. K. Patra, Y. K. Kim, S. C. Ugbolue and S. B. Warner (2005). "Charge consequences in electrospun polyacrylonitrile (pan) nanofibers." Polymer **46**(18): 7191-7200.

Kelly, B. T. (1981). "Physics of graphite." Applied Science **1**.

Kim, B.-H., C. H. Kim, K. S. Yang, A. Rahy and D. J. Yang (2012). "Electrospun vanadium pentoxide/carbon nanofiber composites for supercapacitor electrodes." Electrochimica Acta **83**: 335-340.

Kim, B.-H., K. Seung Yang and H.-G. Woo (2013). "Boron-nitrogen functional groups on porous nanocarbon fibers for electrochemical supercapacitors." Materials Letters **93**: 190-193.

Kim, B.-H., K. S. Yang, Y. H. Bang and S. R. Kim (2011). "Thermally induced porous carbon nanofibers for electrochemical capacitor electrodes from phenylsilane and polyacrylonitrile blend solutions." Materials Letters **65**(23–24): 3479-3481.

Kim, B.-H., K. S. Yang and J. P. Ferraris (2012). "Highly conductive, mesoporous carbon nanofiber web as electrode material for high-performance supercapacitors." Electrochimica Acta **75**: 325-331.

Kim, B.-H., K. S. Yang and H.-G. Woo (2011). "Thin, bendable electrodes consisting of porous carbon nanofibers via the electrospinning of polyacrylonitrile containing tetraethoxy orthosilicate for supercapacitor." Electrochemistry Communications **13**(10): 1042-1046.

Kim, B.-H., K. S. Yang, H.-G. Woo and K. Oshida (2011). "Supercapacitor performance of porous carbon nanofiber composites prepared by electrospinning polymethylhydrosiloxane (pmhs)/polyacrylonitrile (pan) blend solutions." Synthetic Metals **161**(13–14): 1211-1216.

Kim, C.-D., B.-K. Min and W.-S. Jung (2009). "Preparation of graphene sheets by the reduction of carbon monoxide." Carbon **47**(6): 1610--1612.

Kim, C., S.-H. Park, J.-I. Cho, D.-Y. Lee, T.-J. Park, W.-J. Lee and K.-S. Yang (2004). "Raman spectroscopic evaluation of polyacrylonitrile-based carbon nanofibers prepared by electrospinning." Journal of Raman Spectroscopy **35**(11): 928--933.

Kim, C. and K. S. Yang (2003). "Electrochemical properties of carbon nanofiber web as an electrode for supercapacitor prepared by electrospinning." Applied Physics Letters **83**(6): 1216-1218.

Kim, C., K. S. Yang, M. Kojima, K. Yoshida, Y. J. Kim, Y. A. Kim and M. Endo (2006). "Fabrication of electrospinning-derived carbon nanofiber webs for the anode material of lithium-ion secondary batteries." Advanced Functional Materials **16**(18): 2393-2397.

Kim, H., A. A. Abdala and C. W. Macosko (2010). "Graphene/polymer nanocomposites." Macromolecules **43**(16): 6515-6530.

Kim, H. and C. W. Macosko (2008). "Morphology and properties of polyester/exfoliated graphite nanocomposites." Macromolecules **41**(9): 3317-3327.

Kim, S. B., T. Inoue, A. Shimizu and S. Murase (2006). "The electromagnet design for 3-d superconducting actuator using hts bulk." Proceedings of the 18th International Symposium on Superconductivity (ISS 2005) Advances in Superconductivity XVIII Proceedings of the 18th International Symposium on Superconductivity (ISS 2005) **445-448**(0): 1119--1122.

Kim, S. Y., B.-H. Kim, K. S. Yang and K.-Y. Kim (2012). "The formation of silica nanoparticles on the polyacrylonitrile-based carbon nanofibers by graphene via electrospinning." Materials Letters **71**(0): 74-77.

Kim, S. Y., B.-H. Kim, K. S. Yang and K. Oshida (2012). "Supercapacitive properties of porous carbon nanofibers via the electrospinning of metal alkoxide-graphene in polyacrylonitrile." Materials Letters **87**: 157-161.

Ko, F. (2006). Nanofiber technology. Nanomaterials handbook, CRC Press.

Kolla, H. S., S. P. Surwade, X. Zhang, A. G. MacDiarmid and S. K. Manohar (2005). "Absolute molecular weight of polyaniline." Journal of the American Chemical Society **127**(48): 16770-16771.

Kosynkin, D. V., A. L. Higginbotham, A. Sinitskii, J. R. Lomeda, A. Dimiev, B. K. Price and J. M. Tour (2009). "Longitudinal unzipping of carbon nanotubes to form graphene nanoribbons." Nature **458**(7240): 872--876.

Krishnan, A. (1998). "Young's modulus of single-walled nanotubes." Physical Review B **58**(20): 14013--14019.

Kroto, H. W., J. R. Heath, S. C. O'Brien, R. F. Curl and R. E. Smalley (1985). "C60: Buckminsterfullerene." Nature **318**(6042): 162--163.

Kuila, T., S. Bose, C. E. Hong, M. E. Uddin, P. Khanra, N. H. Kim and J. H. Lee (2011). "Preparation of functionalized graphene/linear low density polyethylene composites by a solution mixing method." Carbon **49**(3): 1033--1037.

Kuilla, T., S. Bhadra, D. Yao, N. H. Kim, S. Bose and J. H. Lee (2010). "Recent advances in graphene based polymer composites." Progress in Polymer Science **35**(11): 1350-1375.

Larsen, G., R. Spretz and R. Velarde-Ortiz (2004). "Use of coaxial gas jackets to stabilize taylor cones of volatile solutions and to induce particle-to-fiber transitions." Advanced Materials **16**(2): 166-169.

Lee, C., X. Wei, J. W. Kysar and J. Hone (2008). "Measurement of the elastic properties and intrinsic strength of monolayer graphene." Science **321**(5887): 385-388.

Lee, W. D. and S. S. Im (2007). "Thermomechanical properties and crystallization behavior of layered double hydroxide/poly(ethylene terephthalate) nanocomposites prepared by in-situ polymerization." Journal of Polymer Science Part B: Polymer Physics **45**(1): 28--40.

Lerf, A., H. He, M. Forster and J. Klinowski (1998). "Structure of graphite oxide revisited‖." Journal of Physical Chemistry B **102**(23): 4477-4482.

Letheby, H. (1862). "Xxix.-on the production of a blue substance by the electrolysis of sulphate of aniline." Journal of the Chemical Society **15**: 161-163.

Li, D., A. Babel, S. A. Jenekhe and Y. Xia (2004). "Nanofibers of conjugated polymers prepared by electrospinning with a two-capillary spinneret." Advanced Materials **16**(22): 2062-2066.

Li, D. and R. B. Kaner (2008). "Graphene-based materials." Science **320**(5880): 1170-1171.

Li, D. and Y. Xia (2004). "Direct fabrication of composite and ceramic hollow nanofibers by electrospinning." Nano Letters **4**(5): 933-938.

Li, D. and Y. Xia (2004). "Electrospinning of nanofibers: Reinventing the wheel?" Advanced Materials **16**(14): 1151-1170.

Li, F., Y. Zhao and Y. Song (2010). Core-shell nanofibers: Nano channel and capsule by coaxial electrospinning.

Li, N., Z. Wang, K. Zhao, Z. Shi, Z. Gu and S. Xu (2010). "Large scale synthesis of n-doped multi-layered graphene sheets by simple arc-discharge method." Carbon **48**(1): 255-259.

Li, Q., R. Jiang, Y. Dou, Z. Wu, T. Huang, D. Feng, J. Yang, A. Yu and D. Zhao (2011). "Synthesis of mesoporous carbon spheres with a hierarchical pore structure for the electrochemical double-layer capacitor." Carbon **49**(4): 1248--1257.

Li, X., W. Cai, J. An, S. Kim, J. Nah, D. Yang, R. Piner, A. Velamakanni, I. Jung, E. Tutuc, S. K. Banerjee, L. Colombo and R. S. Ruoff (2009). "Large-area synthesis of high-quality and uniform graphene films on copper foils." Science **324**(5932): 1312-1314.

Liang, J., Y. Huang, L. Zhang, Y. Wang, Y. Ma, T. Guo and Y. Chen (2009). "Molecular-level dispersion of graphene into poly(vinyl alcohol) and effective reinforcement of their nanocomposites." Advanced Functional Materials **19**(14): 2297--2302.

Lifeng, Z. and H. You-Lo (2006). "Nanoporous ultrahigh specific surface polyacrylonitrile fibres." Nanotechnology **17**(17): 4416.

Lin, Q., Y. Li and M. Yang (2012). "Polyaniline nanofiber humidity sensor prepared by electrospinning." Sensors and Actuators B: Chemical **161**(1): 967-972.

Lota, G., B. Grzyb, H. Machnikowska, J. Machnikowski and E. Frackowiak (2005). "Effect of nitrogen in carbon electrode on the supercapacitor performance." Chemical Physics Letters **404**(1--3): 53--58.

Lu, W., M. Zu, J.-H. Byun, B.-S. Kim and T.-W. Chou (2012). "State of the art of carbon nanotube fibers: Opportunities and challenges." Advanced Materials **24**(14): 1805-1833.

Marcano, D. C., D. V. Kosynkin, J. M. Berlin, A. Sinitskii, Z. Sun, A. Slesarev, L. B. Alemany, W. Lu and J. M. Tour (2010). "Improved synthesis of graphene oxide." ACS Nano **4**(8): 4806--4814.

Mattausch, A. and O. Pankratov (2008). "Density functional study of graphene overlayers on sic." physica status solidi (b) **245**(7): 1425--1435.

Moayeri, A. and A. Ajji (2015). "Fabrication of polyaniline/poly(ethylene oxide)/non-covalently functionalized graphene nanofibers via electrospinning." Synthetic Metals **200**: 7-15.

Moniruzzaman, M. and K. I. Winey (2006). "Polymer nanocomposites containing carbon nanotubes." Macromolecules **39**(16): 5194-5205.

Norris, I. D., M. M. Shaker, F. K. Ko and A. G. MacDiarmid (2000). "Electrostatic fabrication of ultrafine conducting fibers: Polyaniline/polyethylene oxide blends." Synthetic Metals **114**(2): 109-114.

Novoselov, K. S., A. K. Geim, S. V. Morozov, D. Jiang, M. I. Katsnelson, I. V. Grigorieva, S. V. Dubonos and A. A. Firsov (2005). "Two-dimensional gas of massless dirac fermions in graphene." Nature **438**(7065): 197--200.

Novoselov, K. S., A. K. Geim, S. V. Morozov, D. Jiang, Y. Zhang, S. V. Dubonos, I. V. Grigorieva and A. A. Firsov (2004). "Electric field effect in atomically thin carbon films." Science **306**(5696): 666-669.

Novoselov, K. S. and A. H. C. Neto (2012). "Two-dimensional crystals-based heterostructures: Materials with tailored properties." Physica Scripta **2012**(T146): 014006.

Park, J.-Y. (2009). Band structure and electron transport physics of one-dimensional swnts. Carbon Nanotube Electronics, Springer US**:** 1-42.

Park, S. and R. Ruoff (2009). "Chemical methods for the production of graphenes." Nature Nanotechnology **4**(4): 217--224.

Peng, S., P. Zhu, Y. Wu, S. G. Mhaisalkar and S. Ramakrishna (2012). "Electrospun conductive polyaniline-polylactic acid composite nanofibers as counter electrodes for rigid and flexible dye-sensitized solar cells." RSC Advances **2**(2): 652-657.

Peres, N. M. R. (2009). "The transport properties of graphene." Journal of Physics-Condensed Matter **21**(32): 323201.

Prasad, K. E., B. Das, U. Maitra, U. Ramamurty and C. N. R. Rao (2009). "Extraordinary synergy in the mechanical properties of polymer matrix composites reinforced with 2 nanocarbons." Proc Natl Acad Sci U S A **106**(32): 13186--13189.

Qin, X.-H., Y.-Q. Wan, J.-H. He, J. Zhang, J.-Y. Yu and S.-Y. Wang (2004). "Effect of licl on electrospinning of pan polymer solution: Theoretical analysis and experimental verification." Polymer **45**(18): 6409-6413.

Qu, H., S. Wei and Z. Guo (2013). "Coaxial electrospun nanostructures and their applications." Journal of Materials Chemistry A **1**(38): 11513-11528.

Ra, E. J., E. Raymundo-Piñero, Y. H. Lee and F. Béguin (2009). "High power supercapacitors using polyacrylonitrile-based carbon nanofiber paper." Carbon **47**(13): 2984--2992.

Rahaman, M. S. A., A. F. Ismail and A. Mustafa (2007). "A review of heat treatment on polyacrylonitrile fiber." Polymer Degradation and Stability **92**(8): 1421-1432.

Rahaman, M. S. A., A. F. Ismail and A. Mustafa (2007). "A review of heat treatment on polyacrylonitrile fiber." Polymer Degradation and Stability **92**(8): 1421--1432.

Ramakrishna, S. (2005). An introduction to electrospinning and nanofibers, World Scientific.

Ramanathan, T., A. A. Abdala, S. Stankovich, D. A. Dikin, M. Herrera-Alonso, R. D. Piner, D. H. Adamson, H. C. Schniepp, X. Chen, R. S. Ruoff, S. T. Nguyen, I. A. Aksay, R. K. Prud'homme and L. C. Brinson (2008). "Functionalized graphene sheets for polymer nanocomposites." Nature Nanotechnology **3**(6): 327--331.

Rao, P. S., S. Subrahmanya and D. N. Sathyanarayana (2003). "Synthesis by inverse emulsion pathway and characterization of conductive polyaniline–poly(ethylene-co-vinyl acetate) blends." Synthetic Metals **139**(2): 397-404.

Reneker, D. H. and I. Chun (1996). "Nanometre diameter fibres of polymer, produced by electrospinning." Nanotechnology **7**(3): 216.

Rodriguez, N. M. (1993). "A review of catalytically grown carbon nanofibers." Journal of Materials Research **8**(12): 3233-3250.

Rollings, E., G. H. Gweon, S. Y. Zhou, B. S. Mun, J. L. McChesney, B. S. Hussain, A. V. Fedorov, P. N. First, W. A. de Heer and A. Lanzara (2006). "Synthesis and characterization of atomically thin graphite films on a silicon carbide substrate." Journal of Physics and Chemistry of Solids **67**(9-10): 2172-2177.

Ruiz, J., B. Gonzalo, J. R. Dios, J. M. Laza, J. L. Vilas and L. M. León (2013). "Improving the processability of conductive polymers: The case of polyaniline." Advances in Polymer Technology **32**(S1): E180-E188.

Salvetat, J.-P. (1999). "Elastic and shear moduli of single-walled carbon nanotube ropes." Physical Review Letters **82**(5): 944--947.

Schadler, L. S., S. K. Kumar, B. C. Benicewicz, S. L. Lewis and S. E. Harton (2007). "Designed interfaces in polymer nanocomposites: A fundamental viewpoint." Mrs Bulletin **32**(4): 335--340.

Schedin, F., A. K. Geim, S. V. Morozov, E. W. Hill, P. Blake, M. I. Katsnelson and K. S. Novoselov (2007). "Detection of individual gas molecules adsorbed on graphene." Nature Materials **6**(9): 652--655.

Shaijumon, M. M., F. S. Ou, L. Ci and P. M. Ajayan (2008). "Synthesis of hybrid nanowire arrays and their application as high power supercapacitor electrodes." Chem. Commun.: 2373-2375.

Shen, B., W. Zhai, C. Chen, D. Lu, J. Wang and W. Zheng (2011). "Melt blending in situ enhances the interaction between polystyrene and graphene through pi-pi stacking." Acs Applied Materials & Interfaces **3**(8): 3103--3109.

Shin, H.-J., K. K. Kim, A. Benayad, S.-M. Yoon, H. K. Park, I.-S. Jung, M. H. Jin, H.-K. Jeong, J. M. Kim, J.-Y. Choi and Y. H. Lee (2009). "Efficient reduction of graphite oxide by sodium borohydride and its effect on electrical conductance." Advanced Functional Materials **19**(12): 1987--1992.

Si, Y. and E. T. Samulski (2008). "Synthesis of water soluble graphene." Nano Letters **8**(6): 1679-1682.

Skotheim, T. A., R. L. Elsenbaumer and J. R. Reynolds (1998). Handbook of conducting polymers, M. Dekker.

Smith, A. W. and N. S. Rasor (1956). "Observed dependence of the low-temperature thermal and electrical conductivity of graphite on temperature, type, neutron irradiation, and bromination." Phys. Rev. **104**: 885--891.

Sprinkle, M., P. Soukiassian, W. A. de Heer, C. Berger and E. H. Conrad (2009). "Epitaxial graphene: The material for graphene electronics." physica status solidi (RRL) -- Rapid Research Letters **3**(6): A91--A94.

Stankovich, S., D. A. Dikin, G. H. B. Dommett, K. M. Kohlhaas, E. J. Zimney, E. A. Stach, R. D. Piner, S. T. Nguyen and R. S. Ruoff (2006). "Graphene-based composite materials." Nature **442**(7100): 282-286.

Stankovich, S., D. A. Dikin, R. D. Piner, K. A. Kohlhaas, A. Kleinhammes, Y. Jia, Y. Wu, S. T. Nguyen and R. S. Ruoff (2007). "Synthesis of graphene-based nanosheets via chemical reduction of exfoliated graphite oxide." Carbon **45**(7): 1558--1565.

Stankovich, S., R. D. Piner, S. T. Nguyen and R. S. Ruoff (2006). "Synthesis and exfoliation of isocyanate-treated graphene oxide nanoplatelets." Carbon **44**(15): 3342-3347.

Staudenmaier, L. (1898). "Verfahren zur darstellung der graphitsäure." Berichte der deutschen chemischen Gesellschaft **31**(2): 1481--1487.

Stenger-Smith, J. D. (1998). "Intrinsically electrically conducting polymers. Synthesis, characterization, and their applications." Progress in Polymer Science **23**(1): 57-79.

Stoller, M. D., S. Park, Y. Zhu, J. An and R. S. Ruoff (2008). "Graphene-based ultracapacitors." Nano Letters **8**(10): 3498-3502.

Subrahmanyam, K. S., A. Ghosh, A. Gomathi, A. Govindaraj and C. N. R. Rao (2009). "Covalent and noncovalent functionalization and solubilization of graphene." Nanoscience and Nanotechnology Letters **1**(1): 28-31.

Sudha, D. Kumar and M. Iwamoto (2013). "Investigation of the chiroptical behavior of optically active polyaniline synthesized from naturally occurring amino acids." Polym J **45**(2): 160-165.

Sun, Z., E. Zussman, A. l. Yarin, J. h. Wendorff and A. Greiner (2003). "Compound core–shell polymer nanofibers by co-electrospinning." Advanced Materials **15**(22): 1929-1932.

Sutter, P. W., J.-I. Flege and E. A. Sutter (2008). "Epitaxial graphene on ruthenium." Nature Materials **7**(5): 406--411.

Syed, A. A. and M. K. Dinesan (1991). "Review: Polyaniline---a novel polymeric material." Talanta **38**(8): 815-837.

Tao, X. and T. Institute (2005). Wearable electronics and photonics, Woodhead.

Teng, C.-C., C.-C. M. Ma, C.-H. Lu, S.-Y. Yang, S.-H. Lee, M.-C. Hsiao, M.-Y. Yen, K.-C. Chiou and T.-M. Lee (2011). "Thermal conductivity and structure of non-covalent functionalized graphene/epoxy composites." Carbon **49**(15): 5107--5116.

Theron, A., E. Zussman and A. L. Yarin (2001). "Electrostatic field-assisted alignment of electrospun nanofibres." Nanotechnology **12**(3): 384.

Tibbetts, G. G., M. L. Lake, K. L. Strong and B. P. Rice (2007). "A review of the fabrication and properties of vapor-grown carbon nanofiber/polymer composites." Composites Science and Technology **67**(7–8): 1709-1718.

Tung, V. C., M. J. Allen, Y. Yang and R. B. Kaner (2009). "High-throughput solution processing of large-scale graphene." Nature Nanotechnology **4**(1): 25--29.

Verdejo, R., M. M. Bernal, L. J. Romasanta and M. A. Lopez-Manchado (2011). "Graphene filled polymer nanocomposites." Journal of Materials Chemistry **21**(10): 3301--3310.

Wajid, A. S., S. Das, F. Irin, H. S. T. Ahmed, J. L. Shelburne, D. Parviz, R. J. Fullerton, A. F. Jankowski, R. C. Hedden and M. J. Green (2012). "Polymer-stabilized graphene dispersions at high concentrations in organic solvents for composite production." Carbon **50**(2): 526-534.

Wallace, G. G., P. R. Teasdale, G. M. Spinks and L. A. P. Kane-Maguire (2002). Conductive electroactive polymers: Intelligent materials systems, second edition, CRC Press.

Wallace, P. R. (1947). "The band theory of graphite." Phys. Rev. **71**: 622--634.

Wang, J., H. Hu, X. Wang, C. Xu, M. Zhang and X. Shang (2011). "Preparation and mechanical and electrical properties of graphene nanosheets-poly(methyl methacrylate) nanocomposites via in situ suspension polymerization." Journal of Applied Polymer Science **122**(3): 1866--1871.

Wang, X., H. You, F. Liu, M. Li, L. Wan, S. Li, Q. Li, Y. Xu, R. Tian, Z. Yu, D. Xiang and J. Cheng (2009). "Large-scale synthesis of few-layered graphene using cvd." Chemical Vapor Deposition **15**(1-3): 53--56.

Wang, Y., S. Serrano and J. J. Santiago-Avilés (2003). "Raman characterization of carbon nanofibers prepared using electrospinning." Synthetic Metals **138**(3): 423-427.

Wangxi, Z., L. Jie and W. Gang (2003). "Evolution of structure and properties of pan precursors during their conversion to carbon fibers." Carbon **41**(14): 2805-2812.

Wessling, B. (1998). "Dispersion as the link between basic research and commercial applications of conductive polymers (polyaniline)." Synthetic Metals **93**(2): 143--154.

Winter, M. and R. J. Brodd (2004). "What are batteries, fuel cells, and supercapacitors?" Chemical Reviews **104**(10): 4245--4270.

Worsley, K. A., P. Ramesh, S. K. Mandal, S. Niyogi, M. E. Itkis and R. C. Haddon (2007). "Soluble graphene derived from graphite fluoride." Chemical Physics Letters **445**(1-3): 51-56.

Wu, M., Q. Wang, K. Li, Y. Wu and H. Liu (2012). "Optimization of stabilization conditions for electrospun polyacrylonitrile nanofibers." Polymer Degradation and Stability **97**(8): 1511-1519.

Xu, Y., H. Bai, G. Lu, C. Li and G. Shi (2008). "Flexible graphene films via the filtration of water-soluble noncovalent functionalized graphene sheets." Journal of the American Chemical Society **130**(18): 5856-5857.

Yang, G. (2010). from http://www.physics.drexel.edu/~gyang/SOLID/lecture113010.pdf.

Yang, X., X. Dou, A. Rouhanipour, L. Zhi, H. J. Räder and K. Müllen (2008). "Two-dimensional graphene nanoribbons." Journal of the American Chemical Society **130**(13): 4216-4217.

Ye, L., X.-Y. Meng, X. Ji, Z.-M. Li and J.-H. Tang (2009). "Synthesis and characterization of expandable graphite--poly(methyl methacrylate) composite particles and their application to flame retardation of rigid polyurethane foams." Polymer Degradation and Stability **94**(6): 971-979.

Yoonessi, M. and J. R. Gaier (2010). "Highly conductive multifunctional graphene polycarbonate nanocomposites." ACS Nano **4**(12): 7211--7220.

Yu, A., P. Ramesh, M. E. Itkis, E. Bekyarova and R. C. Haddon (2007). "Graphite nanoplatelet-epoxy composite thermal interface materials." Journal of Physical Chemistry C **111**(21): 7565--7569.

Yu, J. H., S. V. Fridrikh and G. C. Rutledge (2004). "Production of submicrometer diameter fibers by two-fluid electrospinning." Advanced Materials **16**(17): 1562-1566.

Yun, Y. S., Y. H. Bae, D. H. Kim, J. Y. Lee, I.-J. Chin and H.-J. Jin (2011). "Reinforcing effects of adding alkylated graphene oxide to polypropylene." Carbon **49**(11): 3553--3559.

Zhang, H.-B., W.-G. Zheng, Q. Yan, Y. Yang, J.-W. Wang, Z.-H. Lu, G.-Y. Ji and Z.-Z. Yu (2010). "Electrically conductive polyethylene terephthalate/graphene nanocomposites prepared by melt compounding." Polymer **51**(5): 1191--1196.

Zhang, J., H. Yang, G. Shen, P. Cheng and S. Guo (2010). "Reduction of graphene oxide via l-ascorbic acid." Chemical communications (Cambridge, England) **46**(7): 1112-1114.

Zhang, L., A. Aboagye, A. Kelkar, C. Lai and H. Fong (2014). "A review: Carbon nanofibers from electrospun polyacrylonitrile and their applications." Journal of Materials Science **49**(2): 463-480.

Zhang, L. L. and X. S. Zhao (2009). "Carbon-based materials as supercapacitor electrodes." Chemical Society Reviews **38**(9): 2520-2531.

Zhang, L. L., R. Zhou and X. S. Zhao (2010). "Graphene-based materials as supercapacitor electrodes." Journal of Materials Chemistry **20**: 5983-5992.

Zhang, W., J. Cui, C.-a. Tao, Y. Wu, Z. Li, L. Ma, Y. Wen and G. Li (2009). "A strategy for producing pure single-layer graphene sheets based on a confined self-assembly approach." Angewandte Chemie International Edition **48**(32): 5864--5868.

Zhang, X., F. Gao, X. Cai, M. Zheng, F. Gao, S. Jiang and Q. Wang (2013). "Application of graphene–pyrenebutyric acid nanocomposite as probe oligonucleotide immobilization platform in a DNA biosensor." Materials Science and Engineering: C **33**(7): 3851-3857.

Zhang, Y., Z.-M. Huang, X. Xu, C. T. Lim and S. Ramakrishna (2004). "Preparation of core−shell structured pcl-r-gelatin bi-component nanofibers by coaxial electrospinning." Chemistry of Materials **16**(18): 3406-3409.

Zhang, Y. and G. C. Rutledge (2012). "Electrical conductivity of electrospun polyaniline and polyaniline-blend fibers and mats." Macromolecules **45**(10): 4238-4246.

Zhao, X., Q. Zhang, D. Chen and P. Lu (2011). "Enhanced mechanical properties of graphene-based poly(vinyl alcohol) composites (vol 43, pg 2357, 2010)." Macromolecules **44**(7): 2392--2392.

Zheng, W., X. Lu and S.-C. Wong (2004). "Electrical and mechanical properties of expanded graphite-reinforced high-density polyethylene." Journal of Applied Polymer Science **91**(5): 2781--2788.

Zhi, L. and K. Mullen (2008). "A bottom-up approach from molecular nanographenes to unconventional carbon materials." Journal of Materials Chemistry **18**: 1472-1484.

Zhou, T., F. Chen, K. Liu, H. Deng, Q. Zhang, J. Feng and Q. Fu (2010). "A simple and efficient method to prepare graphene by reduction of graphite oxide with sodium hydrosulfite." Nanotechnology **22**(4): 045704.

Zhou, X., T. Wu, B. Hu, G. Yang and B. Han (2010). "Synthesis of graphene/polyaniline composite nanosheets mediated by polymerized ionic liquid." Chemical Communications **46**(21): 3663--3665.

Zhu, Y., S. Murali, M. D. Stoller, A. Velamakanni, R. D. Piner and R. S. Ruoff (2010). "Microwave assisted exfoliation and reduction of graphite oxide for ultracapacitors." Carbon **48**(7): 2118--2122.

Zussman, E., X. Chen, W. Ding, L. Calabri, D. A. Dikin, J. P. Quintana and R. S. Ruoff (2005). "Mechanical and structural characterization of electrospun pan-derived carbon nanofibers." Carbon **43**(10): 2175-2185.